TABLE OF CONTENTS

LIST OF TABLES

LIST OF FIGURES

CHAPTER 1: INTRODUCTION

1.1 General

Noise pollution affects more people than any other kind of pollution in the modern industrialized world [Sandberg and Ejsmont 2002]. Among the many sources of noise, the one that clearly dominates is the road traffic noise. In the United States, more people are exposed to highway noise than from any other single noise source [AASHTO 1974]. Noise pollution is especially problematic in densely congested urban settings where residents live near highways and main transportation thoroughfares. Road traffic noise has traditionally been associated with engine and exhaust noise of vehicles. However, of late, while the emission and propagation noise from these sources are greatly reduced, the emission from tire-road interaction has become more prominent. This effect has been reported to be more significant in Portland Cement Concrete (PCC) pavements [Onstenk et al 1993, BE 3415 1994].

Currently, the most commonly adopted solution to reduce the noise generated by traffic is the installation of sound barriers. While the construction of sound barriers impedes the sound transmission path between vehicles and the neighboring development alongside the highways resulting in noise abatement, they tend to be extremely costly, unsightly, and not practical for bridges and/or urban highways. This, coupled with the understanding that the pavement surface has a significant effect on noise generation mechanisms, has led to the development of techniques to achieve quieter PCC riding surfaces. Some of the most commonly used techniques include special surface texturing

like tines, use of exposed aggregates, chip sealing with small aggregates, grinding etc [BE 3415 1994, Descornet et al. 2000].

1.2 Modifying the Material Structure to Reduce Noise

The most common noise reducing methods focus on modifying the surface texture of the pavement to absorb noise. However, the use of porous concrete (Enhanced Porosity Concrete – EPC) is a method where the noise reduction is achieved by introducing porosity in the material structure by gap grading the aggregates, i.e., the porosity lies in the non-aggregate component of the material. The mechanisms by which such pavements reduce noise is attributed to their potential to absorb and dissipate a significant portion of air through their pore network, and the ability of air in these pores to vibrate, thereby reducing energy through friction. Detailed treatment of the methods of manufacture, physical and mechanical properties, and noise absorption characteristics of porous concrete is incorporated in a previous report [Neithalath et al. 2003]. It is interesting to note that while these porous materials have shown exceptional promise with respect to sound absorption, the propensity of these pores to clog with debris over time is a cause for concern that can lead to reduction in performance with time [Onstenk et al. 1993].

1.3 The Concept of Inclusions

The previous section discusses the prospect of introducing porosity in the non-aggregate component of the mixture to achieve sound absorption. Another potential method involves the use of "aggregates" with a higher than typical porosity, i.e., increasing the porosity of the aggregate component. It is postulated that inclusions made from porous, elastic materials will have the ability to combine the conventional (viscous and frictional damping) mechanism of sound absorption with structural damping effects. It is built on the premise that relatively high volume fractions of porous inclusions in the matrix will provide a pore network that can absorb sound and dissipate structure-borne vibrations. Materials considered include porous particles made from materials like sintered fly ash, expanded shale, cellular concrete fragments, and cellulose fibers. Thus, this research is an effort to incorporate an absorbent material with cement and tailor its microstructure to improve the overall acoustic performance. It is anticipated that the use of low stiffness 'aggregate/fiber' inclusions may provide an effective means to reduce the stiffness of the pavement and increase the viscous-damping capacity of the concrete. By increasing the impedance incompatibility between the concrete components, the sound transmission path can be interrupted which could possibly increase the damping capacity of the pavement. Lightweight concrete with inclusions can also have other potential applications in buildings as partitions, apartment separating floors etc.

1.4 Organization of this Report

This report is organized in two parts – Part A describes the use of morphologically altered cellulose fibers as inclusion materials in conventional cement-sand mortar. Part B comprises of the study of Enhanced Porosity Concrete (EPC) reinforced with polypropylene fibers. The reasons for choosing these materials as inclusions are elucidated in Chapter 2. The tests that are conducted to arrive at those conclusions are also explained. Based on the results from these tests, the objectives for the research study are also outlined in this chapter.

1.4.1 Organisation of Part A: Cellulose-Cement Composites

A detailed review of literature of the types of cellulose fibers, their manufacture and properties, cellulose fibers in cementitious matrices, and the physical, mechanical, and durability characteristics of cellulose fiber reinforced cementitious materials is given in Chapter 3.

Chapter 4 gives the details of materials, mixture proportions, and mixing procedure of cellulose-cement composites. The characteristics of three types of morphologically altered cellulose fibers are explained. The test procedures employed to evaluate the physical, mechanical, and damping properties are also explained in this chapter.

The physical and mechanical properties of cellulose-cement composites including porosity, compressive and flexural strengths and the modulus of elasticity are discussed

in Chapter 5. These properties are dealt with in detail, with emphasis on the influence of fiber morphology and volume on these properties.

Chapter 6 discusses the influence of the volume and morphology of cellulose fibers on the sound absorption and vibration damping characteristics of cellulose-cement composites. Specifically, this chapter compares the acoustic effectiveness and damping features of morphologically altered cellulose fiber-cement composites.

The durability studies conducted on cellulose-cement composites are described in Chapter 7. Hot water soak test carried out to ascertain the stability of fibers in the cementitious matrix is explained. Freezing and thawing tests are also carried out on cellulose-cement composites, and electrical conductivity used as a measure of damage.

Chapter 8 summarizes the results of the tests, lists the findings, and identifies scope for further research.

1.4.2 Organization of Part B: Fiber Reinforced Enhanced Porosity Concrete

Chapter 9 encompasses a concise summary of literature on the mechanisms, materials and manufacture, use, and properties of Enhanced Porosity Concrete (EPC). There has been no reported literature on fiber reinforced EPC to the authors' knowledge.

Chapter 10 explains the materials used in this study, mixture proportions adopted, and the test methods employed to study the various properties of fiber reinforced Enhanced Porosity Concrete. Detailed descriptions of the experimental set up developed, and the testing method are provided.

The physical and mechanical properties of fiber reinforced EPC forms part of Chapter 11. The properties studied are the porosity and flexural strength. The influence of fibers in both is brought out.

Chapter 12 is a detailed discussion on the acoustic absorption behavior of EPC. The influence of fibers in the acoustic absorption of both single sized and blended aggregates is explained. The mechanisms by which fibers influence acoustic absorption, as well as the influence of pore structure features is also dealt with.

Chapter 13 summarizes the research findings, and outlines the future direction of research.

CHAPTER 2: SCREENING OF POTENTIAL MATERIALS AS SOUND ABSORBING INCLUSIONS

2.1 General

The primary goal of this research study is to extend the concept of Enhanced Porosity Concrete (EPC) where porosity is introduced in the non-aggregate component of the material, to the concept of "compliant inclusions", where porosity is incorporated in the aggregate component. The premise of this work is that porous, compliant inclusions will have the capacity to combine the conventional sound absorbing mechanism (viscous and frictional effects) with structural damping. To achieve this end, several lightweight, porous materials were investigated with respect to their effectiveness in acoustic absorption and damping capacity. These tests were used to screen the different materials that were expected to exhibit significant potential as inclusions.

2.2 Screening Tests

As described in the previous section, acoustic absorption coefficient (α), and specific damping capacity (ψ) were used as the parameters to evaluate the efficiency of inclusions. The test procedures are described in this section.

2.2.1 Determination of Acoustic Absorption Coefficient (α)

To evaluate the acoustic absorption characteristics of inclusion materials, a Brüel & Kjær™ impedance tube was employed, as shown in Figure 2.1. Cylindrical mortar specimens (diameter of 95 mm) with inclusions were used for the test. The sample was placed inside a thin cylindrical Teflon sleeve, into which it fits snuggly. The sample assembly was placed against a rigid backing at one end of the impedance tube which is equipped with a sound source. A plane acoustic wave generated by the sound source was propagated along the axis of the tube. Microphones placed along the axis of the tube were used to detect the sound wave pressure transmitted to the sample and the portion of the wave that is reflected (ASTM E-1050). The pressure reflection coefficient (R) is the ratio of the pressure of reflected wave to that of incoming wave, at a particular frequency, expressed as:

$$R = \frac{e^{jkd_1} - e^{jkd_2} P}{e^{-jkd_2} P - e^{-jkd_1}} \qquad 2.1$$

where d_1 and d_2 are the distances from the specimen surface to the closest and farthest active microphones respectively, j is an imaginary number ($\sqrt{-1}$), k is the wave number (ratio of angular frequency to the wave speed in the medium) and P is the ratio of acoustic pressures at the two active microphone locations.

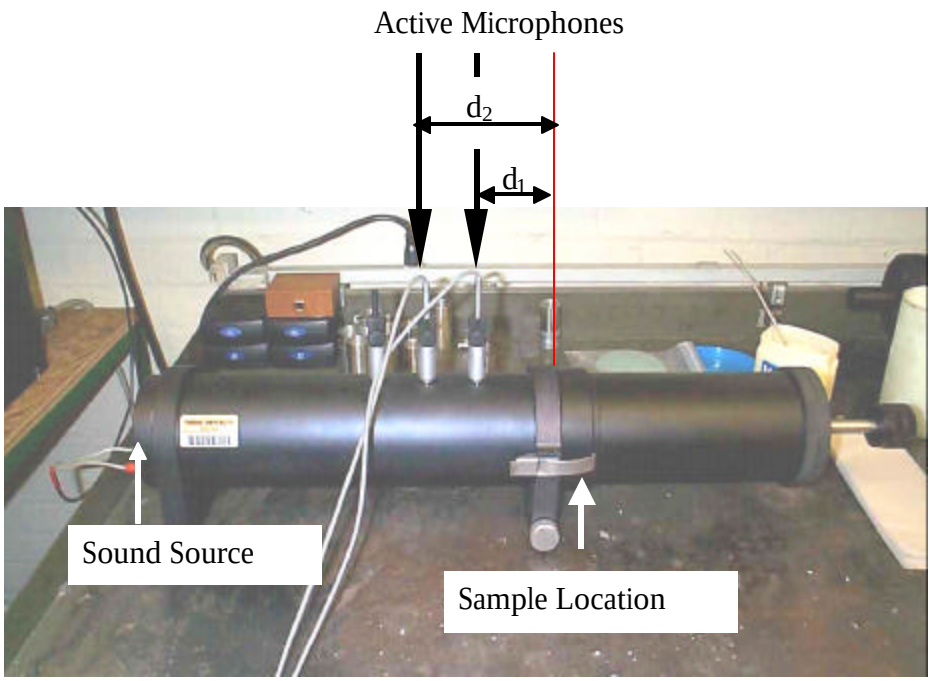

Figure 2.1 Impedance tube set up

A data acquisition system (PULSE ™) is attached to the impedance tube, which converts the signals in the time domain to one in the frequency domain. A software program written in Matlab™ allows graphic display of the real and imaginary components of the impedance with respect to the frequency. The program has also been tailored to output the variation of acoustic absorption coefficient with frequency.

The absorption coefficient (α) is commonly reported as a measure of a material's ability to absorb sound. A material with an absorption coefficient of 1.0 indicates a purely absorbing material whereas a material with an absorption coefficient of 0 indicates that it is purely reflective. The absorption coefficient at each frequency can be calculated from the pressure reflection coefficient (R) as given in Equation 2.2.

$$\alpha = 1-|R|^2 \qquad 2.2$$

In this work the frequency range of interest was limited from 100 Hz to 1600 Hz. A threshold of 100 Hz was established because at very low frequencies, the acoustic pressures were difficult to stabilize. Frequencies higher than 1600 Hz could be measured accurately only when the impedance tube has a small diameter. (To achieve acoustic measurements over the widest range of frequencies, and to ensure that a "standing wave" is generated inside the impedance tube, its diameter should be as small as possible). Preparation of concrete / mortar samples of such small sizes is not practical.

2.2.2 Determination of Specific Damping Capacity (ψ)

The Specific Damping Capacity (χ) was determined using Grindosonic™ equipment according to the decaying sine wave method.

$$\chi = \frac{A_i - A_{n+i}}{A_i} \times 100\% \qquad 2.3$$

where A_i is the amplitude of the i^{th} period and A_{n+i}, that of $(n+i)^{th}$ period.

The specific damping capacity reported is at the resonant frequency of the material. The beam specimens were supported at 0.224L (L is the specimen length), as per ASTM E 1876-01. The pick up of the Grindosonic equipment was positioned on the center of the side face of the specimen and a light impact was given on the center of the top face of the specimen to transmit flexural waves through the specimen. The instrument indicated the fundamental flexural frequency as well as the specific damping capacity in percentage.

2.3 Materials Considered and Specimen Preparation

The inclusion materials considered for this study are:

(i) Lightweight expanded shale aggregate

(ii) Crimped rubber inclusions

(iii) Morphologically altered Cellulose fibers

(iv) Foamed Cellular Concrete

(v) Polypropylene fibers in Enhanced Porosity Concrete (EPC)

The material characteristics and specimen preparation details for the screening tests are described in the following sections. The cement used was Lonestar Type I, and fine aggregate, locally available river sand.

2.3.1 Expanded Shale Aggregates

The expanded shale aggregates used in this study was Haydite, manufactured in a rotary kiln in Brooklyn, Indiana. The aggregate size used was one passing # 4 sieve (4.75 mm) and retained on # 8 sieve (2.36 mm). The specific gravity and water absorption values of these aggregates were 2.0 and 7.0% respectively.

The mortar mixtures prepared using Haydite aggregates contained 65% by volume of aggregates. A water-to-cement ratio of 0.50 was used. The cement and the aggregates were mixed dry in a Hobart mixer for one minute, and the required amount of water added. The mixer was run for further two minutes, after which it was stopped for a duration of two minutes. A final two minute run ensured that the contents were mixed homogeneously. Cylindrical specimens 95 mm in diameter and 75 mm in length were

cast for acoustic absorption, and beam specimens 25 mm x 75 mm x 250 mm for specific damping capacity tests.

2.3.2 Crimped Rubber Inclusions

The rubber inclusions used for this study was in the form of shredded fibers, approximately 10-15 mm in length and 1-2 mm in width. The rubber particles were added at 10% by weight of cement. The water-to-cement ratio adopted was 0.50. The mortar mixture had an aggregate volume of 50%. The cement and sand were first mixed dry in the mixer, and the rubber particles were slowly added while mixing. Water was subsequently added while the mixer was running. The ingredients were mixed for two minutes before the mixer was stopped for two minutes. This was followed by further two minutes of mixing. The specimens for acoustic absorption and specific damping capacity were cast as explained in the previous section.

2.3.3 Morphologically Altered Cellulose Fibers

Morphologically altered cellulose fibers were provided by Weyerhaeuser Co. The macronodule fibers used for the screening tests consisted of agglomeration of treated individual fibers. The size of these ranged from 2 mm to 8 mm. The agglomeration resulted in making these materials porous. A cement-sand mortar with 50% sand volume was used. The fibers being porous, absorb large amounts of water, and for the screening test, a very high fiber volume was used (7.5%). Hence, even with the use of a high range water-reducer, the water-to-cement ratio had to be increased to 0.69.

The cement and sand was first mixed at low speed for one minute and then the fibers were added, while mixing. Approximately three quarters of the water needed was added and all ingredients were mixed at medium speed for two minutes. The remaining water was then added with water reducer and mixed until a uniform mixture was obtained (typically at one minute). Care was taken to ensure that the mixer did not run at higher than required speeds or for longer than required durations so that the fiber nodules are not broken down in the mixer. An accelerator was added at 1% by weight of cement to avoid retardation due to incorporation of high amounts of cellulose fibers. The specimens for acoustic absorption and damping capacity tests were cast as previously described.

2.3.4 Foamed Cellular Concrete

The foamed cellular concrete specimens of varying densities for this study was provided by Elastizell™ Corporation. The densities that were used were 450, 560, and 720 kg/m^3 respectively.

2.3.5 Polypropylene Fibers in Enhanced Porosity Concrete (EPC)

Enhanced Porosity Concrete (EPC) is proportioned by gap grading selected coarse aggregate sizes so as to create a network of interconnected porosity in the material. It has been found that EPC has better sound absorbing characteristics as compared to normal concrete because of the interconnected and tortuous pore network that allows sound waves to propagate inside and lose energy [Onstenk et al. 1993, Nelson 1994, Marolf et al. 2003, Neithalath et al. 2003]. In this study, the influence of polypropylene fiber reinforcement on the acoustic absorption behavior of EPC was explored.

EPC used for the screening tests was proportioned with aggregates retained on # 4 (4.75 mm) sieve. The weighed quantity of aggregates was added to the mixer, followed by cement. Water was slowly added while the dry materials were being mixed in a pan mixer. The fibers were slowly added into the rotating pan. The mixer was allowed to run for three minutes. At the end of three minutes, the bottom and sides of the mixer were scrapped, and the mixer was allowed to rest for three minutes. A final two minutes of mixing followed this step. The acoustic absorption tests were carried out on 95 mm diameter cylindrical specimens, 150 mm long.

2.4 Acoustic Absorption Coefficient (α)

The acoustic absorption coefficients of mortars / concrete incorporating the inclusion materials are described in this section. The acoustic absorption spectra of mortars / concrete containing each of these inclusion materials are compared to the spectra of normal mortar / concrete.

2.4.1 Influence of Expanded Shale Aggregate

The acoustic absorption spectra of cement mortar with expanded shale lightweight aggregates as inclusions are shown in Figure 2.2. The specimens are of 75 mm length.

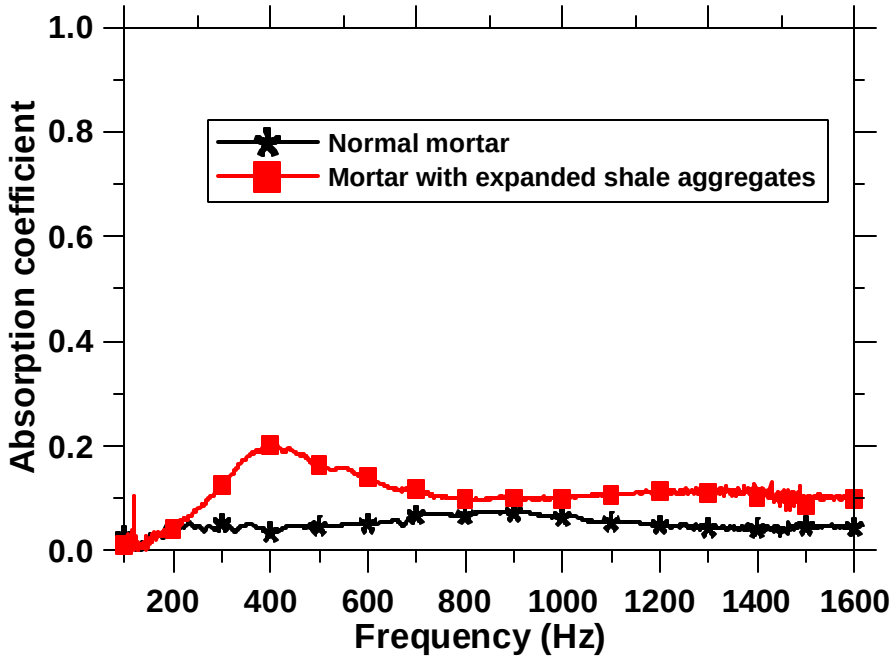

Figure 2.2 Comparison of acoustic absorption spectra of mortars with and without expanded shale aggregate

It can be observed from this figure that the maximum acoustic absorption coefficient (α) for normal mortars is around 0.05-0.10, and there is no selective absorption at any particular frequencies. For mortars incorporating expanded shale aggregates, the maximum absorption coefficient is around 0.25, at a frequency of about 400 Hz. This increase in α could be attributed to the fact that porous aggregates exposed to the incoming sound waves absorb some amount of energy depending on their porosity.

2.4.2 Influence of Crimped Rubber Inclusions

Figure 2.3 depicts the acoustic absorption spectra of mortars incorporating crimped rubber inclusions at 10% by weight of cement.

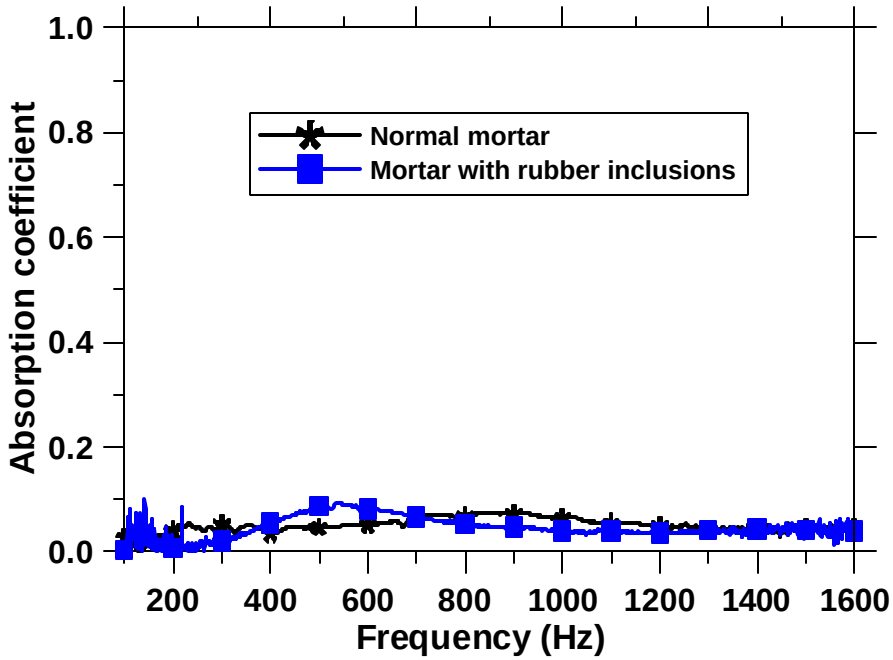

Figure 2.3 Comparison of acoustic absorption spectra of mortars with and without crimped rubber inclusions

This figure shows that the absorption spectra of mortars with and without crimped rubber inclusions are not significantly different, and the maximum absorption coefficient is around 0.10 for both the cases. The reason for this similarity is that, for mortars incorporating crimped rubber inclusions, there is no open porosity at the surface where sound waves can enter and attenuate, much like a normal mortar.

2.4.3 Influence of Cellulose Fibers

Macronodule fibers were used at 7.5% by volume of the matrix to study its influence on the acoustic absorption capacity. Figure 2.4 shows the comparison between mortar mixtures with and without macronodule cellulose fibers. The efficiency in acoustic absorption of mixtures with cellulose fibers is evident from this figure. While normal mortar has a maximum absorption coefficient of about 0.05-0.10, mortars

incorporating 7.5% cellulose fibers exhibit α values of about 0.45, at a frequency of approximately 450 Hz. This is due the fact that macronodule fibers are porous by themselves, and results in connected pathways inside the material for sound waves to propagate and attenuate.

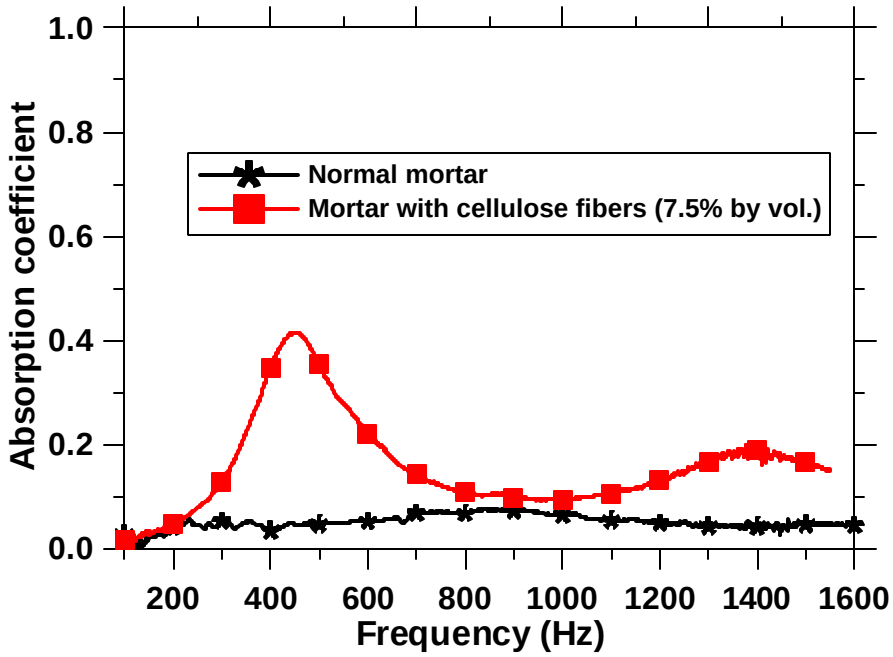

Figure 2.4 Comparison of acoustic absorption spectra of mortars with and without macronodule cellulose fibers

2.4.4 Foamed Cellular Concrete

The acoustic absorption spectra of foamed cellular concretes of three different densities, along with the normal mortar are shown in Figure 2.5. It can be easily seen that with a reduction in density, the maximum acoustic absorption coefficient increases. However, the increase in α values are not as significant as the decrease in densities. The

closed cell structure of foamed cellular concretes, which does not allow sound waves to propagate through them, can be the reason for such a behavior.

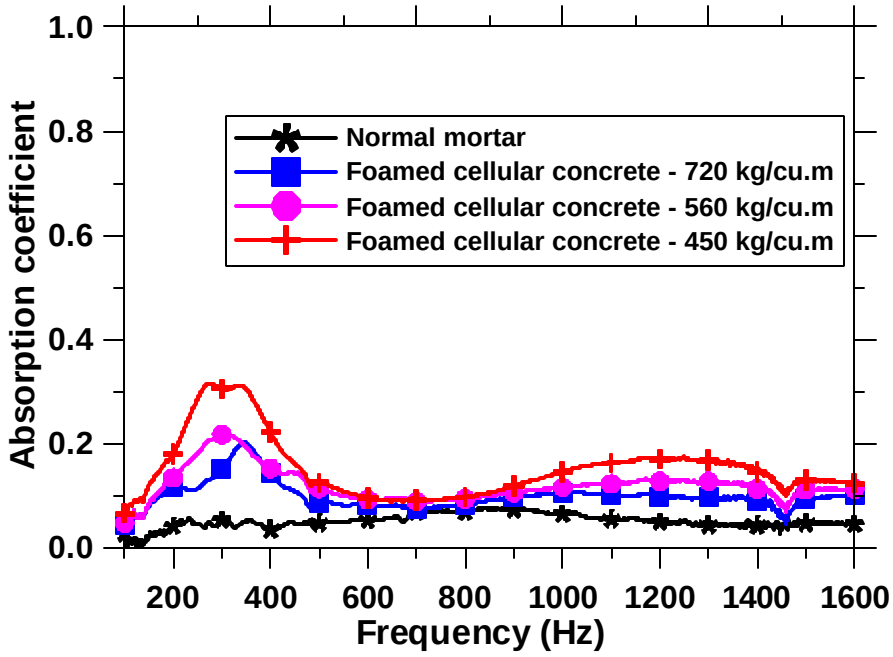

Figure 2.5 Comparison of acoustic absorption spectra of normal mortar and foamed cellular concretes of different densities

2.4.5 Influence of Polypropylene Fibers in Enhanced Porosity Concrete

Enhanced Porosity Concrete (EPC) is reported to be very efficient in acoustic absorption because of its pore structure and large porosity [Nelson 1994, Marolf et al. 2003, Neithalath et al. 2003]. The influence of polypropylene fibers on acoustic absorption of EPC made with aggregates retained on # 4 sieve (4.75 mm) is shown in Figure 2.6. It can easily be seen that the maximum acoustic absorption coefficient for EPC even without fibers is much higher than normal mortar. Addition of 1.5% by volume of polypropylene fibers increases the absorption coefficient further. Among all

the alternatives discussed previously, the fiber reinforced EPC performs the best with respect to acoustic absorption.

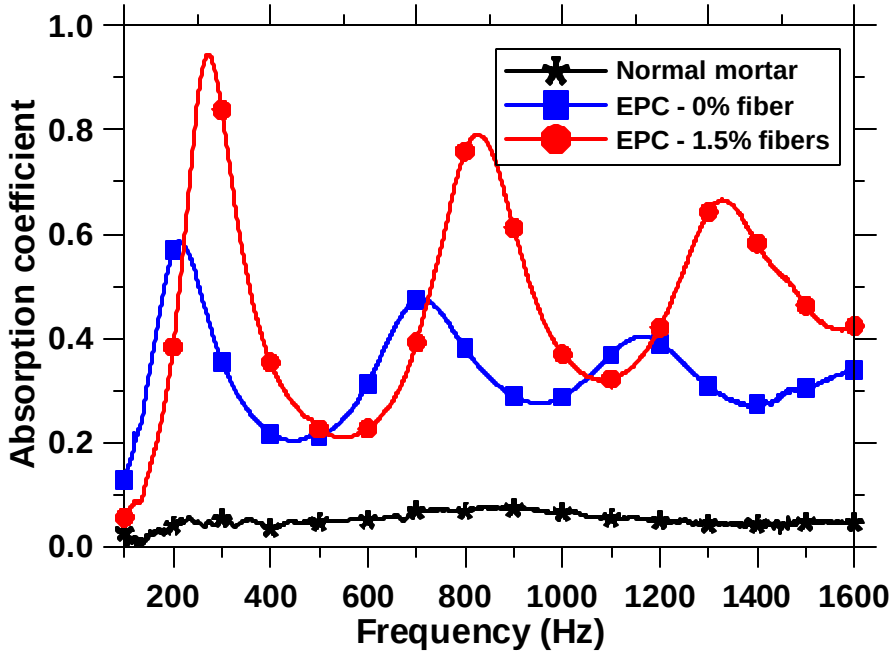

Figure 2.6 Acoustic absorption spectra of EPC with and without polypropylene fibers, compared to that of normal mortar

2.5 Specific Damping Capacity (ψ)

Specific damping capacity is a measure of the energy dissipation capacity of the material. The specific damping capacities of mortars / concrete made with the selected inclusion materials are shown in Table 2.1. Damping capacity tests were not carried out on fiber reinforced EPC specimens because the highly porous nature of these materials. The damping capacity measurements being extremely sensitive to specimen geometry and locations of the impact and pick up, the EPC specimens did not give consistent results.

Table 2.1 Specific damping capacities for the chosen inclusion materials

Material	Details	Specific Damping Capacity (%)
Normal mortar	Cement-sand mortar – 50% aggregate volume	8
Mortar with expanded shale aggregate	65% aggregate volume, maximum size of aggregates – 4.75 mm	10
Mortar with crimped rubber inclusions	Cement-sand mortar – 50% aggregate volume, crimped rubber10% by weight of cement	19
Mortar with morphologically altered cellulose fibers	Cement-sand mortar – 50% aggregate volume, macronodule fibers 7.5% by volume	23
Foamed Cellular Concrete	Three different densities – 450, 560 and 720 kg/m^3	450 kg/m^3 – 28 560 kg/m^3 – 16 720 kg/m^3 – 11
Fiber reinforced EPC	Aggregates retained on # 4 sieve (4.75 mm), no sand. 0% and 1.5% polypropylene fibers by volume	--

2.6 Selection of Potential Inclusion Materials

From the tests on acoustic absorption and specific damping capacity, it was found that morphologically altered fibers in cementitious matrix, and fiber reinforced EPC have significant potential in absorbing sound and / or dissipating energy. Though the mixtures with rubber inclusions have appreciable energy dissipation through damping, the absorption capacity is almost negligible. Expanded shale aggregate mortars perform better than mortars with rubber inclusions in acoustic absorption, but fares poorly in damping capacity. Foamed cellular concrete shows increasing absorption with reducing density, but at low densities, the strength becomes very low. For further studies, therefore, morphologically altered cellulose fibers in a cementitious matrix, and polypropylene fiber reinforced Enhanced Porosity Concrete were chosen.

2.7 Objectives of this Study

Two potential classes of materials that can be used to mitigate tire-pavement interaction noise have been identified. The objectives of this research study are as follows:

2.7.1 Part A: Cellulose-Cement Composites

(i) To study the influence of fiber volume and morphology on the mechanical characteristics, porosity, and acoustic absorption of cellulose-cement composites

(ii) To ascertain the efficiency of cellulose fibers on the damping behavior of the composite

(iii) To characterize the porosity and pore network of cellulose-cement composites and relate pore features to the acoustic and damping characteristics

(iv) To study the durability characteristics of cellulose-cement composites

2.7.2 Part B: Fiber Reinforced Enhanced Porosity Concrete

(i) To study the influence of polypropylene fibers on the mechanical characteristics, porosity, and acoustic absorption of Enhanced Porosity Concrete

(ii) To characterize the porosity and pore network of fiber reinforced EPC and relate pore features to the acoustic characteristics

2.8 Summary

This chapter provides an outline of the methodology chosen to select potential inclusion materials that have the capacity to absorb sound or dissipate energy. Five different inclusion materials were selected and evaluated. Measurement of acoustic absorption coefficient by impedance tube, and specific damping capacity by impulse excitation of vibration were used as the screening tests. From the standpoint of acoustic

absorption, fiber reinforced EPC performed the best, with maximum absorption coefficients of about 0.95 for mixtures with 1.5% fibers by volume. Cement composites with morphologically altered cellulose fibers showed moderate absorption capacities (~0.45 at 7.5% fibers by volume) and high specific damping capacities (23% after 7 day moist curing). Hence, these two materials were chosen for further studies. The following chapters describe the materials and methods of manufacture, testing procedures, and analysis of physical, mechanical, acoustic, and durability characteristics of concretes with selected inclusion materials. Part A of this report deals with cellulose fiber inclusions where as Part B deals with Enhanced Porosity Concrete reinforced with Polypropylene fibers.

PART A: CELLULOSE FIBER REINFORCED CEMENT COMPOSITES

CHAPTER 3: LITERATURE REVIEW ON CELLULOSE-CEMENT COMPOSITES

3.1 General

Based on the screening tests as explained in the previous chapter, it was found that morphologically altered cellulose fibers have the potential to serve as porous, flexible inclusions in cement mortar, because of their sound absorption and specific damping capacity. This chapter reviews pertinent literature on the manufacture, mechanical properties, and durability aspects of cementitious composites with cellulose fibers.

3.2 Cellulose Fibers

Cellulose fibers have found wide acceptance in the cement composite industry as a replacement for asbestos. Good mechanical properties and high processability, as well as the lower production energy required are the two main criteria that establish the viability of using cellulose fibers in a cementitious matrix [Kim et al. 1999, Vinson and Daniel 1990]. This section deals with the manufacture and properties of different kinds of cellulose fibers. It is to be noted that only the natural cellulose fibers are discussed here; the man-made variety of cellulose fibers are not touched upon.

3.2.1 Manufacture of Cellulose Fibers

Trees are the major raw materials for cellulose fibers. Commercially, the trees harvested for the production of cellulose fibers are known as “softwoods” and “hardwoods”. The so-called “long fibers” are produced from softwoods. They range in length from about 2.5 mm to 7 mm, the majority lying in the length range from 3 to 5 mm. The width or diameter of these fibers ranges from about 15 to 80 μm. Hardwoods yield cellulose fibers that are about one-half to one-third the length, and about one-half the width of fibers produced from softwoods [Soroushian and Marikunte 1990]. The cells in softwoods and hardwoods are bonded together by a layer of cementing material. The fiber production process (pulping) breaks these cells.

Pulping process can be chemical, semi-chemical, or mechanical. In the chemical process, wood cells are separated from one another by dissolving and removing the cementing material. In the mechanical pulping process, the cells are separated by frictional forces, often aided by steam pressure. The semi-chemical process uses a combination of both the chemical reactions and the frictional forces. The fibers produced by one of these means can be further subdivided by hydrolysis followed by mechanical disintegration into microfibrils [Bledzki and Gassan 1999].

3.2.2 Properties of Cellulose Fibers

The characteristic values of Young’s modulus for cellulose fibers are reported to be close to that of E-glass fibers (~ 40 GPa), however, the range is also large, as is the case with all natural products. The elastic modulus of bulk natural fibers like wood is around 10 GPa. Elastic modulus of up to 70 GPa can be obtained by mechanical

disintegration of cellulose fibers into microfibrils. Theoretically, the elastic moduli of cellulose chains give values of up to 250 GPa. The tensile strength of cellulose fibers depends on the test length. For a test length of zero, as in the case for glass fibers, the tensile strength has been reported to be 1000 MPa. A decrease in fiber fineness leads to a higher tensile strength [Bledzki and Gassan 1999]. In another study on cotton and wood based cellulose fibers, the Young's modulus was estimated as 4 GPa and 2 GPa respectively. The mean tensile strength for cotton based cellulose fiber was close to 500 MPa whereas it was reported to be 175 MPa for wood based fibers [Kompella and Lambros 2002].

3.3 Cellulose-Cement Composites

The basic components of cellulose-cement composites are cellulose fiber and cementitious binder. Fine aggregates (sand) are also used in cellulose-cement composites.

3.4 Manufacture of Cellulose-Cement Composites

Cellulose-cement composites are produced by two different methods: (i) conventional molding process, similar to preparation of normal cement mortars, and (ii) Slurry dewatering method.

In the conventional molding process, cement and a portion of the mix water are added to the mixer, mixed at low speed until a uniform mixture is obtained. The cellulose fibers and the remaining water are then added, and mixed at medium / high speeds till a homogeneous mixture is obtained. Water reducers are typically added to

increase workability, and lower the water-cementitious materials ratio. Molding process is generally used to produce beam, cylindrical, and cubical specimens [Blankenhorn et al. 2001, Bouguerra et al. 1998, Soroushian and Marikunte 1990, Sarigaphuti et al. 1993].

Slurry dewatering method is common for manufacturing cellulose-cement composites in the form of sheets or boards. This method is based on the Hatschek process for producing fiber reinforced composites. The fibers are dispersed using high speed mixing in an appropriate quantity of water. The mix constituents are added and mixed at high speeds till uniform dispersion is achieved. To achieve agglomeration of cement particles in the slurry (and consequently avoid loss of fines), a flocculent is added. The slurry is poured into evacuable molds fitted with an assembly of permeable screens, and vacuum is applied at the rate of about 60 KPa/g, to remove excess water. The sheet is removed from the filter screen, and pressed under constant pressure until the remaining water is removed [Marikunte and Soroushian 1994, Vinson and Daniel 1990, Soroushian et al. 1995, Majumdar and Walton 1991].

3.5 Influence of Cellulose Fibers on the Fresh Properties of the Composite

Studies have been reported on the water requirement, workability, unit weight, air content, and setting time of cellulose-cement composites. It has been observed that to achieve similar workability, the water requirement increases with increase in cellulose fiber volume fraction. Higher volume fraction of fibers implies higher surface area, and hence more water to wet the surfaces. Also, cellulose fibers absorb water from the mixture, reducing the workability [Soroushian and Marikunte 1991]. The drop in workability with time is comparable in cellulose fiber reinforced and plain mixtures.

Cellulose fibers are observed to reduce the unit weight of fresh cement based materials. This is probably because of the fact that the air content increases with addition of cellulose fibers. The increase in air content could be attributed to the difficulty of compacting cement composites incorporating high volumes of fibers.

The setting times are also found to increase with increase in fiber volume. This could be because of the fact that some constituents of the fiber can act as set retarders [Soroushian and Marikunte 1990].

3.6 Physical Properties of Cellulose-Cement Composites

The physical properties commonly reported for cellulose-cement composites are its water absorption and specific gravity [Soroushian et al. 1995].

3.6.1 Water Absorption

The water absorption capacity of cellulose-cement composites was reported to be affected by both the fiber content and the binder type. An increase in fiber content increases the water absorption because of the tendency of the fibers to absorb water. Addition of silica fume, by densifying the paste structure, reduces the water absorption capacity.

3.6.2 Specific Gravity

Addition of cellulose fibers to cementitious matrices reduces the specific gravity of the composite. Fibers being lighter than the cementitious matrix, this is expected. This behavior is more pronounced at higher volume fractions [Vinson and Daniel 1990, Bledzki and Gassan 1999].

3.7 Mechanical Properties of Cellulose-Cement Composites

The mechanical properties of composites generally evaluated are compressive strength, flexural strength, toughness, and shrinkage.

3.7.1 Compressive Strength

The compressive strength of cellulose fiber-cement composites vary depending on the fiber volume fraction and the type of fibers used. It has been reported that the compressive strength decreases with increase in fiber content [Wolfe and Gjinolli 1996, Blankenhorn et al. 2001]. Treating cellulose fibers with acrylic or alkylalkoxysilane was found to result in increased compressive strength of the composite as compared to the untreated ones. Composites with longer fibers fare poorly than shorter fibers in compressive strength.

3.7.2 Flexural Strength

The flexural strength of cellulose fiber reinforced cement composites is reported to increase with fiber volume up to a certain optimal fiber volume fraction and then decrease. Both early age and later age strengths are reported to increase when processed cellulose fibers are used as the reinforcement [Soroushian and Ravanbakhsh 1999]. The drop in strength past the optimal volume fraction is attributed to the tendency of fibers to pack less efficiently as fiber mass increases beyond this point [Wolfe and Gjinolli 1996]. Large increase in flexural strength with 2-3% of fibers is reported [Soroushian and Marikunte 1990]. Vinson and Daniel [1990] reported no uniform trends between fiber volume and flexural strength. Oven drying of cellulose-cement composites does not increase the flexural strength significantly as compared to plain mortars. The performance of recycled waste paper cellulose fiber reinforced composites was found to be comparable to those made with virgin fibers [Soroushian et al. 1995].

3.7.3 Toughness

The fracture toughness of cellulose fiber reinforced cement composites increases continuously with increasing fiber content. An increase in toughness of about 200% has been reported with addition of 2% of cellulose fibers by volume [Soroushian and Marikunte 1991]. Use of waste paper fibers increased the flexural toughness of the composites [Soroushian et al. 1995]. The flexural toughness is reduced when the composites are oven dried.

3.7.4 Shrinkage

Addition of cellulose fibers in the amount of about 0.5% by volume can substantially reduce the crack width of concrete resulting from restrained shrinkage. The performance of cellulose fibers in crack control is comparable to that of polypropylene fibers if similar amounts are used. Restrained shrinkage cracking tests were conducted using ring-type concrete specimens [Sarigaphuti et al. 1993, Soroushian and Ravanbakhsh 1999].

3.8 Durability of Cellulose-Cement Composites

A key concern to the use of cellulose fibers in cementitious matrices relates to the long-term durability of fibers, particularly when the product is under sever exposure conditions. Cellulose fibers are particularly sensitive to alkali attack. Investigations concerned with the use of cellulose fibers in cement composites suggest that the mechanism of ageing process is directly related to the type of matrix, porosity, fiber type, and ageing mechanism [Akers and Studinka 1989, Mac Vivar et al. 1999]. The main degradation mechanisms in fiber reinforced composites are fiber degradation, fiber-matrix interfacial physical interaction, fiber-matrix chemical interaction, and volume stability and cracking sensitivity of the composite [Bentur 1994]. The accelerated ageing tests commonly adopted to ascertain the durability of cellulose-cement composites are briefly explained in this section.

3.8.1 Accelerated Ageing Tests

The accelerated carbonation method was designed to assess the changes in physical and mechanical properties of the composite after exposure to cycles of heat ageing, water soak, followed by a saturated carbon di-oxide atmosphere [Mac Vivar 1999]. Accelerated ageing in carbon di-oxide rich environment lead to an increase in strength and elastic modulus. It is reported that accelerated ageing in CO_2 rich environment compares favorably with natural ageing process [Akers and Studinka 1989].

The hot-water soak test [ASTM C 1185] investigates the long term chemical interaction of constituent materials [Marikunte and Soroushian 1994, Sarigaphuti et al. 1993]. In this method, wet and elevated temperature conditions are used to accelerate the tests. The test specimens are saturated in water and maintained at $60\pm2^{o}C$ for 56 days and tested for flexural performance. Flexural toughness considerably deteriorated with ageing, where as the flexural strength increases with ageing. Ageing causes densification of the interfaces and petrification of cellulose fibers, thus improving the flexural strength and reducing the toughness of the composites.

The influence of accelerated wetting and drying on the performance of cellulose-cement composites has been studied [Marikunte and Soroushian 1994, Akers and Studinka 1989]. The flexural strength of the composite was found to increase slightly, and toughness decreased considerably. The fiber content is said to have a drastic effect on the toughness reduction.

Cyclic freezing and thawing tests have also been carried out on cellulose-cement composites. It has been reported that such testing did not produce any ageing effects

similar to those caused by natural weather or accelerated carbonation [Mac Vivar et al. 1999]

3.8.2 Aging and Physical Properties

The porosity and permeability of cementitious composites are vital to their durability. Accelerated carbonation decreases the porosity, either due to densification of the matrix resulting from shrinkage brought about by carbonation, and / or densification due to continued hydration process within the matrix. Cyclic soaking and drying with exposure to CO_2 is known to accelerate carbonation [Akers and Studinka 1999]. Consequently, the carbonation products fill the matrix structure, increase the density of the product, and reduce its porosity.

CHAPTER 4: MATERIALS, MIXTURES, AND TEST METHODS FOR CELLULOSE-CEMENT COMPOSITES

4.1 General

This chapter provides an overview of the materials, mixture proportions, and test methods adopted in the study of Cellulose-Cement composites. The determination of acoustic absorption coefficient, and specific damping capacity were explained as part of the screening studies, and hence they will not be explained in this chapter.

4.2 Materials

This section gives an outline about the various materials used in the experimental investigations. The materials are kept constant throughout the study so as to nullify the influence of change in materials on the physical, mechanical, and durability characteristics of cellulose-cement composites.

4.2.1 Cement

Commercially available Type I Ordinary Portland Cement manufactured by Lonestar Industries was used for the entire study. Table 4.1 summarizes the chemical properties of the cement.

Table 4.1 Chemical properties of cement

C_3S (%)	C_3A (%)	Total Alkali (%)	Insoluble Residue (%)	Loss on Ignition (%)	MgO (%)	SO_3 (%)
--	15.0 (max)	--	0.8 (max)	3.0 (max)	6.0 (max)	4.5 (max)
62.0	9.0	0.5	1.94	0.58	1.82	2.67

4.2.2 Fine Aggregate

The fine aggregate used for the study was a locally available river sand, with an absorption of 2.3%. The sand conforms to ASTM C 128-94.

4.2.3 Cellulose Fibers

Morphologically altered cellulose fibers for this study were obtained from Weyerhaeuser group. The three types of cellulose fibers used in this study are shown in Figure 4.1. The first type consisted of fiber agglomerates (nodules), ranging from 1 mm-8 mm in size, formed by a flaking process that did not separate the fibers during manufacture; they are termed macro nodules, for this study. The second type consisted of typical cellulose fibers, 2-3 mm long and 20-60μm in diameter and is referred to as discrete fibers. The third type consisted of a mixture of small fiber nodules and normal short fibers, and will be referred to as petite nodules. All the fibers were bleached soft wood fibers. The latter two types of fibers, discrete fibers and petite nodules, to a certain degree, could be dispersed fairly easily into individual units in water whereas

macronodules were not easily dispersible. The fiber nodules or clumps are porous since they are formed by the agglomeration of individual fibers.

(a)

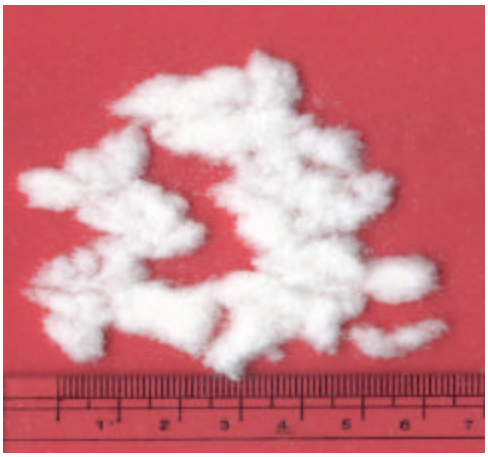

(b)

(c)

Figure 4.1 Morphology of three types of cellulose fibers used in this study: (a) Macronodules, (b) Discrete fibers, (c) Petite nodules

4.2.4 Water Reducer

A commercial high range water reducer conforming to ASTM C 494 Type F was used to reduce the water demand and increase the workability of the cellulose-cement mixtures.

4.2.5 Accelerator

A commercial non-chloride accelerator was used in conjunction with mixtures that incorporated high volumes of cellulose fibers. Though the fibers used were treated fibers, it is conceivable that, at high volumes, there is enough lignin present to retard the setting of cement.

4.3 Composition of Composite Mixtures

A cement-sand mortar, with 50% of sand by volume of the matrix phase has been used throughout this study. Fiber volume chosen for the three selected fibers varied with the type of fiber. For macro nodule fibers, 1.5, 3.0, 4.5, 6.0 and 7.5% of the matrix volume was replaced by fibers whereas for discrete fibers and petite nodules, 1.5, 3.0 and 4.5% replacement was chosen. Two different series of fiber volumes were selected based on two criteria: (i) macro nodules, by virtue of their particle size and porosity, were assumed to provide the kind of porosity that could be beneficial for sound absorption and (ii) at higher volumes, discrete fibers and petite nodules tend to clump together in the matrix and the water content required to achieve desired consistency increases drastically.

In contrast, macro nodules being more "aggregate-like" retain their physical form during mixing and require less water to reach the desired consistency.

For all fibers, the water demand increased with the addition of fibers to the mixture. Since the addition of water reducer was not effective in maintaining constant water-to-cement ratio (w/c) for all mixtures, the w/c was adjusted to maintain fresh mix workability at a reasonably practical level, represented by flow values determined in accordance with ASTM C 1437. Table 4.2 gives the details of the fresh properties of the mixtures.

Table 4.2 Ingredients and flow properties of cellulose-cement mixtures investigated

Fiber type	Fiber volume (%)	Water-cement ratio	Water reducer (% by weight of cement)	Accelerator (% by weight of cement)	Flow (%)
--	0.0	0.47	0.0	0	70
Macro Nodules	1.5	0.50	1.0	0	65
	3.0	0.52	1.0	0	55
	4.5	0.57	1.5	0	55
	6.0	0.65	2.0	1	50
	7.5	0.69	2.5	1	45
Discrete Fibers	1.5	0.50	1.0	0	70
	3.0	0.52	1.0	0	65
	4.5	0.56	1.5	0	55
Petite Nodules	1.5	0.50	1.0	0	70
	3.0	0.52	1.0	0	60
	4.5	0.57	1.5	0	55

4.4 Mixing Procedure

The mixing procedure adopted in this study was varied depending on the type of fibers that were used. For mixtures with macro nodules, cement and sand was first mixed at low speed for one minute and then the fibers were added, while mixing. Approximately three quarters of the water needed was added and all ingredients were mixed at medium speed for two minutes. The remaining water was then added with water reducer and mixed until a uniform mixture was obtained (typically at one minute). Care was taken to ensure that the mixer did not run at higher than required speeds or for longer than required durations so that the fiber nodules are not broken down in the mixer. For mixtures with high volumes of fiber (6.0 and 7.5%), an accelerator was added since it was noticed that there was considerable set retardation otherwise. Discrete fibers and petite nodules were initially mixed with about three quarters of the mixing water for one minute while the mixer was running at low speed. This enabled the fibers to be dispersed. Cement and sand were then added and mixed at medium speed for two minutes, stopped for one minute, followed by the addition of remaining water and water reducer till a uniform mixture was obtained.

For each mixture, cylindrical specimens were cast for acoustic absorption (95 mm diameter, 100 mm long) and compressive strength (100 mm diameter, 200 mm long), and prismatic specimens for specific damping capacity, and flexural strength (250 mm x 75 mm x 25 mm) determination. All the specimens were consolidated using external vibration and were kept damp inside the molds for 24 hours, after which they were moist cured (at >98% RH, 23^{o}C) until the test age. Slices (75 mm x 25 mm x 25mm) were cut from the prismatic specimens for porosity determination.

4.5 Test Methods

This section describes the various test procedures employed to study the properties of cellulose-cement composites. Methods to determine the acoustic absorption coefficient, and specific damping capacity could be found in the section dealing with screening of potential inclusion materials.

4.5.1 Porosity Determination

Porosity was determined on 75 mm x 75 mm x 25 mm prisms of composite specimens obtained as mentioned in the previous section. The method of vacuum saturation as described in RILEM CPC 11.3 has been followed in the determination of porosity. The prisms were dried in an oven at 105± 5°C until no change in measured weight was noticed. The specimens were then kept dry in a vacuum chamber for 3 hours before water was introduced to the chamber, under vacuum. The vacuum was maintained for 6 more hours after which time the specimens were left in water for 18 hours. The saturated surface dried weight was then determined. For the fiber-reinforced specimens, the water absorbed by the fibers was accounted for in the vacuum saturated weight so as to obtain the effective porosity. Porosity of a plain (control) mortar was also determined.

4.5.2 Flexural Strength Determination

Flexural strength was determined in accordance with ASTM C 78-02. Three specimens (250 mm x 75 mm x 25 mm) were tested for each mixture, and the average strength reported.

4.5.3 Compressive Strength Determination

The compressive strength was determined in accordance with ASTM C 39-01. Two specimens (75 mm diameter and 150 mm long) were tested for each mixture and the average strength reported.

4.5.4 Electrical Impedance Spectroscopy

Electrical Impedance Spectroscopy (EIS) was used to determine the bulk resistance of cellulose-cement composites, in order to estimate the conductivities. EIS measurements were conducted in this study using a Solartron 1260 ™ Impedance / Gain-Phase analyzer that was interfaced with a personal computer for data acquisition. A typical Nyquist plot (plot of real versus imaginary impedance) obtained from EIS measurements consists of two arcs – the bulk arc and the electrode arc. The two arcs meet at a point where the imaginary component of the impedance is minimum, and the corresponding real impedance is the bulk resistance (R_b) of the sample.

Figure 4.6 shows the specimen set up that was used for the EIS experiments. The cylindrical specimens, 75 mm in diameter, and 75 mm long were saturated in the electrolyte. The bottom of the specimen was sealed to a stainless steel plate using silicone sealant, and another stainless steel plate with a small acrylic dyke was placed at the top of the specimen, with a piece of porous foam in between. The entire set up was firmly gripped with adjustable clamping mechanism. The stainless steel plates served as the electrodes and alligator plugs from the impedance analyzer were attached to the electrodes. The impedance measurements were made over the frequency range of 1 MHz to 10 Hz using a 250 mV AC signal.

Using the bulk resistance (R_b) obtained from the Nyquist plots, the effective electrical conductivity (σ_{eff}) of the sample was calculated as:

$$s_{eff} = \frac{l}{R_b A} \qquad 4.5$$

where l is the specimen length and A is the cross sectional area of the specimen.

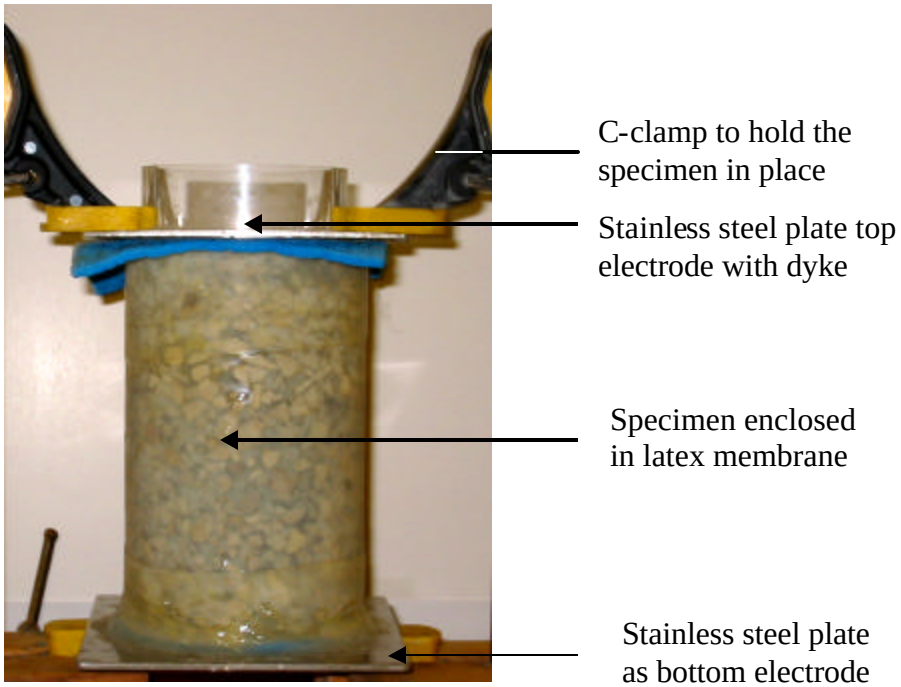

Figure 4.5 Specimen set up for EIS experiments

4.5.5 Dynamic Modulus of Elasticity

The dynamic modulus of elasticity was determined using Grindosonic ™ equipment, as per ASTM E 1876-01. The specimen was supported on rollers at a distance of 0.224L from the edges (L is the specimen length). The pick up of the Grindosonic equipment was positioned on the center of the side face of the specimen and a light impact was given on the center of the top face of the specimen to transmit flexural waves through the specimen. The instrument indicated the fundamental flexural

frequency. The procedure was repeated for three times (a very consistent reading was obtained in this case) and the average was taken as the fundamental flexural frequency of the specimen. The dynamic modulus of elasticity is given by:

$$E = 0.9465 m f_f^2 \frac{L^3}{t^3 b} T_1 \qquad 4.6$$

where E is the dynamic modulus of elasticity in Pa, m is the mass of the specimen in g, f_f is the fundamental flexural frequency of the specimen in Hz, L is the specimen length in mm, t and b are the specimen thickness and width respectively in mm, and T_1 is a correction factor to account for the finite length of the bar, Poisson's ratio and so forth. The equation for calculation of T_1 is given in ASTM E 1876.

4.5.6 Freezing and Thawing

Freezing and thawing studies on cellulose-cement composites were carried out in a controlled temperature chamber. The temperature of the chamber cycled from -17 ^{o}C to 23 ^{o}C, and one cycle of freezing and thawing occurs in a day. The specimens were subjected to freezing and thawing, both under water, and in air. After specified number of cycles, the fundamental flexural resonant frequencies of the specimens were determined using the procedure determined in Section 4.5.5. Reduction in resonant frequencies is indicative of damage.

CHAPTER 5: PHYSICAL AND MECHANICAL PROPERTIES OF CELLULOSE-CEMENT COMPOSITES

5.1 General

Though the main purpose of developing cellulose-cement composites using morphologically altered cellulose fibers is to ascertain their efficiency in acoustic absorption, it is imperative to study the physical and mechanical properties of the material in order to establish their practical utility. The properties that studied include the porosity, compressive and flexural strengths and the modulus of elasticity. This chapter discusses these properties in detail, with emphasis on the influence of fiber morphology and volume on these properties.

5.2 Porosity

For sound absorbing materials, porosity (ϕ) is one of the primary factors that govern its acoustic behavior. The attenuation of sound is believed to be effected by the porosity incorporated into the system by the addition of porous fiber nodules or clumps. Porosity also plays a significant role in determining the mechanical properties of the composite. As explained in the previous chapter, the porosity of cellulose-cement composites was determined using the procedure stated in RILEM CPC 11.3.

5.2.1 Influence of Fiber Volume and Morphology on Porosity

A plot of normalized porosity ($f_{composite} / f_{mortar}$) versus fiber volume for composites with all the three fiber types is shown in Figure 5.1.

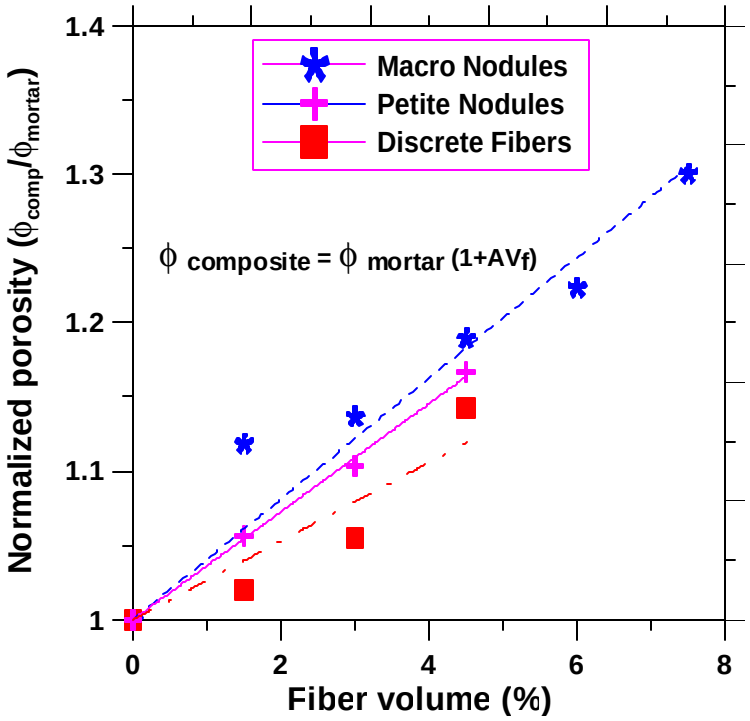

Figure 5.1 Influence of fiber volume and morphology on composite porosity

It can be observed from this figure that the increase in porosity is highest for specimens with macro nodules and lowest for those with discrete fibers. The relationship is linear (R^2 values of 0.93, 0.99 and 0.87 for macro nodules, petite nodules and discrete fibers respectively), with porosity increasing with fiber volume. The relationship between the porosity of the composite at any fiber volume and the porosity of the mortar can be given by:

$$\phi_{composite} = \phi_{mortar} (1 + A\ V_f) \qquad 5.1$$

where the value of the constant A can be considered as an indicator of the contribution of the fiber phase to the total porosity of the composite. In the present study, the constant A assumes values of 0.041, 0.036 and 0.023 for composites with macro nodules, petite nodules and discrete fibers respectively.

The increase in porosity with increasing fiber volume in mixtures containing macro nodules and petite nodules can be explained by the fact that in addition to being porous themselves, these nodules are composed of porous fibers that can absorb water. For specimens with discrete fibers, the increased porosity may be due to the tendency of fibers to clump together while mixing, entrapping water filled spaces, which consequently turn into voids. Increased fiber volume enhances the potential for fiber clumping.

5.3 Flexural Strength

The flexural strengths of cellulose-cement composites comprising of all three different fiber types (macronodules, discrete fibers, and petite nodules) were determined as per ASTM C 78. The strengths were determined after curing the specimens for 7 days, and 14 days. In addition, the flexural strength after oven-drying the specimen at 105^{o}C after 14 days of moist curing was also determined.

The flexural strengths of composites incorporating macronodule fibers as a function of fiber volume are shown in Figure 5.2. The wet flexural strengths of 7 day and 14 day moist cured specimens decrease with increase in fiber volume, and the trend is very similar. The reduction in strength with increase in fiber volume in the wet condition can be attributed to a variety of reasons: (i) the macronodule fibers as soft inclusions reduces the load carrying capacity of the matrix, (ii) the cellulose fibers have a reduced strength in wet condition, (iii) fibers entrap water filled spaces, and (iv) reduced fiber-to-matrix bond strength. When oven dried after 14 days of moist curing, the flexural strength is found to increase with fiber volume until an optimal fiber volume, and then

decreases. The reason for this behavior could be that in the dry condition, there is an increased fiber-to-matrix bond, and the failure is due to fiber fracture than fiber pull-out. This behavior is dominant up to a certain fiber volume, but after that the influence of soft inclusions begins to take over, resulting in reduced flexural strengths at higher fiber volumes.

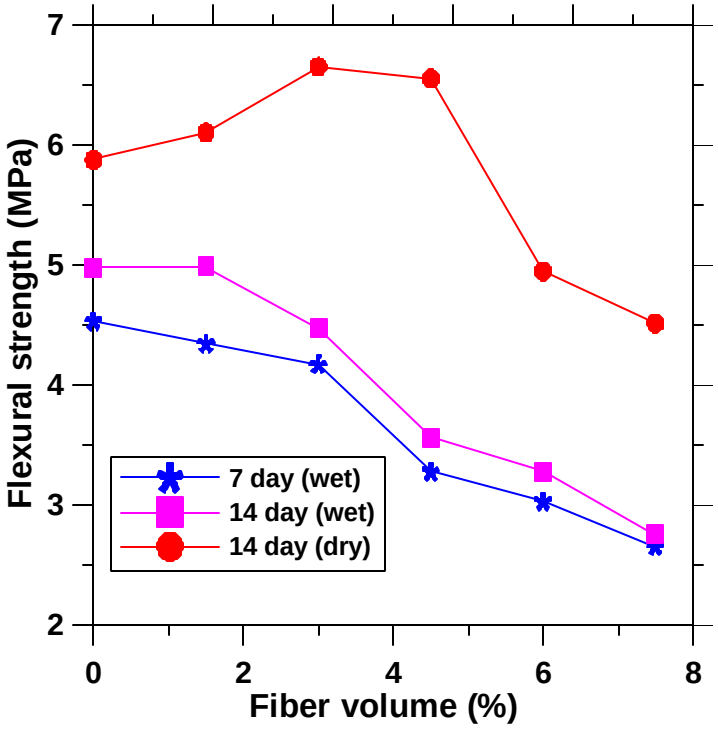

Figure 5.2 Flexural strength vs. fiber volume (macronodules)

Figures 5.3 and 5.4 show the flexural strengths of composites incorporating discrete fibers and petite nodules respectively as a function of fiber volume. The trends are similar to that obtained for macronodules. The same reasons as described earlier could be attributed to this case also.

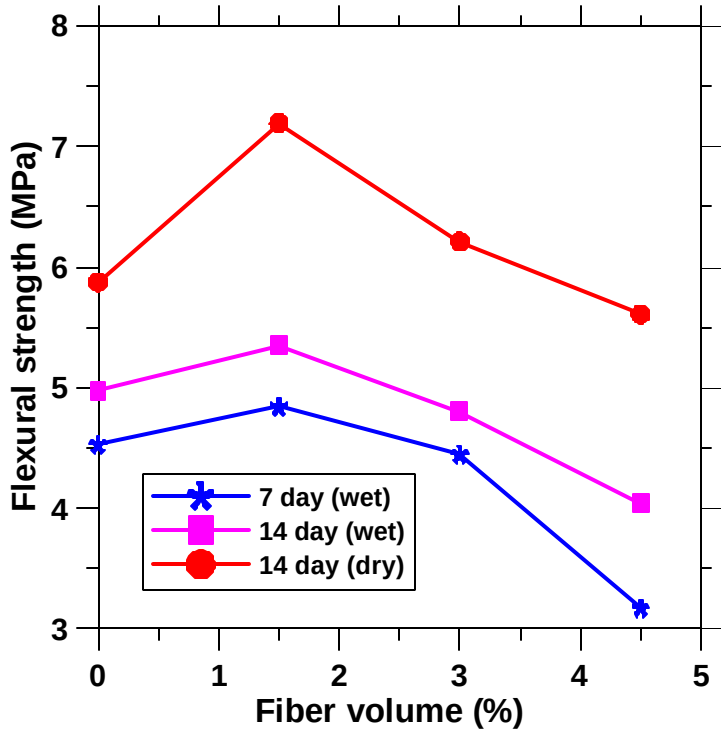

Figure 5.3 Flexural strength vs. fiber volume (discrete fibers)

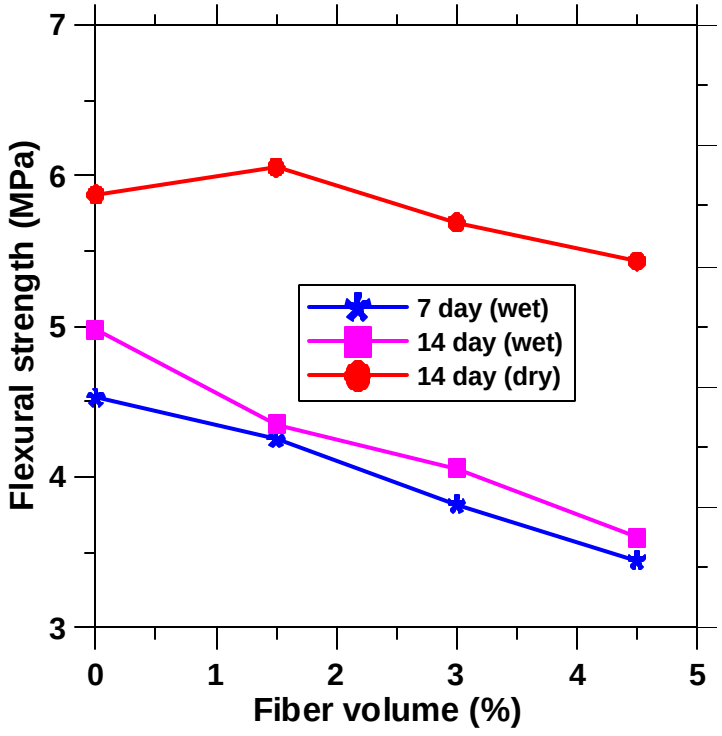

Figure 5.4 Flexural strength vs. fiber volume (petite nodules)

A comparison of flexural strengths of 7-day cured composites incorporating different volumes of macronodules, discrete fibers, and petite nodules is shown in Figure 5.5.

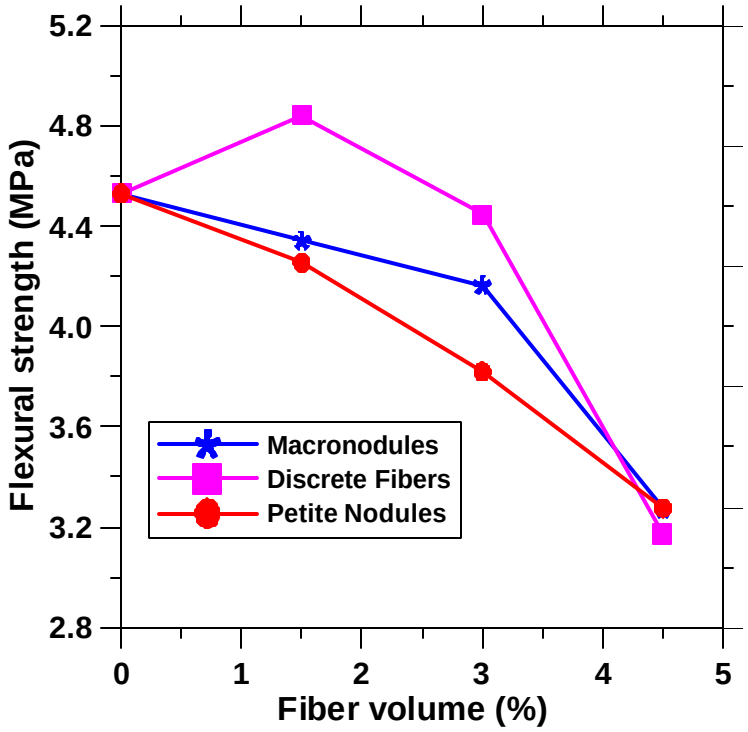

Figure 5.5 Comparison of flexural strengths between different fiber types (7 day cured)

For a given fiber volume, discrete fibers show the highest flexural strength. The reason for this can be that macronodules and petite nodules, because of their clumped nature, provide large areas of preferential weakness in the matrix, resulting in a reduction in flexural strength. With increase in fiber volume, the flexural strength reduces for composites incorporating any of the fiber types, and at about 4.5% fiber volume, the flexural strength is essentially the same. At higher fiber volumes, there are increased chances of fiber clumping, creating voids that reduce the flexural strength.

5.4 Compressive Strength

The variation of compressive strength of composites reinforced with macronodule fibers with 1-porosity (1-ϕ) is shown in Figure 5.6

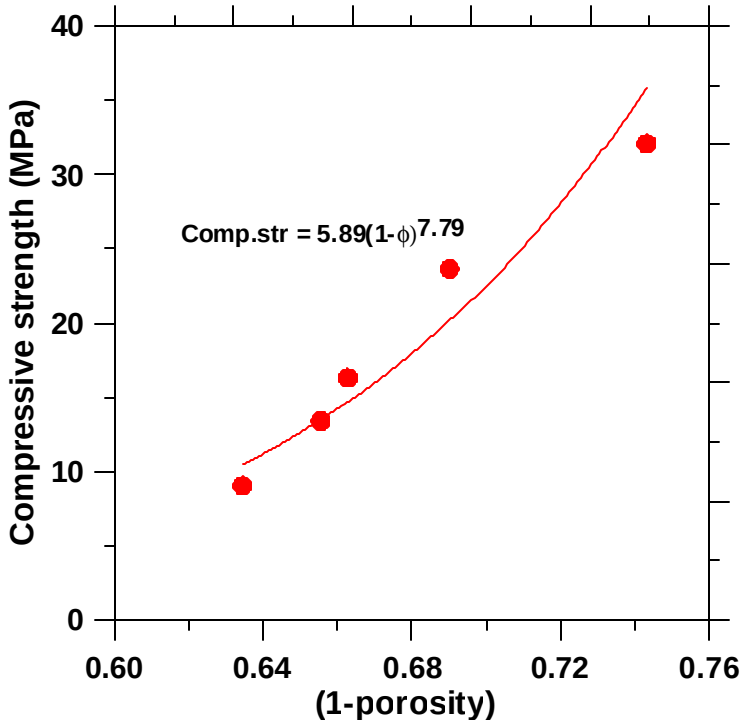

Figure 5.6 Variation of compressive strength with (1-porosity) (composites with macronodules)

The relationship between compressive strength and (1-ϕ) conforms to a power law. This is similar to the porosity-compressive strength relationships reported for concretes and mortar [Neville].

5.5 Dynamic Modulus of Elasticity

The dynamic modulus of elasticity of the composites was determined as per ASTM 1259-01.

The dynamic modulus of elasticity is a function of frequency, and in composite materials, it depends on constituent properties and morphology of the individual phases [Wang and Torng 2001]. The variation of normalized dynamic modulus ($E_{composite}$ / E_{mortar}) with fiber volume for composites containing macro nodules for two ages of curing and moisture condition is shown in Figure 5.7. This figure depicts a gradual reduction in dynamic modulus with increase in fiber content. Moisture condition "wet" implies that the testing was done immediately after removing the specimen from 98% RH and "dry" indicates that the testing was done after conditioning the specimens at 105^{o}C for 24 hours after the desired moist curing duration and then allowing it to return to ambient conditions.

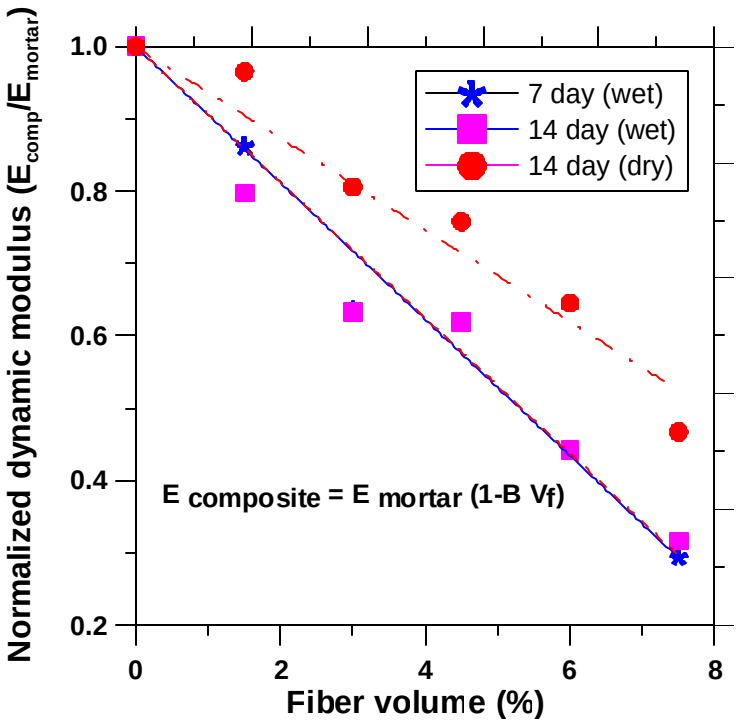

Figure 5.7 Influence of fiber volume on dynamic modulus of elasticity (composites with macronodules)

The dynamic elastic modulus of the composite at any fiber volume can be related to that of the mortar as:

$$E_{composite} = E_{mortar} (1-BV_f) \qquad 5.2$$

The constant B is invariant for "wet" composites, irrespective of the curing duration. B for "dry" composites is found to be less than that of the wet composites, indicating that wet composites exhibit higher loss in modulus with increasing fiber volume.

A comparison of reduction in dynamic modulus of all the fibrous systems is shown in Figure 5.8.

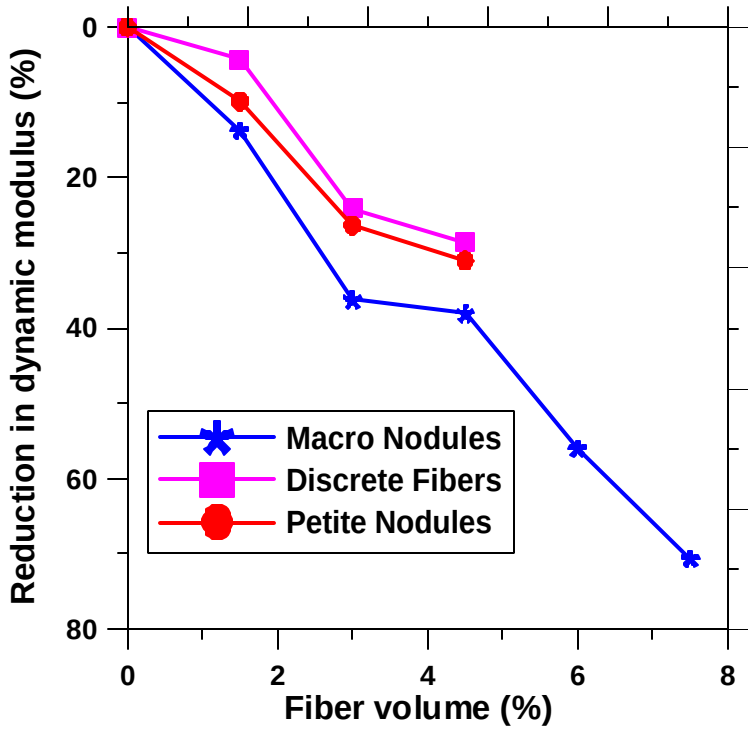

Figure 5.8 Reduction in dynamic modulus of elasticity as a function of fiber volume

The reduction in modulus is highest for composites reinforced with macronodules, followed by those with petite nodules and then by discrete fibers. An increase in composite porosity with the addition of fibers can be attributed to this behavior – higher loss in modulus exhibited by the system with higher porosity.

5.6 Summary

This chapter discussed the physical and mechanical properties of cellulose fiber reinforced composites. The influence of volume of the three different fiber types on porosity of composite was studied. The composites reinforced with macronodules exhibited the highest porosity. The flexural strength of the composites in the wet condition was found to be lower than those in the dry condition. This could be attributed to an increased fiber-to-matrix bond in the dry condition. Increase in fiber volume resulted in reduction in flexural strength for all the types of fibers used. For a given fiber volume, composites with discrete fibers exhibited the highest flexural strength. The compressive strength of macronodule fibers was also found to decrease with increase in fiber volume. An increase in fiber volume also results in a reduction in dynamic modulus of elasticity for all types of fibers investigated.

CHAPTER 6: ACOUSTIC PERFORMANCE AND DAMPING BEHAVIOR OF CELLULOSE-CEMENT COMPOSITES

6.1 General

This chapter discusses the influence of the volume and morphology of cellulose fibers on the sound absorption and vibration damping characteristics of cellulose-cement composites. Specifically, this chapter compares the acoustic effectiveness and damping features of morphologically altered cellulose fiber-cement composites. As described earlier, three types of morphologically altered cellulose fibers were used in this study, viz. macronodules, discrete fibers and petite nodules. Section 4.2.3 has elaborated on the various aspects of these fibers.

6.2 Acoustic Absorption of Cellulose Cement Composites

Cylindrical specimens (95 mm diameter and 75 mm long, cut from 100 mm long specimens) were tested in an air dry state to obtain the absorption spectra (plot of absorption coefficients at different frequencies) for composites with varying volumes of different types of cellulose fibers. This section deals with the influence of fiber volume and morphology, as well as the porosity of the composite on the acoustic absorption characteristics.

6.2.1 Influence of Fiber Volume and Morphology

The acoustic absorption spectra for composites with macro nodules as inclusions are given in Figure 6.1. For the 75 mm long specimens, the absorption peak occurs at a frequency of approximately 500 Hz. It can be seen that an increase in fiber content increases the maximum absorption coefficient. For a sample with no fiber, maximum α is approximately 0.05 and it steadily increases to approximately 0.40 for the composite with 7.5% volume of macro nodules.

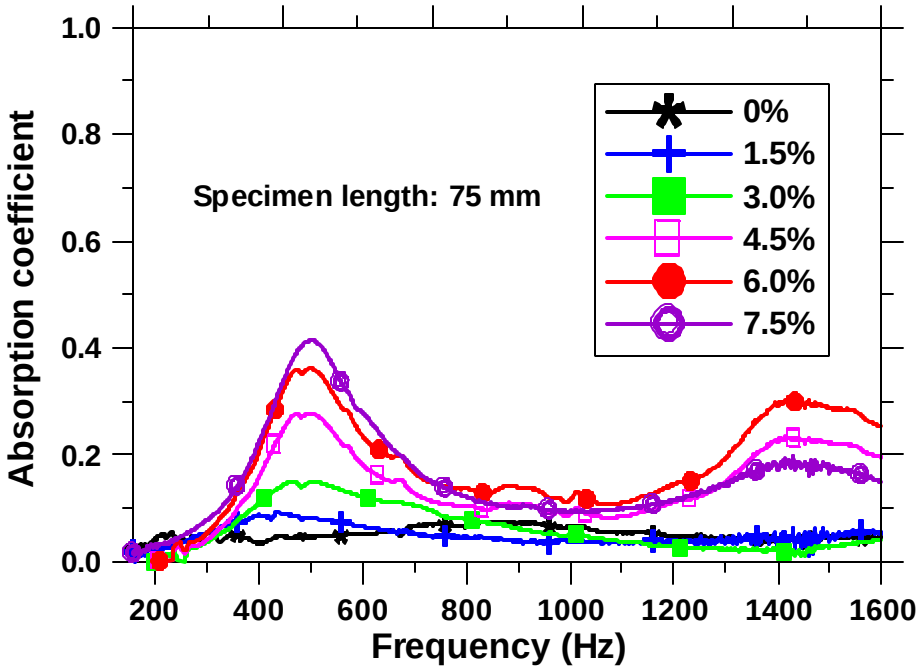

Figure 6.1 Acoustic absorption spectra of composites with macronodules

The macro nodules appear to provide porous channels inside the specimen where the incident sound energy can enter and attenuate. With an increase in fiber volume, it is expected that there is an increase in the number of connected porous channels, leading to an increase in sound absorption. Discrete fibers and petite nodules are less effective in

acoustic absorption, showing only about 50% of the improvement shown by the composites with macro nodules, as is evident from Figure 6.2. This observation justifies the premise that fiber morphology has a significant influence on the acoustic absorption behavior of the composite.

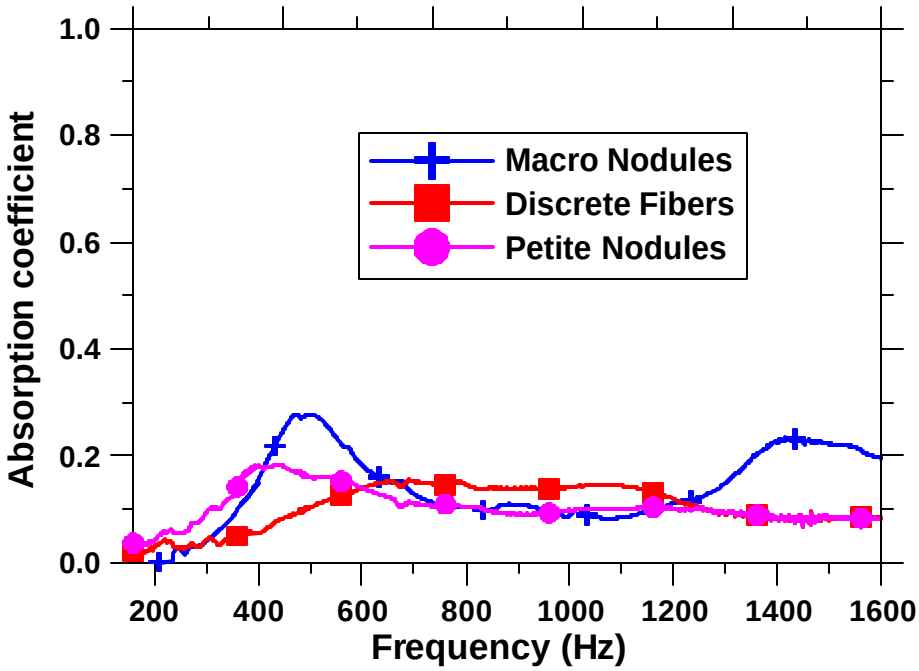

Figure 6.2 Comparison of absorption spectra at 4.5% for the three morphologies

6.2.2 Influence of Porosity of the Composite

Acoustic absorption is closely related to porosity [Voronina 1997, Wang and Torng 2001, Marolf et al. 2003]. Though it is understood that the porosity accessible to the sound waves is provided by the fiber clumps, it can be safely assumed that the total composite porosity as a function of fiber volume is some indicator of accessible porosity. The variation of maximum acoustic absorption coefficient in relation to the normalized porosity of the composites is shown in Figure 6.3, which indicates an increase in

maximum absorption coefficient with porosity. It can also be noted that all the three fiber types demonstrate similar response.

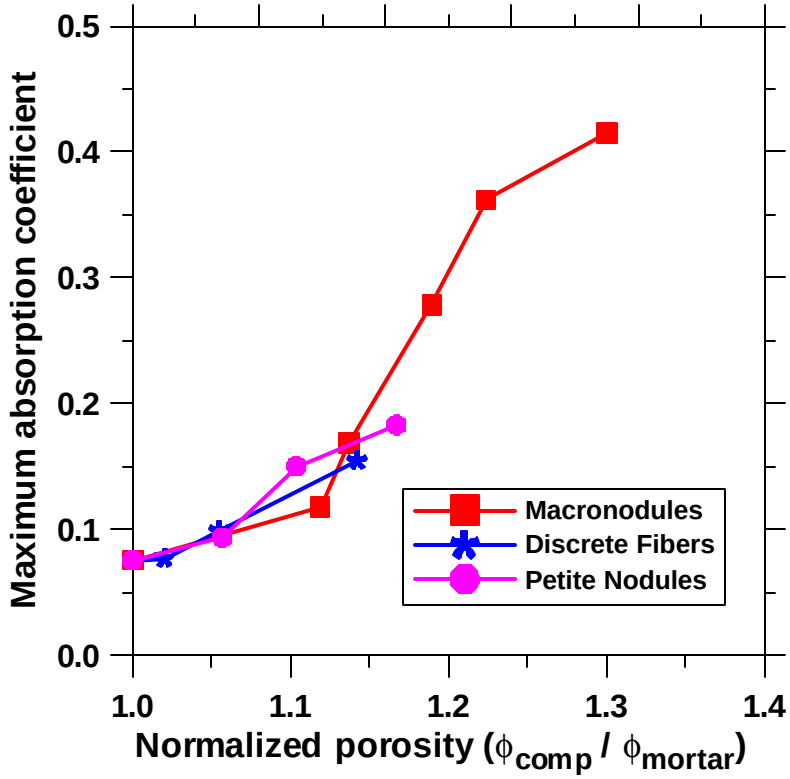

Figure 6.3 Variation of maximum absorption coefficient with normalized porosity

6.3 Elastic Damping in Cellulose-Cement Composites

Damping defines the energy dissipation properties of a material. Viscoelastic materials can be used for damping mechanical vibrations and dissipating sound waves [Chen and Lakes 1993, Lakes 2001]. Damping in concrete is believed to be associated with the presence of water and air voids, microcracks, and acoustical impedance mismatch at the boundaries of different component phases. Damping is sensitive not only to the morphology of individual phases in a multiphase system but also to their spatial relations and individual displacements.

6.3.1 Influence of Fiber Volume and Morphology on Specific Damping Capacity

For specimens with macro nodule inclusions, Figure 6.4 shows the relationship between fiber content and specific damping capacity for two different ages of curing and three different moisture conditions (wet, dry, and rewetted).

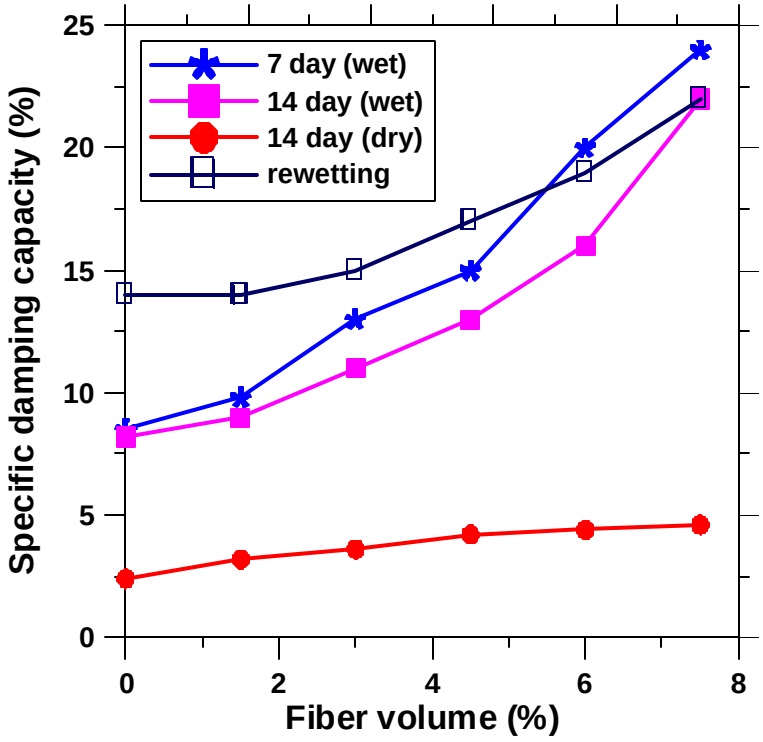

Figure 6.4 Relationship between fiber volume and specific damping capacity for composites with macronodule inclusions

There is a marked increase in damping capacity with an increase in fiber content, especially for wet specimens. This may be attributed to the fact that an increase in volume of macro nodules increases the stiffness mismatch, resulting in higher energy dissipation in the material than it would have for a sample without fibers. This is also consistent with observations from a study on damping mechanisms in hardened pastes, mortar and concrete which indicated that the damping capacity is related to the

percentage of water-filled pores in the system [Chowdhury 1999], with increased moisture leading to a higher degree of damping. Higher volumes of macro nodules effectively increase the amount of water filled pores in the system, thereby resulting in high damping capacity values. For the same curing conditions, it can be observed that the damping capacity decreases with age, probably due to reduction in porosity and pore water content as a result of cement hydration. The reduction, though, is not very large in this case.

The specific damping capacity was found to be dependent on the fiber morphology also, as seen from Figure 6.5, which shows its variation with fiber content at the age of 7 days, in the wet condition.

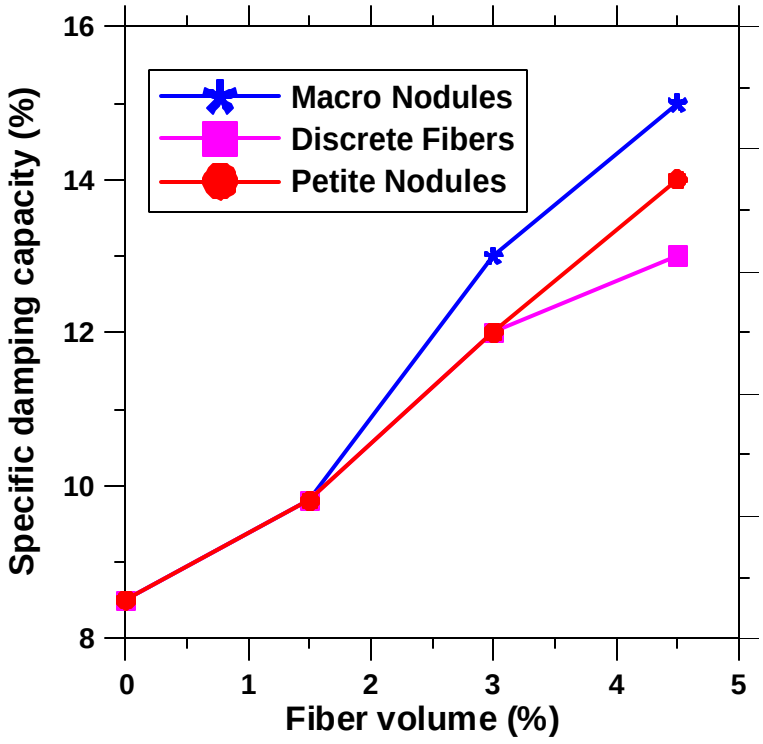

Figure 6.5 Comparison of specific damping capacities of composites with different fiber types (7 day wet condition)

For low fiber volumes, there is no appreciable difference in damping capacity between the three kinds of fibers investigated. Discrete fibers and petite nodules do not seem to be very different as far as damping capacities of their composites are concerned, whereas composites with macro nodules show higher damping than the others. Macro nodules were found to be effective in increasing the damping capacity of the composite, when added at higher fiber volumes.

6.3.2 Influence of Moisture Condition on Specific Damping Capacity

The damping capacity of all specimens showed a large degree of sensitivity to moisture content. The values were reduced to one-fifth of the measured saturated values for composites reinforced with 7.5% macro nodules when the specimens were dried at $105^{o}C$, as is evident from Figure 6.4. The loss of moisture and development of microcracking may have opposing effects on damping [Chowdhury 1999]. The presence of microcracks increases damping whereas the loss of moisture decreases damping. When the specimens are dried at $105^{o}C$, there are chances of formation of microcracks, but it appears that the increase in damping capacity due to microcracking is much smaller than the decrease due to water loss. As a result, dry specimens possess a smaller damping capacity than wet ones. The variation in damping capacity with fiber volume is also smaller for dried specimens. This brings out another interesting observation. Though the acoustical mismatch may seem to be the driving force for increased damping of composites with higher fiber volumes, the influence of presence of large amounts of water in these mixes cannot be neglected. It appears that both, the vibration of water

molecules in the pores and the presence of porous fibers, dissipate significant amount of energy.

On rewetting of the 14 day old specimens, it can be seen from Figure 6.4 that, for composites with macro nodules, the damping capacity increases again. The increase this time is very significant and the value is higher than that observed for 7 day moist cured mixes, especially at low fiber contents. This could be due to the synergestic effects of both microcracking as well as the presence of water molecules. At higher fiber contents, this value approaches the damping capacity observed for 7 day and 14 day wet composites.

6.3.3 Stiffness-Loss Relationships for Cellulose-Cement Composites

The loss tangent (the tangent of the phase angle between stress and strain in sinusoidal loading) is another useful measure of material damping characteristics. It is also defined as the ratio of the imaginary and the real parts of the complex dynamic modulus E^* ($E^*=E'+iE''$; Storage modulus $E'=E\cos\delta$, and Loss modulus $E''=E\sin\delta$, so that loss tangent $\tan\delta = E''/E'$). Using the measured specific damping capacity χ, the viscoelastic loss tangent can be obtained as $\tan d = \frac{y}{2p}$, which is proportional to the energy loss per cycle within the framework of linear viscoelasticity [Lakes et al. 2002]. Most materials used in structural applications have very low loss tangents ($\approx$0.01). In general, materials with high loss tangents tend to be more compliant, therefore these are generally not of structural interest. A stiff material with low to moderate loss tangents would be of use in structural damping of noise and vibration.

Stiffness-loss plot of $|E^*|$ or E' vs tan δ (it is obvious that for composites with low damping, $|E^*|$ and E' values are very nearly the same) for composites with fiber volume ranging from 0 to 7.5% of macro nodules is shown in Figure 6.6.

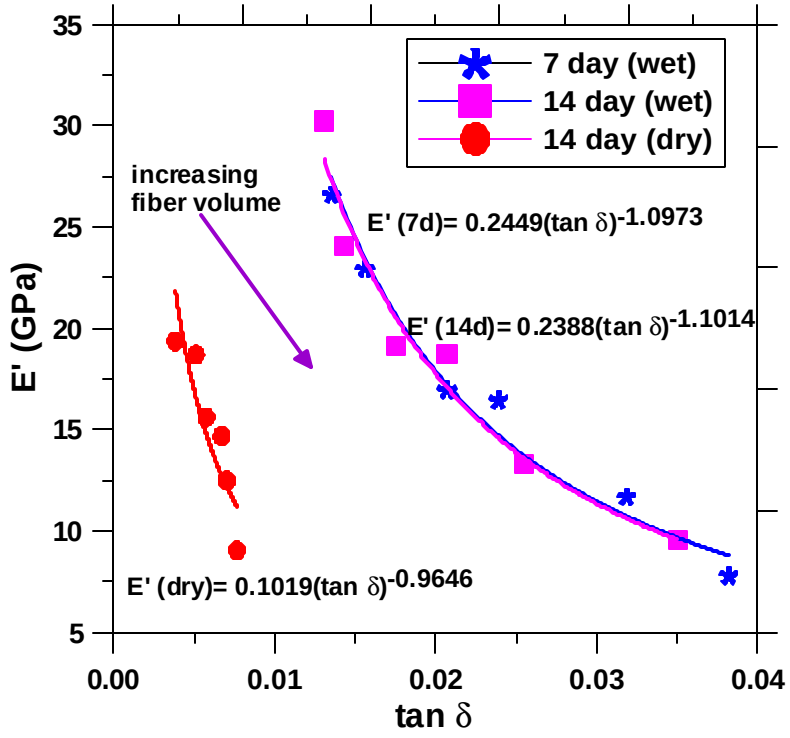

Figure 6.6 Stiffness-Loss plot of composites with macronodules

Increasing fiber volume results in reduced stiffness and increased loss tangent for the moist cured mixes. But when these parameters are plotted for the dried composites, it is seen that the increase in loss is not commensurate with the reduction in stiffness, the reason for which has been explained in the previous section. Stiffness-loss relationship seems to be dependent on the moisture condition of the specimens only and not necessarily on the curing duration as can be infered from the similarity in curves for both 7 and 14 day cured specimens. The trend shows that the storage modulus is inversely related to the loss tangent (E'=0.2499 tan $\delta^{-1.10}$ and 0.2388 tan $\delta^{-1.10}$ for 7 and 14

day moist cured specimens tested wet, and $E'=0.1019 \tan \delta^{-0.96}$ for oven dried specimens respectively). The constant that relates loss tangent and storage modulus can be thought of as an indicator of the moisture condition of the specimens.

6.3.4 Influence of Moisture Condition on the Loss Tangent

A plot of fiber volume of macro nodules versus loss tangent for saturated as well as dry composites is given in Figure 6.7.

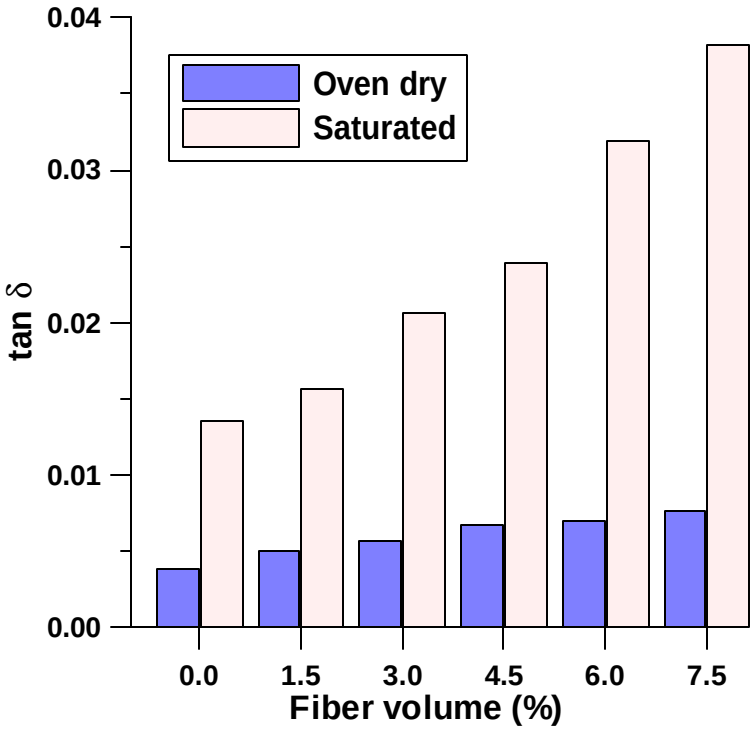

Figure 6.7 Influence of moisture condition on loss tangent for different fiber volumes (composites with macronodules)

It can be seen that for oven-dried composites, the increase in fiber content does not lead to a substantial increase in loss tangent as compared to saturated composites. The ratio of loss tangents in the saturated to the oven dry condition increases with

increase in fiber volume. This reiterates the significance of both enhanced porosity and moisture content in increasing damping.

6.3.5 Rule of Mixtures Approach to Stiffness-Loss Relationships

Since Voigt's (series) and Reuss' (parallel) rule of mixtures represent upper and lower bound for elastic constants of composites, the experimental values of dynamic elastic modulus and loss tangent are compared with those predicted by Voigt's and Reuss' rules. The dynamic Young's modulii E can be converted into complex modulii by the relation:

$$E^* = E\, e^{id} \qquad 6.1$$

Considering the elastic modulus of the mortar phase as E_m and that of fiber phase as E_f and their representative volume fractions as V_m and V_f, the composite elastic modulus using Voigt's rule can be calculated as:

$$E_c^* = E_m^*\, V_m + E_f^*\, V_f \qquad 6.2$$

and by Reuss' rule:

$$\frac{1}{E_c^*} = \frac{V_m}{E_m^*} + \frac{V_f}{E_f^*} \qquad 6.3$$

The loss tangents for Voigt and Reuss composites can be expressed by separating the real and imaginary parts of E_c^* [Chen and Lakes 1993].

$$\tan d_c^{\,Voigt} = \frac{V_m \tan d_m + V_f \dfrac{E_f'}{E_m'} \tan d_f}{V_m + \dfrac{E_f'}{E_m'} V_f} \qquad 6.4$$

$$\tan d_c^{\,Reuss} = \frac{(\tan d_m + \tan d_f)\left[V_m + V_f \frac{E_m'}{E_f'}\right] - (1 - \tan d_m \tan d_f)\left[V_m \tan d_f + V_f \tan d_m \frac{E_m'}{E_f'}\right]}{(1 - \tan d_m \tan d_f)\left[V_m + V_f \frac{E_m'}{E_f'}\right] + (\tan d_m + \tan d_f)\left[V_m \tan d_f + V_f \tan d_m \frac{E_m'}{E_f'}\right]}$$

6.5

$\tan \delta_m$ is the loss tangent for the matrix, $\tan \delta_f$ is the loss tangent for the fiber inclusion, which is assumed as 0.9 (for a soft, lossy phase), $E_m' = E_m \cos \delta_m$ and $E_f' = E_f \cos \delta_f$. E_f, based on tensile test of cellulose fibers was obtained as 2 GPa [Kompella and Lambros 2002].

The stiffness-loss relationships for the composites with macro nodules based on elastic moduli and loss tangents calculated using both Voigt's and Reuss' rules for 7-day moist cured composites are compared to the actual test data in Figure 6.8. A small volume of fiber is seen to result in a large increase in loss for the Reuss structure whereas it results in a large reduction in stiffness with little loss for the Voigt structure. The composite with soft cellulose fiber inclusions is found to behave very similarly to the Voigt composite in that a small volume of soft material has a minimal effect on loss tangent, but reduces the stiffness to a large extent. The behavior of 14-day moist cured composites is also found to be similar.

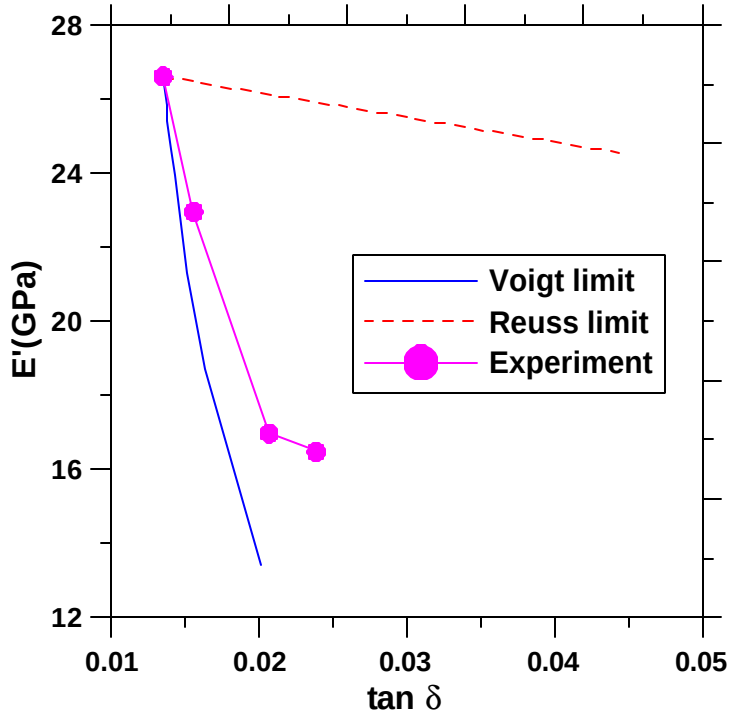

Figure 6.8 Comparison of Stiffness-Loss relationships based on Rule of Mixtures with actual test data (composites with macronodules)

6.3.6 Loss Modulus and its Prediction

The product of E' and tan δ is the loss modulus E", which is frequently considered as an index of damping characteristics of materials[Fu and Chung 1996, Lakes et al. 2002]. The loss modulus combines the storage modulus and damping capacity, thereby best reflecting the energy dissipation capability of the material.

For a given material composition, E' and tan δ of a composite depends on the fiber volume as well as the moisture condition of the specimen. Under a constant moisture condition, say, saturated or oven dry state, the storage modulus and loss tangent can be represented by just one parameter - the fiber volume. The plots of fiber volume against E' and tan δ are shown in Figures 6.9 and 6.10 respectively for composites with macro nodules wet cured for 7 days, 14 days and oven dried.

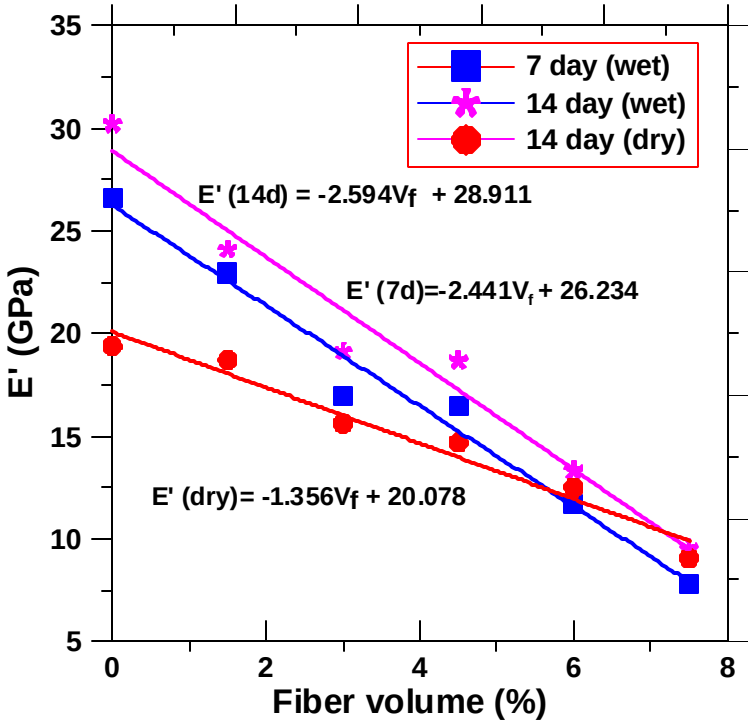

Figure 6.9 Variation of storage modulus with fiber volume for composites with macronodules

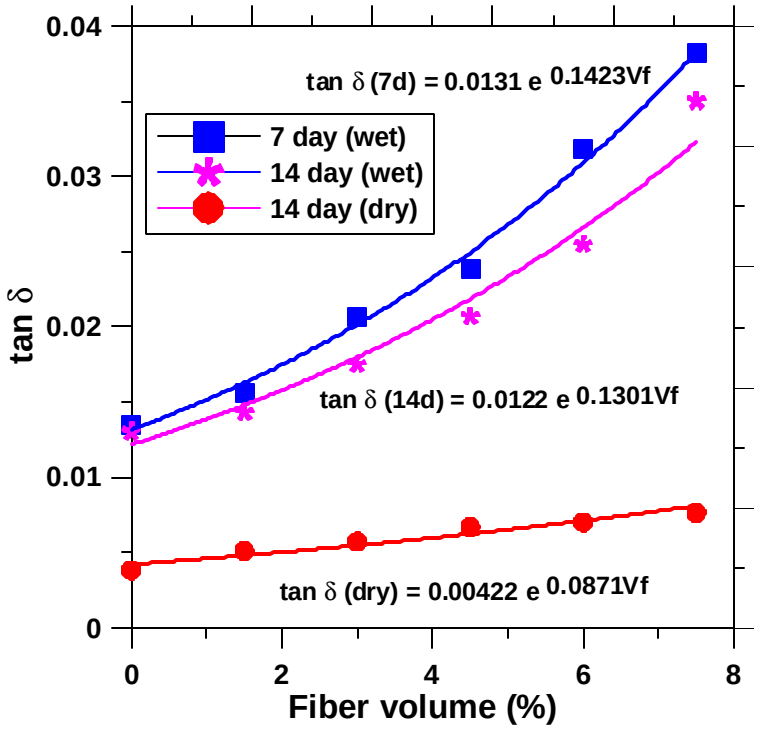

Figure 6.10 Variation of loss tangent with fiber volume for composites with macronodules

A fairly linear relationship can be observed between the fiber volume and storage modulus whereas the relationship between fiber volume and loss tangent can be more adequately expressed in terms of an exponential function. From the relationships between fiber volume and dynamic parameters, relationships between V_f and E9 tan δ can be easily determined. They are given as follows:

$$E' \tan\delta \text{ (7-day)} = (0.3437 - 0.032\ V_f)\ e^{0.1423\ Vf} \qquad 6.6$$

$$E' \tan\delta \text{ (14-day)} = (0.3527 - 0.032\ V_f)\ e^{0.1301\ Vf} \qquad 6.7$$

$$E' \tan\delta \text{ (oven dry)} = (0.085 - 0.0057\ V_f)\ e^{0.0811\ Vf} \qquad 6.8$$

Equations 6.6 and 6.7 show that for saturated condition, the coefficients are similar, however they change for the oven-dried condition. These equations help to confirm the observation that the moisture condition of the specimens has a significant influence on the stiffness-loss relationship.

In Figure 6.11, the loss modulus determined experimentally as well as from the equations presented above is plotted against volume of macro nodules. The exponential predictive equations match the experimental data especially at higher fiber volumes. The deviation from curvilinear behavior in the lower ranges of fiber volume may be attributed to the fact that the loss modulus has a certain optimal value, after which a decrease in storage modulus more than compensates for an increase in loss tangent, effectively resulting in a reduced loss modulus. For the composites that are oven dried, E' tan δ remains more or less constant with fiber volume, i.e., a decrease in storage modulus as a result of increase in fiber volume is compensated by increase in tan δ. For the other cases, as can be seen from the figure, there is an optimum fiber volume at which E' tan δ is maximum, beyond which a decreasing storage modulus dictates the value of loss

modulus. For conflicting requirements of stiffness and damping, E'tanδ may provide a suitable parameter that can aid in the selection of materials for noise isolation and vibration damping purposes.

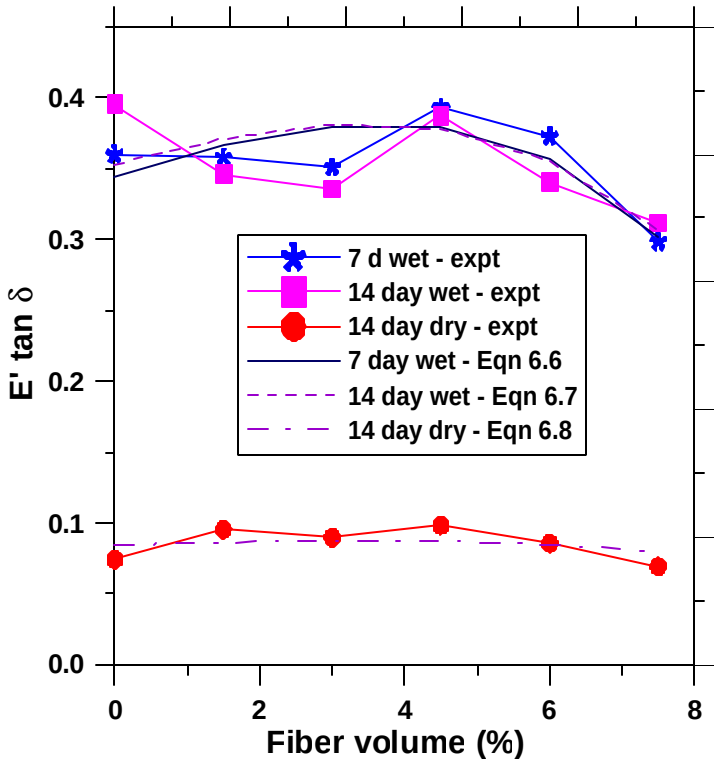

Figure 6.11 Variation of loss modulus with fiber volume for different moisture conditions (composites with macronodules)

The plot of E tan δ vs. fiber volume for composites with macro nodules cured for 7 days is also shown so as to compare the rule of mixtures with the experimental values and those obtained from Equation 6.6 (Figure 6.12). It can be observed that E tan δ values obtained from experiments and the values predicted by Voigt's rule follow the similar trend. The same could not be said of Reuss composites. This again corroborates the fact that the composite containing soft high loss inclusions in a stiff matrix, as is the case with cellulose fibers in cementitious matrix, behaves similarly to a

Voigt composite. In this case also, the loss modulus predicted by Equation 10 matches well with the experimental values.

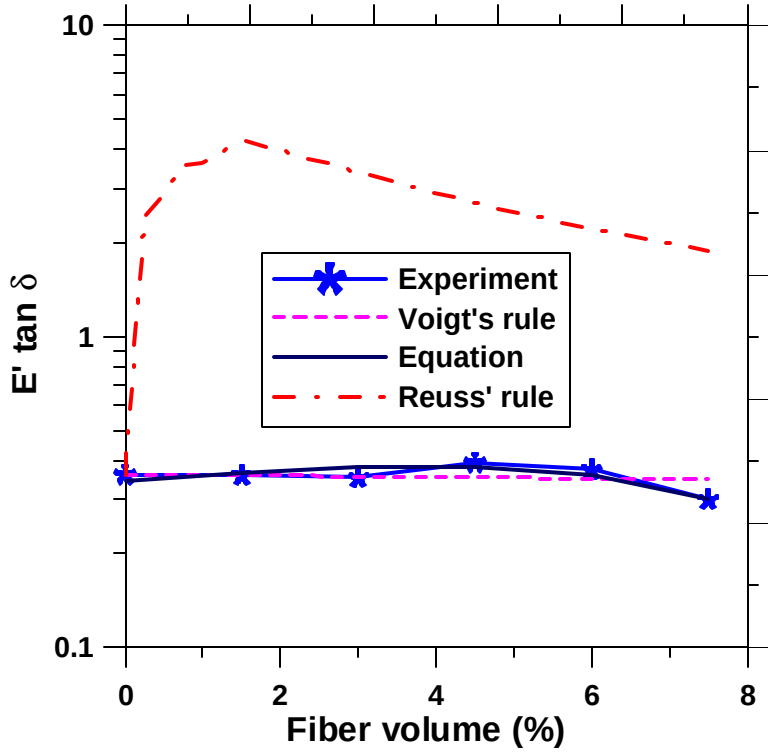

Figure 6.12 Comparison of loss modulus obtained from actual test data, rules of mixtures and predictive equation (composites with macronodules)

CHAPTER 7: DURABILITY OF CELLULOSE-CEMENT COMPOSITES

7.1 General

A significant concern to the use of cellulose fiber reinforced cement composites is the long-term durability of fibers in the cementitious matrix, especially under severe exposure conditions. The lignin in the natural fibers is attacked by the highly alkaline pore water, weakening the link between the individual fiber cells that constitute the cellulose fiber [Marikunte and Soroushian 1994].

This chapter presents results on the durability studies carried out on cellulose-cement composites. Composites made with only macronodules were considered for this study since it was found to be most effective in acoustic absorption and vibration damping. The fiber volumes used were 2.5%, 5.0%, and 7.5%, along with control specimens. The test methods adopted to evaluate durability were (i) cyclic freezing and thawing, and (ii) hot water soaking. For the freezing and thawing test, electrical impedance spectroscopy was used to monitor the resistance of the specimens. For both the tests, resonant frequency was monitored at fixed intervals, and the flexural strength evaluated at the end of the test period.

7.2 Resistance to Freezing and Thawing

The cellulose-cement composites were subjected to cyclic freezing and thawing in a controlled temperature chamber where the temperature cycled from -17 ^{o}C to 23 ^{o}C,

with one freezing and thawing cycle every day. The change in electrical resistance was monitored on cylindrical specimens 100 mm in diameter and 100 mm long, while the changes in specific damping capacity were monitored on 250 mm x 75 mm x 25 mm prismatic members. The flexural strength test specimens were also beams of size 250 mm x 75 mm x 25 mm. The specimens were subjected to freezing and thawing after moist curing them for 14 days.

7.2.1 Electrical Measurements to Monitor Freezing and Thawing Damage

Electrical Impedance Spectroscopy (EIS) was used to monitor the electrical resistance of cellulose-cement composites undergoing freezing and thawing. Figure 7.1 depicts the number of freeze-thaw cycles (after 14 days of moist curing) plotted against the bulk resistance for different fiber volumes. It could be observed from this plot that the bulk resistance increases initially, until around 20 cycles of freezing and thawing, and then starts dropping down. The resistance ideally should be decreasing consistently, if damage is developed in the system due to freezing and thawing. The two possible reasons for this behavior are (i) there is continuing hydration even after 14 days, rendering the pore structure dense, thereby increasing the bulk resistance of the sample, and (ii) when a specimen is frozen, pore water tends to flow towards the freezing sites, and when it is thawed, there is a period of time before the pore water drains back into the paste microstructure [Corr et al. 2002]. During this time, it is postulated that hydration products grow in the open spaces. This renders the microstructure denser, increasing the apparent resistance of the sample. Hence, even when there is slight damage due to freezing and thawing, it is the densification of the microstructure that is dominant at this

stage. After around 20 cycles of freezing and thawing, the resistance consistently decreases, indicating that there is damage induced in the specimen due to freezing and thawing.

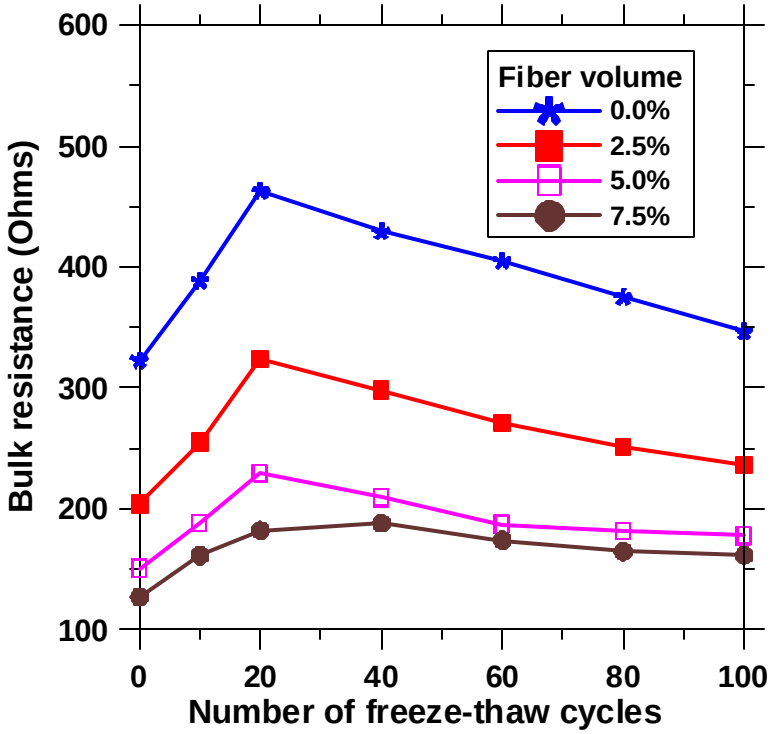

Figure 7.1 Variation in bulk resistance as a function of number of freeze-thaw cycles

The variation in bulk resistance with fiber volume is shown in Figure 7.2, for specimens moist cured for 100 days as well as those subjected to freezing and thawing for 100 cycles. It could be seen from this figure that the bulk resistance decreases with increase in fiber volume for specimens subjected to both the exposure regimes. The reduction in resistance is relatively higher for plain specimens as compared to fiber reinforced specimens, and with increase in fiber volume, the difference in resistance between the specimens moist cured for 100 days, and those subjected to 100 freezing and thawing cycles decreases. This shows that the degree of damage induced by freezing and thawing is higher for specimens without fibers, and the resistance increases with increase

in fiber volume. This is because of the fact that macronodule fibers are porous by themselves, and allow for movement of water when freezing happens in the pores, thereby reducing the stresses generated.

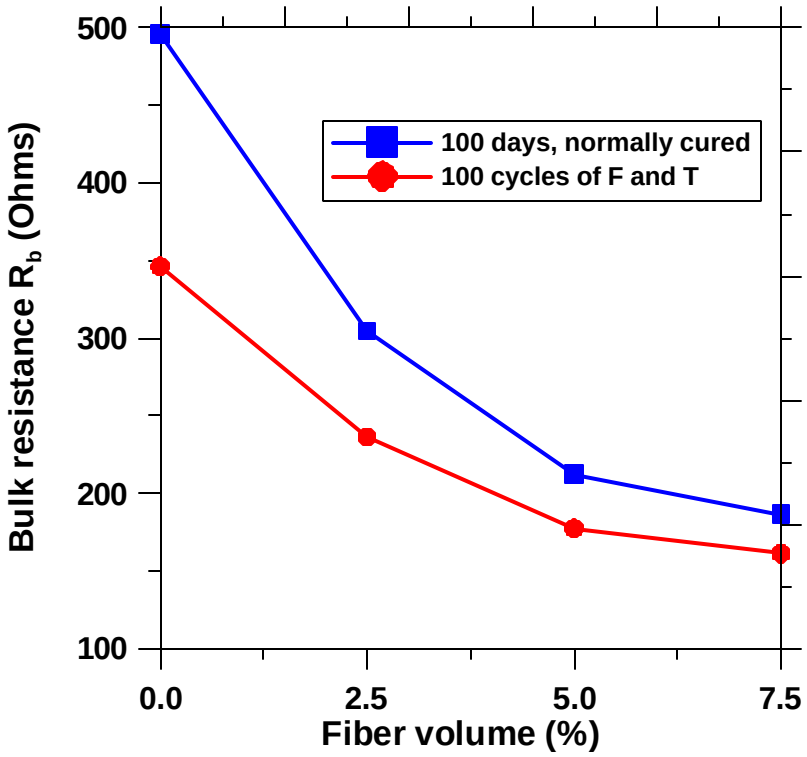

Figure 7.2 Comparison between bulk resistances of normally cured specimens and those subjected to 100 cycles of freezing and thawing

7.2.2 Specific Damping Capacity as a Measure of Damage

The specific damping capacity (ψ) determined using dynamic excitation of vibration was used to obtain an indication of the damage developed in the composites after repeated cycles of freezing and thawing. The variation in specific damping capacity as a function of the number of freezing and thawing cycles is shown in Figure 7.3

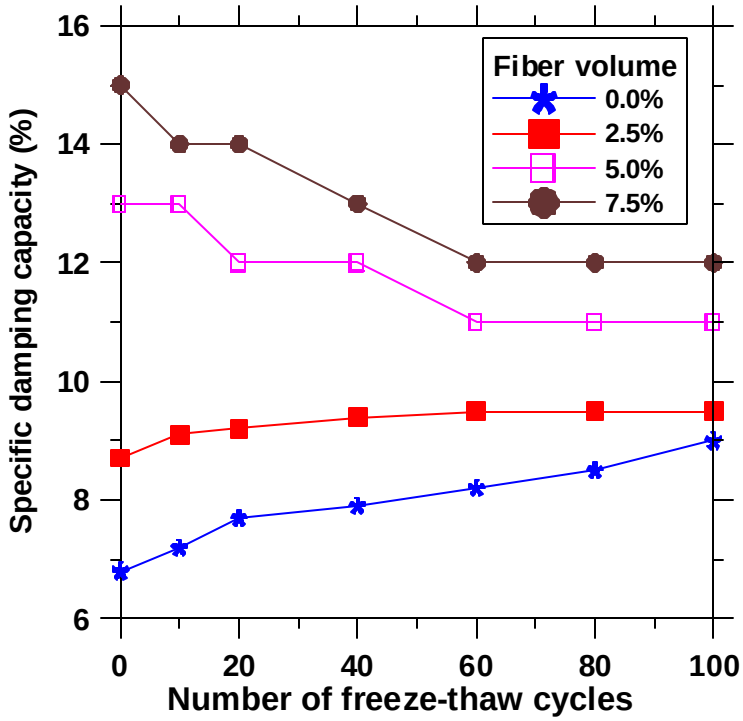

Figure 7.3 Variation in specific damping capacity as a function of number of freeze-thaw cycles

Specific damping capacity depends on the presence of water and air voids, and cracks in concrete. It could be observed from Figure 15.3 that for mixtures with no fibers, the specific damping capacity increases with the number of freeze-thaw cycles. This points to the fact that there is microcracking and associated damage occurring in the specimen with increasing number of freeze-thaw cycles. For a mixture with 2.5% of fibers by volume, the specific damping capacity essentially plateaus off after about 40 cycles, indicating that the porous fiber nodules are capable of allowing water movement due to freezing and thawing, resulting in reduced stresses, and consequently reduced damage. Interestingly, for higher fiber volumes, it is seen that the specific damping capacity reduces with number of freeze-thaw cycles, before it plateaus off. This could probably be because of the increased deposition of hydration products in the void structure of the composite at lower number of freezing and thawing cycles, and the

efficiency of increased fiber volume to prevent cracking by allowing water movement at higher number of freezing and thawing cycles.

The influence of high volume of fibers on the resistance of the composite to freezing and thawing is shown in Figure 7.4.

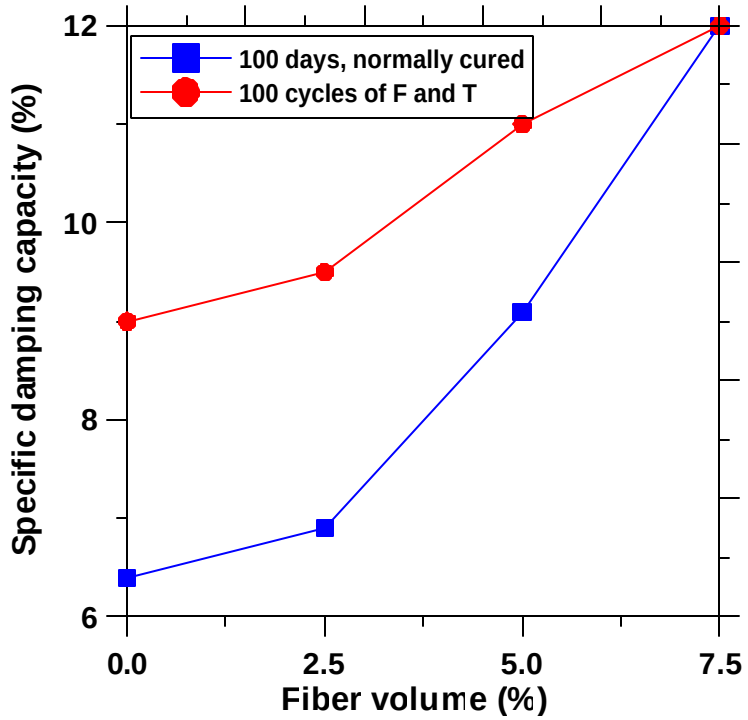

Figure 7.4 Comparison between specific damping capacities of normally cured specimens and those subjected to 100 cycles of freezing and thawing

It could be seen from this figure that the increase in specific damping capacity with fiber volume is drastically higher for composites that are moist cured than for those subjected to freezing and thawing cycles. At a fiber volume of 7.5%, the specific damping capacities for specimens subjected to both exposure regimes are essentially the same. This corroborates the observation made in the previous section that the degree of damage induced by freezing and thawing is higher for specimens without fibers than those with fibers.

7.2.3 Flexural Strength of Composites Subjected to Freezing and Thawing

Figure 7.5 shows the relationship between flexural strength and fiber volume for cellulose-cement composites moist cured for 100 days, and those subjected to 100 cycles of freezing and thawing.

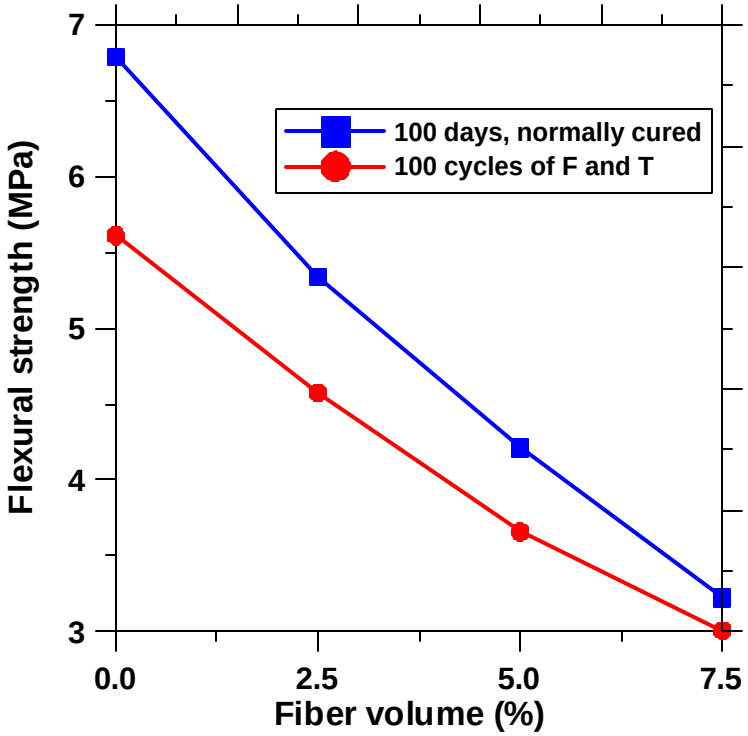

Figure 7.5 Comparison between flexural strengths of normally cured specimens and those subjected to 100 cycles of freezing and thawing

The flexural strength decreases with increase in fiber volume for both the cases, the reasons for which have been explained in Chapter 5. The difference between the flexural strengths is larger for specimens with out fibers, and it reduces with increase in fiber volume. This trend is similar to those observed for electrical resistances as well as specific damping capacity, and proves that increasing the fiber volume results in reducing the damage induced in the composite due to freezing and thawing.

7.3 Resistance to Hot Water Soak

Prismatic specimens 250 mm x 75 mm x 25 mm were subjected to hot water soaking at a temperature of 60±2 ^{o}C for a period of 100 days. Specific damping capacity and flexural strength measurements were carried out to detect deterioration in the specimens.

7.3.1 Specific Damping Capacity Measurements

Figure 7.6 shows the variation in specific damping capacity as a function of the number of freezing and thawing cycles.

With increase in exposure time to hot water, the specific damping capacity increases till about 60 days and then starts to decrease. The increase in specific damping capacity could be attributed to the progressive cracking of the matrix. Beyond that period, cellulose fibers degrade under continued exposure to high temperature conditions, and the petrification of cellulose fibers has the effect of densification of the matrix, resulting in a reduction in damping capacity.

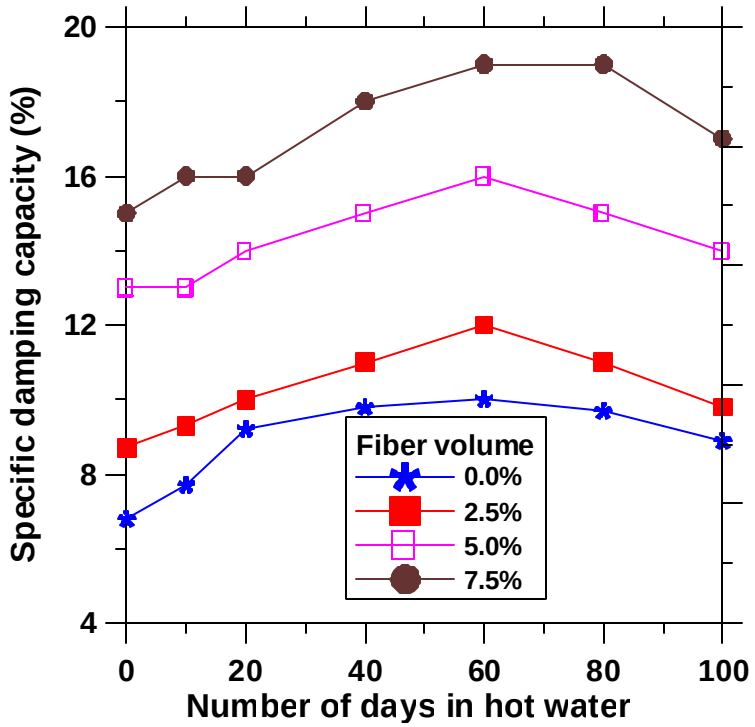

Figure 7.6 Variation in specific damping capacity as a function of number of days in hot water

The variation in specific damping capacity with fiber volume for composite specimens cured normally, as well as those subjected to 100 days of hot water soaking is shown in Figure 7.7. The specific damping capacities of hot water soaked specimens are considerably higher than those cured under normal conditions. The specific damping capacities increase with increase in fiber volume, as expected. It can be noticed from this figure that the difference in damping capacities between specimens cured under normal conditions and those soaked in hot water for 100 days increases with increase in fiber volume. This is an indication that exposure to wet conditions at 60±2 ^{o}C result in fiber deterioration more than matrix damage.

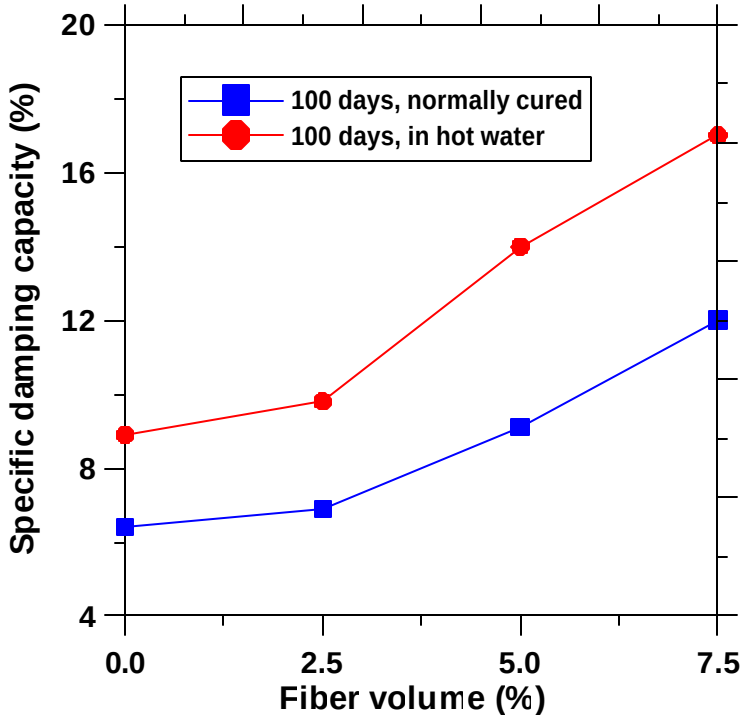

Figure 7.7 Comparison between specific damping capacities of normally cured specimens and those subjected to 100 days of hot water soaking

7.3.2 Flexural Strength of Composites Subjected to Hot-Water Soak

Figure 7.8 depicts the relationship between flexural strength and fiber volume for composites moist cured for 100 days, and those subjected to 100 days of hot water soaking. There is a drop in flexural strength with increase in fiber volume, the reasons for the same have been explained in the previous sections. The flexural strength drop seems to be rather uniform between the specimens subjected to both the exposure conditions, though a relatively larger drop would be expected for specimens with higher volume of fibers, based on the results of specific damping capacity.

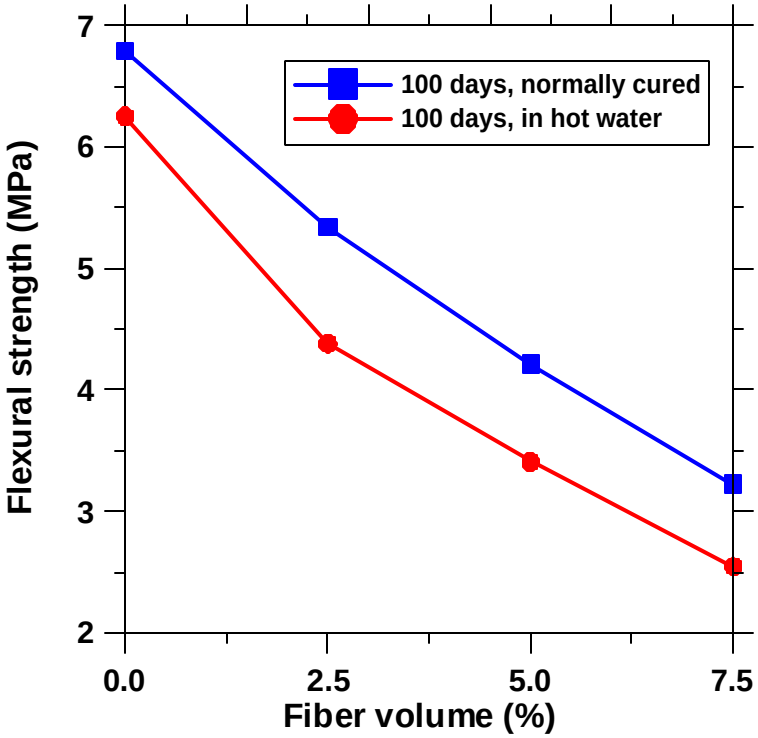

Figure 7.8 Comparison between flexural strengths of normally cured specimens and those subjected to 100 days of hot water soaking

7.4 Comparison between the Two Methods to Evaluate the Durability Characteristics

In the previous sections, two different exposure conditions – freezing and thawing, and hot water soak – that were used to evaluate the durability characteristics of cellulose-cement composites were described. This section aims at comparing the two test methods and identifying the influence of these test methods on the constituents of the composite.

Figure 7.9 shows the variation in specific damping capacity with fiber volume for specimens subjected to all the three exposure conditions – i.e. 100 days of normal curing, 100 cycles of freezing and thawing, or 100 days in hot water. As expected, the specific damping capacities of normally cured specimens are the lowest, followed by those

subjected to freezing and thawing. The specific damping capacities of specimens subjected to hot water soaking were found to be the highest.

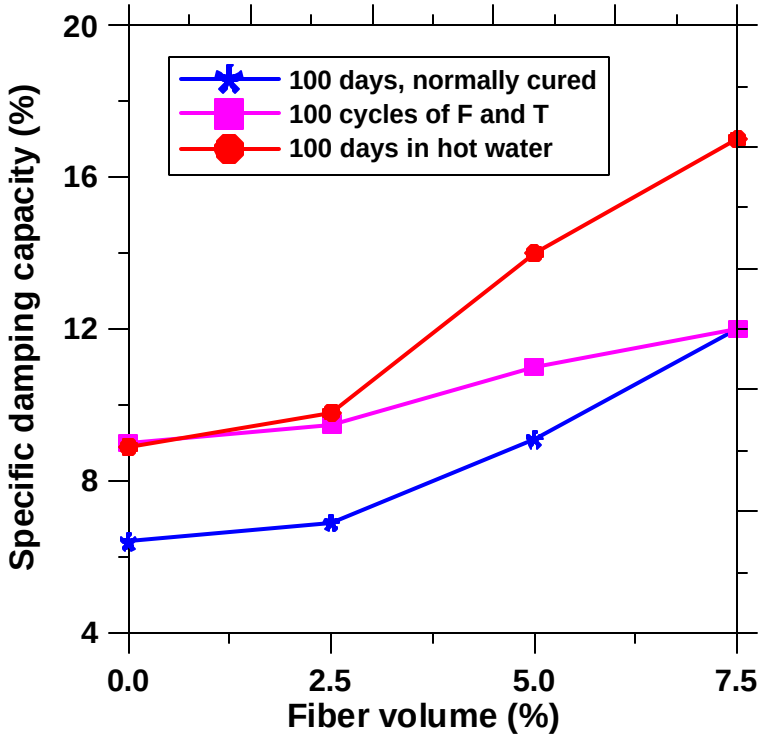

Figure 7.9 Variation of specific damping capacity with fiber volume, for all three exposure conditions

It could be observed from this plot that the relative damage induced due to freezing and thawing is less with increasing fiber volume, as compared to hot water soaking. This points to the fact that the fibers are effective in mitigating freezing and thawing damage, whereas they deteriorate on exposure to wet conditions and high temperature.

Similar plot for the variation in flexural strength with fiber volume is shown in Figure 7.10. The flexural strength for the hot water soaked mixtures without fibers is higher than the same mixture subjected to 100 cycles of freezing and thawing. But, with the introduction of fibers in the mixture, the strength of the hot water soaked specimens

falls below that of the specimens subjected to freezing and thawing. This shows that, under conditions of hot water soaking, it is the damage to the fibers that dictate the performance of the composite.

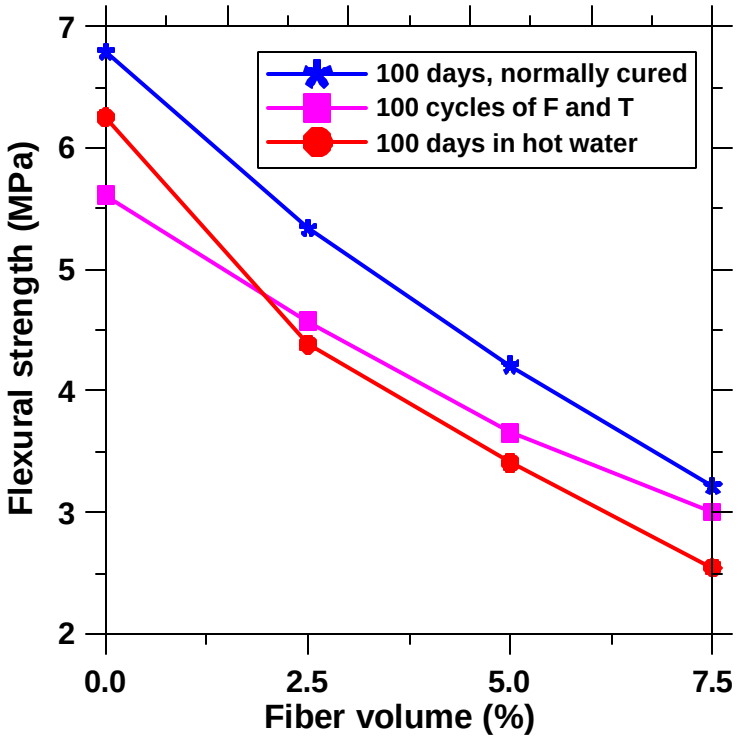

Figure 7.10 Variation of flexural strength with fiber volume, for all three exposure conditions

A comparison of flexural strength loss for specimens subjected to both freezing and thawing, and hot water soak (as compared to the normally cured specimens), is shown in Figure 7.11. Flexural strength loss increases with increasing fiber volume for specimens subjected to hot water soak, whereas it decreases for specimens subjected to freezing and thawing, again proving that an increased fiber volume is beneficial in resisting freezing and thawing damage while it is detrimental in high temperature, wet environment.

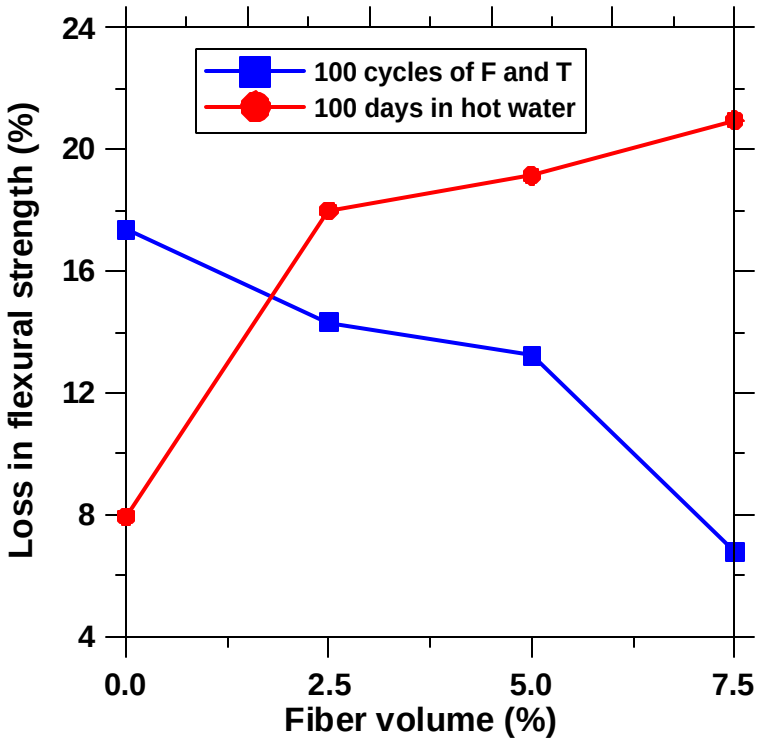

Figure 7.11 Comparison of loss in flexural strength between specimens subjected to freezing and thawing, and hot water soak

7.5 Summary

This chapter has dealt with the issues of durability of cellulose-cement composites. Two test methods were adopted to evaluate the durability - cyclic freezing and thawing, and soaking in hot water. Electrical resistance, specific damping capacity, and flexural strength measurements were used to evaluate the damage. It was observed that the fiber nodules restrict damage due to freezing and thawing. But on subjecting to hot water soaking, it is the fibers that suffer the damage, resulting in reduced performance characteristics of the composite.

CHAPTER 8: SUMMARY AND CONCLUSIONS (PART – A)

8.1 Summary

The basic tenet of this phase of the research was to investigate whether flexible, compliant inclusions incorporated in mortar / concrete could aid in absorbing sound and dissipating energy. Towards this end, several lightweight, porous, "aggregate-like" materials were evaluated. It was found that morphologically altered cellulose fibers were most effective in absorbing sound and damping the vibrations. Several mixtures incorporating varying volumes of three different types of morphologically altered cellulose fibers were prepared and tested for physical properties (density, porosity), mechanical properties (compressive and flexural strengths, modulus of elasticity), acoustic absorption, and vibration damping capacity. The mechanical and acoustic behavior of cellulose-cement composites with varying volumes and types of fibers has been explained in detail. Elastic damping in these composites were modeled using composite rule of mixtures. From detailed studies, it was observed that the macronodule fibers were the most efficient in absorbing sound, and dissipating vibrational energy. The durability of composites with varying volumes of these fibers as inclusions was studied in detail. The composites were subjected to cyclic freezing and thawing, and accelerated aging by hot water soaking to understand the response of the constituents of the composite to severe exposure conditions.

8.2 Conclusions

The conclusions from this phase of the research study are listed in this section. The findings pertaining to each sub-section are listed separately.

8.2.1 Physical and Mechanical Properties

1. Morphologically altered cellulose fibers aid in increasing the porosity of the composite. The porosity increases with increasing volume of fibers. This aspect is most evident in composites with macronodule fibers as inclusions, since the fibers themselves are porous in this case.
2. Flexural strength was observed to reduce with increase in fiber volume. This could be attributed to the following reasons: (i) the macronodule fibers are soft inclusions in the matrix, which reduces the load carrying capacity of the composite, (ii) the cellulose fibers have a reduced strength in wet condition, (iii) fibers entrap water filled spaces, and (iv) fiber-to-matrix bond strength is reduced.
3. The dynamic modulus of elasticity also was found to decrease with increase in fiber volume; as expected, this could be attributed to the increased porosity with increasing fiber volume.

8.2.2 Acoustic Absorption and Elastic Damping

4. Cellulose-cement composites have the potential for absorbing sound. The absorption coefficient increases with an increase in fiber volume, possibly

due to the generation of increased number of interconnected porous channels in the matrix.

5. Sound absorption is related to fiber morphology. Macro nodules (large fiber clumps) are found to be more effective than discrete (small, well distributed) fibers.
6. Specific damping capacity increases with increase in fiber content, presumably due to an increased impedance mismatch between the cementitious matrix and the cellulose phases.
7. An increase in moisture contents of the specimen increases the damping capacity. Drying at 105^{o}C drastically reduces the damping capacity of all specimens. Though the microcracking caused by drying increases the damping, the loss of water offsets this effect to a much higher degree, resulting in reduced damping capacity.
8. The storage modulus and loss modulus for cellulose-cement composites are inversely proportional, and follow an exponential relationship. For dried composites, this relationship tends to be linear.
9. Cellulose composites containing a stiff, low loss phase (cement matrix), and a compliant, high loss phase (cellulose fibers) behave similarly to a Voigt (series) composite, which shows a large reduction in stiffness and a low loss tangent.
10. A series of equations have been developed to describe the loss modulus of cellulose-cement composites as a function of fiber volume. These equations are found to match well with experimental values as well as

those idealized to Voigt composites. For water-saturated composites, there appears to be an optimal fiber volume at which E' tan δ is maximized, beyond which a decreasing storage modulus dictates the value of the loss modulus. E' tan δ practically remains constant for oven-dried composites irrespective of fiber volume

8.2.3 Durability of Cellulose-Cement Composites

11. Electrical resistance and specific damping capacity measurements could be used to detect the damage in cellulose-cement composites due to freezing and thawing. However, at early ages, there is an anomaly in the resistance results, which could be explained by the fact that hydration continues, and dominates the damage due to freezing and thawing.
12. Specific damping capacity and flexural strength measurements indicate that, with increase in fiber volume, the composites subjected to freezing and thawing undergo relatively lesser damage as compared to hot water soaked composites. This indicates that the porous fibers act as locations to relieve the stresses caused due to expanding water in the composites subjected to freezing and thawing. However, the hot water soaked composites show higher damage with increasing fiber volume, probably due to the fact that at elevated temperatures and in wet conditions, the fibers disintegrate, increasing the porosity of the composite, and affecting the integrity of the material.

PART B: FIBER REINFORCED ENHANCED POROSITY CONCRETE

CHAPTER 9: LITERATURE REVIEW ON FIBER REINFORCED ENHANCED POROSITY CONCRETE

9.1 General

This chapter presents a review of pertinent literature on Enhanced Porosity Concrete (EPC). To the authors' understanding, there has been no reported study on the influence of fibers in EPC.

Concretes with higher than normal porosity and pore sizes, which enable water to drain through them quickly, are known as porous concretes, pervious concretes or Enhanced Porosity Concretes (EPC). The latter term will be used throughout this study. They are typically produced by gap grading aggregates, eliminating / minimizing the use of sand, and using low binder contents. It has been reported that an EPC layer over a conventional concrete base is one of the efficient means of reducing pavement noise [BE 3415 1994, Christory et al. 1993, Descornet et al. 2000, Sandberg and Ejsmont 2002].

Though EPC was used in pedestrian areas and parking lots in Japan as early as 1983, its use in United States and Europe was not popular till the 1990s when the tire-pavement interaction noise became a prominent issue. It was reported that EPC resulted in a 6 dB(A) (A-weighted average – Sandberg and Ejsmont 2002, Nelson 1994) reduction in noise level compared to the conventional pavement in a study in Belgium [Descornet et al. 2000]. A 5-6 dB(A) reduction was also reported by Nissoux et al. (1993).

9.2 Requirements for an Effective EPC Pavement

For EPC to perform effectively with respect to its acoustic behavior, it has been recommended that 15-25% interconnected porosity is required [Christory et al. 1993, Nelson and Phillips 1994, Onstenk et al. 1993, BE 3415 1994, Descornet et al. 2000]. But it is also necessary that the material has adequate mechanical resistance and durability. A listing of the desirable properties has been given by Onstenk et al. (1993).

(i) Significant noise reduction and drainage properties,
(ii) Acceptable strength and stiffness,
(iii) Adequate surface properties with respect to traffic safety – skid resistance, evenness,
(iv) Sufficient service life – bonding to underlying dense concrete, freeze-thaw resistance,
(v) Construction by means of available techniques, and
(vi) Costs comparable to conventional pavements.

9.3 Advantages of EPC Pavements

The advantages of using an EPC pavement in place of a conventional pavement are three-fold, as shown in Figure 2.6 – (i) Ground water recharging, (ii) Reduced hydroplaning, and (iii) Noise reduction. The first two were the prominent reasons for using EPC before the tire-pavement noise issues took center stage, and its efficiency in acoustic absorption ascertained. EPC were used in the design of foundations for pavement structures to provide continuous drainage necessary for extending the service life of these structures. EPC was also reported to be used on the runway of airports, primarily for its better drainage capacities. EPC pavements also exhibited reduced hydroplaning [Christory et al. 1993].

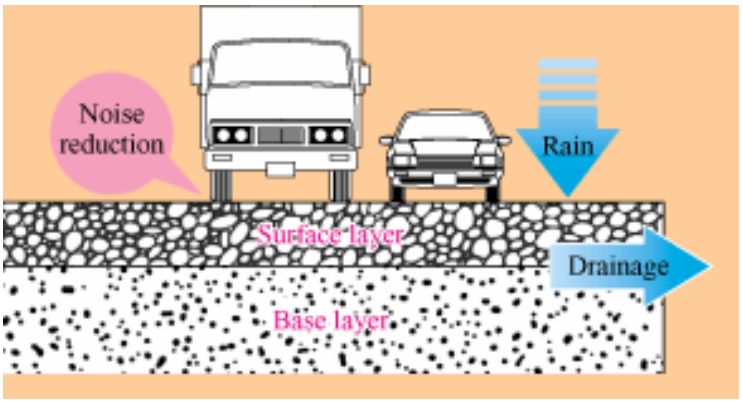

Figure 9.1 3-fold advantage of EPC (from www.hepc.go.jp)

9.4 Materials, Mixture Proportioning, and Construction Procedure of EPC Pavements

In order to achieve such desirable properties with high porosity, materials and mixture proportioning method should be chosen taking into account a host of factors. Those parameters are described as follows.

9.4.1 Aggregate Sizes and Gradation

To ensure that EPC contains about 15-25% open porosity, careful selection and gradation of aggregates are necessary. Gap-graded aggregates, resulting in lack of material to fill out the space between the larger aggregates, are the most favored choice. The accessible porosity and strength are reported to be a function of the grain size of the fine aggregate in relation to that of the coarse aggregate [BE 3415 1994]. The maximum grain size of coarse aggregate has to be limited to 10 mm as per another study [Onstenk et al. 1993]. This study also reports that the grain size of fine aggregate has a major effect on accessible porosity and strength, while the grain size of coarse aggregate does

not have a major effect. Gerharz (1999) recommends that the aggregate size for EPC lie between 4 and 8 mm. A 6-10 mm aggregate size range has been used for a demonstration project [Nissoux et al.]. The use of coarse aggregates of size up to 30 mm and sand of size less than 2.5 mm has been reported [Jing and Guoliang 2002]. The use of larger aggregate sizes (20 mm maximum size) has been recommended for EPC since they result in large sized pathways in the material, thereby preventing clogging [Nelson 1994].

9.4.2 Cement Content

EPC is proportioned with just enough cement content required to bind the aggregates together. This is to minimize the occurrence of excess cement paste seeping through the material structure, reducing its openness. The water-binder ratio also is kept low for the same reasons. It is recommended to conduct binder drainage tests to ascertain the optimum binder content for the aggregate gradation chosen [Nelson 1994]. This procedure is expected to ensure high residual porosity, with acceptable strength characteristics.

9.4.3 Additives

The use of silica fume (10% by weight of cement), and a superplasticizer were reported not to increase the strength of EPC [Onstenk et al. 1993]. Polymer additives were reported to result in an increase in strength as well as freeze-thaw resistance of EPC. Since the cement content of EPC is low, fine mineral admixtures and organic intensifier (polymer) were incorporated in concrete to improve the microstructure and strength of EPC [Jing and Guoliang 2002].

9.4.4 Construction Procedure

From a construction point of view, two alternatives are stated in literature for EPC – (i) wet on wet, and (ii) wet on dry [BE 3415 1994].

The "wet-on-wet" process consists of laying the conventional concrete base layer and the EPC top layer within a short time so that the base layer has not begun to set when laying the top layer. The benefit of this system is that no additional products are required to bond the two layers. In some cases, a retarding admixture is applied to the base layer so that it does not set before the EPC layer is placed. This process requires careful planning of the construction process – either two pavers, or modified pavers which can simultaneously lay two layers of different materials, are needed. It also necessitates the use of two mixing plants with different capacities, due to the different thicknesses used in both layers.

The "wet-on-dry" process consists of laying the EPC layer once the conventional concrete in the base layer has hardened enough to sustain a roller on it. The bond between the two layers is obtained through the use of an adherent material which can be cement based or polymer based. This may result in an increased cost. Moreover, the joints in the lower layer need to be sawed, and sealed to avoid cement paste from the top layer penetrating into it.

9.5 Mechanical Properties and Durability Characteristics of EPC

This section describes the different mechanical properties and durability characteristics of EPC as described by various authors.

9.5.1 Compressive and Flexural Strengths

The strength of EPC depends on the grain size distribution, accessible porosity, and the type and amount of additive used. A maximum compressive strength of about 18 MPa, at an accessible porosity of 25% has been reported. The maximum flexural tensile strength at this porosity was found to be about 4 MPa. Increase in tensile strength was observed when a polymer additive was used [Onstenk et al. 1993]. Flexural tensile strength of about 3 MPa was achieved for a total porosity of 25%, using 6-10 mm aggregates [Nissoux et al.]. A 28-day compressive strength of 20 MPa, and flexural strength of 3 MPa has been reported for an EPC with 25% porosity in another study [BE 3415 1994]. Increase in aggregate size resulted in a reduced compressive strength, where as the addition of polymer and mineral admixture resulted in an increased strength [Jing and Guoliang 2002].

9.5.2 Water Permeation

The water permeation capacity or the drainage properties are closely related to the accessible porosity. For an accessible porosity of 20-29%, the coefficient of permeability is about 0.01 m/s [BE 3415 1994]. It has also been found from this study that the fine aggregate determines the permeability. A permeability of around 36 $l/s/m^2$ has been reported for EPC in another study [Nissoux et al. 1993].

9.5.3 Durability Characteristics

Since EPC forms the top layer of the pavement, it is exposed to the most severe conditions. Some studies have suggested that a polymer additive is required to develop

sufficient freeze-thaw resistance in EPC [BE 3415 1994, Gerharz 1999, Onstenk et al. 1993], whereas results of field implementation of EPC in low volume pavements show that EPC proportioned with gap graded aggregates and with a porosity of around 20% sustained freeze-thaw cycles without any additives [GCPA 2003]. Freeze-thaw tests have also been conducted by submerging the lower part of EPC in 3% NaCl solution. This type of testing is reported to be more severe than the conventional freeze and thaw tests [Onstenk et al. 1993].

9.6 Acoustic Absorption of EPC

Several studies on the acoustic absorption of EPC have concluded that the porosity accessible to the sound waves, and the thickness of the porous layer are the significant factors that determine the acoustic absorption of EPC [Nelson 1994, Francois and Michel 1993, Onstenk et al. 1993, BE 3415 1994, Descornet et al. 1993]. The frequencies and amplitudes of the maxima and minima of the absorption coefficients are related to the porosity of the surface layer, air flow resistance, tortuosity of the pore network, and the thickness of the porous layer [Descornet et al. 2000]. Varying the thickness affects the frequency at which the maximum acoustic absorption occurs while increasing the porosity is said to be beneficial in increasing the absorption at any frequency. The first absorption peak determines the effectiveness of the material in terms of noise reduction. The optimization of acoustic properties of EPC therefore depends on the efficiency in obtaining the maximum amplitude and width of the first peak, which in turn depends on the four above-mentioned parameters. However, from a practical standpoint, only the porosity and thickness can be designed and achieved by proper

mixture proportioning whereas the tortuosity and flow resistivity can be determined later only. Normal variations in air flow resistivity and tortuosity of the pore channels are reported to have only a marginal effect in the acoustic absorption of EPC [Nelson 1994]. A layer thickness of between 5 and 8 cm was arrived at as the optimum thickness to reduce tire-pavement noise, from this study. To ensure significant acoustical effectiveness (3 dB(A) reduction as compared to a dense surface), porous surfaces are reported to require a minimum voids content of 20%, and a minimum thickness of 40 mm [Descornet et al. 2000]. It has been stated in this study that the maximum acoustic absorption coefficient (α) measured using a standing wave tube on cores of 100 mm diameter should satisfy those given in Table 9.1. In a German study, an EPC pavement of 80 mm thickness and 25% porosity exhibited an average noise reduction of about 6 dB(A) [Descornet et al. 2000].

Table 9.1 Maximum acoustic absorption coefficient measured from cores, for different frequencies (Italian specifications, Descornet et al. 2000)

Frequency (Hz)	Acoustic absorption coefficient (α)
400-630	≥ 0.15
800-1600	≥ 0.30
2000-2500	≥ 0.30

9.7 Noise Reduction Mechanisms in EPC

The primary effect of EPC is on acoustic sources of tire-pavement interaction noise and air-borne sound. There are several mechanisms by which EPC reduce noise

[Sandberg and Ejsmont 2002, Nelson and Phillips 1994, Descornet et al. 2000]. They are briefly described in this section.

(i) The open porosity prevents the development of high pressure gradients at the edges of the tire-road contact patch, and also within the contact patch. This is responsible for the reduction or even elimination of all air displacement noise generation mechanisms
(ii) Small chippings in the surface results in the impact mechanism being not a very dominant effect
(iii) The porosity in the EPC results in acoustic absorption so that sound waves are dissipated into heat in the small pores inside the material. The acoustic absorption effect will influence not only the tire-pavement noise but also other types of vehicle noise
(iv) If sound is reflected between the pavement surface and the underbody of the vehicle a number of times, each reflection causes loss of acoustic energy
(v) The acoustically "soft" EPC surface will affect the acoustical impedance in and around the tire-road contact patch, as well as between the source and receiver. This is similar to the explanation of Section 2.3.1. The absence of a reflecting plane eliminates the horn effect.

9.8 Fiber Reinforced EPC

Though there is no reported literature on the use and performance of fiber reinforced EPC, it was thought that the addition of fibers can result in enhanced mechanical properties (flexural strength). It was also believed that the use of flexible fibers can influence the acoustic absorption behavior of EPC. The following chapters delve into this hypothesis in more detail.

CHAPTER 10: MATERIALS, MIXTURE PROPORTIONING, AND TEST METHODS FOR FIBER REINFORCED EPC

10.1 Introduction

This chapter explains the materials used in this study, mixture proportions adopted, and the test methods employed to study the various properties of fiber reinforced Enhanced Porosity Concrete. Detailed descriptions of the experimental set up developed, and the testing method are provided.

10.2 Materials

This section gives an outline about the various materials used in the experimental investigations. The materials are kept constant throughout the study so as to nullify the influence of change in materials on the properties of F-EPC.

10.2.1 Cement

Commercially available Type I Ordinary Portland Cement manufactured by Lonestar Industries was used for the entire study. Table 10.1 summarizes the chemical properties of the cement.

Table 10.1 Chemical properties of cement

C_3S (%)	C_3A (%)	Total Alkali (%)	Insoluble Residue (%)	Loss on Ignition (%)	MgO (%)	SO_3 (%)
--	15.0 (max)	--	0.8 (max)	3.0 (max)	6.0 (max)	4.5 (max)
62.0	9.0	0.5	1.94	0.58	1.82	2.67

10.2.2 Fine Aggregate

The fine aggregate used for the study was a locally available river sand, with a water absorption of 2.3%. The sand conforms to ASTM C 128-94.

10.2.3 Coarse Aggregate

Limestone aggregates were used as coarse aggregates in this study. Aggregates were sieved into different size fractions to create gap grading used in this study. The aggregate sizes used were: # 8 (passing 4.75 mm and retained on 2.36 mm sieve), # 4 (passing 9.5 mm and retained on 4.75 mm sieve), and 3/8" (passing 12.5 mm and retained on 9.75 mm sieve).

10.2.4 Fibers

Polypropylene fibers, 50 mm long and 1-2 mm wide were used to reinforce EPC. The fibers had a density of 910 kg/m^3.

10.3 Mixture Proportioning and Specimen Preparation

This section describes the mixture proportions used in this study, mixing procedure and the method of preparing specimens for the various tests that are described later.

10.3.1 Mixture Proportions

The water-cement (w/c) ratio used for all the mixtures investigated in this study was kept constant at 0.33. The cement content was established by providing just enough paste to coat the aggregates since an excessive amount of paste may drain through the pores of the material. It was found out from a trial and error process that the aggregate-cement ratio could be kept around 5.6 at the selected w/c to achieve this. The mixtures were prepared with either the single sized aggregates alone, or binary blends of these mixtures. Equal weights of two aggregate sizes were used in blended mixtures. The fiber volumes used for this study were 0.5% and 1.5%.

10.3.2 Mixing and Placing Procedure

The constituent materials were batched immediately prior to mixing. The weighed quantity of aggregates was added to the mixer, followed by cement. Water was slowly added while the dry materials were being mixed in a pan mixer. Fibers were then slowly added, with the mixer in motion. The mixer was allowed to run for three minutes. At the end of three minutes, the bottom and sides of the mixer were scrapped, and the mixer was allowed to rest for three minutes. A final two minutes of mixing followed this step.

The contents of the mixer were then discharged from the mixing pan into the molds using scoops. The concrete was placed in the forms in two equal lifts. The forms were vibrated on a table vibrator while the concrete was being placed. In addition, the sides of the forms were struck with rubber mallet so as to ensure that the molds are properly filled. No needle vibrator was used since the workability is low because of gap graded aggregates and low cement content. The forms were finished and were kept under wet burlap for the first 24 hours. After this period, the specimens were removed from the molds, and were kept in the curing chamber at a relative humidity of greater than 98% till further testing.

10.4 Test Procedures

The following section gives an outline of the various test procedures employed in this study to obtain the material properties of EPC.

10.4.1 Flexural Strength Determination

Flexural strength was determined in accordance with ASTM C 78-02. Two tests were conducted on each mixture from a single beam (150 mm x 150 mm x 700 mm), and the average strength reported. Figure 10.1 shows the loading arrangement for flexural strength testing. The first flexural strength test was conducted on 450 mm span of the beam and the second test on the longer remaining portion of the beam after the first flexural failure.

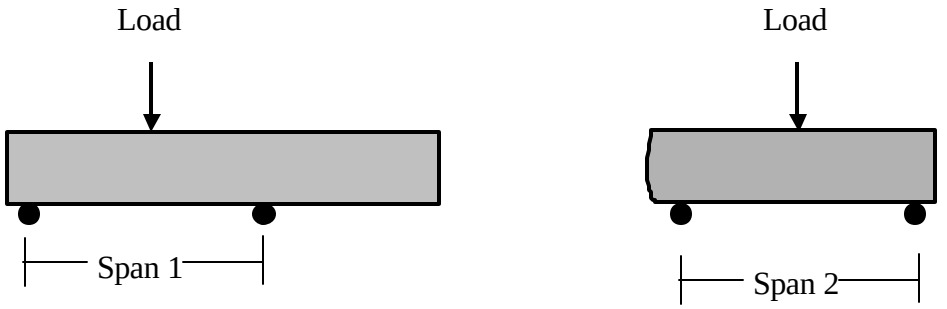

Figure 10.1 Flexural strength determination

10.4.2 Porosity Determination using Volume Method

Because of the presence of large interconnected pores in the F-EPC system, the following procedure was adopted to determine the volume porosity. The cylindrical specimens (95 mm in diameter and 150 mm long) that were cored from the beams (150 mm x 150 mm x 700 mm) were immersed in water for 24 hours to saturate the pores in the matrix. After this period, the sample was removed from water and allowed to achieve SSD condition. The sample was then enclosed in a latex membrane and the bottom of the cylinder was sealed using a stainless steel plate with silicone sealant. The mass of the sample, latex membrane, and the steel plate (M_1) was measured. Water was added to the top of the sample until it was filled, which indicated that all the interconnected pores were saturated. The mass of the system filled with water was taken (M_2). The difference in the mass $\Delta M = (M_2-M_1)$ represents the water in the pores. This mass was converted into a volume, expressed as a percentage of the total volume of the specimen to provide an indication of the total porosity.

10.4.3 Measurement of Acoustic Absorption

To evaluate the acoustic absorption characteristics of F-EPC, a Brüel & Kjær™ impedance tube was employed, as shown in Figure 4.4. Cylindrical specimens with a diameter of 95 mm were cored from beams after they were tested in flexure. The specimen length used was 150 mm. The sample was placed inside a thin cylindrical Teflon sleeve, into which it fits snuggly. The sample assembly was placed against a rigid backing at one end of the impedance tube which is equipped with a sound source. A plane acoustic wave generated by the sound source was propagated along the axis of the tube. Microphones placed along the axis of the tube were used to detect the sound wave pressure transmitted to the sample and the portion of the wave that is reflected (ASTM E-1050). The pressure reflection coefficient (R) is the ratio of the pressure of reflected wave to that of incoming wave, at a particular frequency, expressed as:

$$R = \frac{e^{jkd_1} - e^{jkd_2} P}{e^{-jkd_2} P - e^{-jkd_1}} \qquad 10.1$$

where d_1 and d_2 are the distances from the specimen surface to the closest and farthest active microphones respectively, j is an imaginary number ($\sqrt{-1}$), k is the wave number (ratio of angular frequency to the wave speed in the medium) and P is the ratio of acoustic pressures at the two active microphone locations.

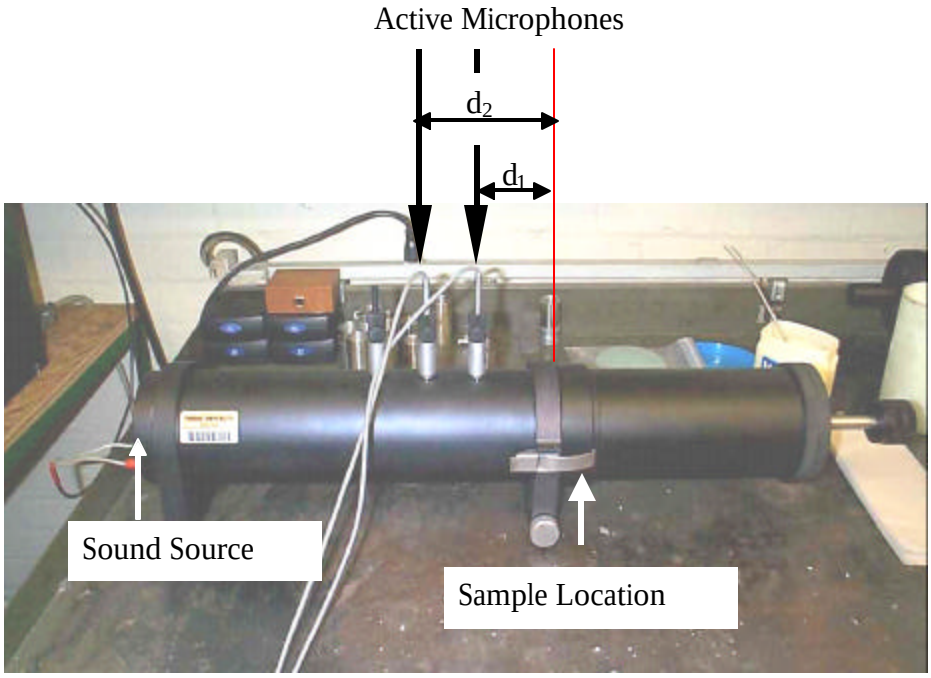

Figure 10.2 Impedance tube set up

A data acquisition system (PULSE ™) is attached to the impedance tube, which converts the signals in the time domain to one in the frequency domain. A software program written in Matlab™ allows graphic display of the real and imaginary components of the impedance with respect to the frequency. The program has also been tailored to output the variation of acoustic absorption coefficient with frequency.

The absorption coefficient (α) is commonly reported as a measure of a material's ability to absorb sound. A material with an absorption coefficient of 1.0 indicates a purely absorbing material whereas a material with an absorption coefficient of 0 indicates that it is purely reflective. The absorption coefficient at each frequency can be calculated from the pressure reflection coefficient (R) as given in Equation 10.2.

$$\alpha = 1-|R|^2 \qquad 10.2$$

In this work the frequency range of interest was limited from 100 Hz to 1600 Hz. A threshold of 100 Hz was established because at very low frequencies, the acoustic

pressures were difficult to stabilize. Frequencies higher than 1600 Hz could be measured accurately only when the impedance tube has a small diameter. (To achieve acoustic measurements over the widest range of frequencies, and to ensure that a "standing wave" is generated inside the impedance tube, its diameter should be as small as possible). Preparation of homogeneous concrete samples of such small sizes tends to be difficult due to the size of the aggregates.

10.4.4 Electrical Impedance Spectroscopy

Electrical Impedance Spectroscopy (EIS) was used to determine the bulk resistance of F-EPC samples, in order to estimate the conductivities. EIS measurements were conducted in this study using a Solartron 1260 ™ Impedance / Gain-Phase analyzer that was interfaced with a personal computer for data acquisition. A typical Nyquist plot (plot of real versus imaginary impedance) obtained from EIS measurements consists of two arcs – the bulk arc and the electrode arc. The two arcs meet at a point where the imaginary component of the impedance is minimum, and the corresponding real impedance is the bulk resistance (R_b) of the sample.

Figure 10.3 shows the specimen set up that was used for the EIS experiments. The cylindrical specimen, 95 mm in diameter, and 150 mm long was enclosed in a latex membrane to contain the electrolyte. The bottom of the specimen was sealed to a stainless steel plate using silicone sealant. The specimen was saturated with the electrolyte and another stainless steel plate with a small acrylic dyke was placed at the top of the specimen, with a piece of porous foam in between. The entire set up was firmly gripped with adjustable clamping mechanism. The stainless steel plates served as

the electrodes and alligator plugs from the impedance analyzer were attached to the electrodes. The impedance measurements were made over the frequency range of 1 MHz to 10 Hz using a 250 mV AC signal.

Using the bulk resistance (R_b) obtained from the Nyquist plots, the effective electrical conductivity (σ_{eff}) of the sample was calculated as:

$$s_{eff} = \frac{l}{R_b A} \qquad 10.4$$

where l is the specimen length and A is the cross sectional area of the specimen.

The electrolytes used in this study were sodium chloride (NaCl) solutions of varying concentrations (3%, and 10%). The conductivity of 3% NaCl solution was 4.40 S/m whereas that of 10% solution was 12.40 S/m.

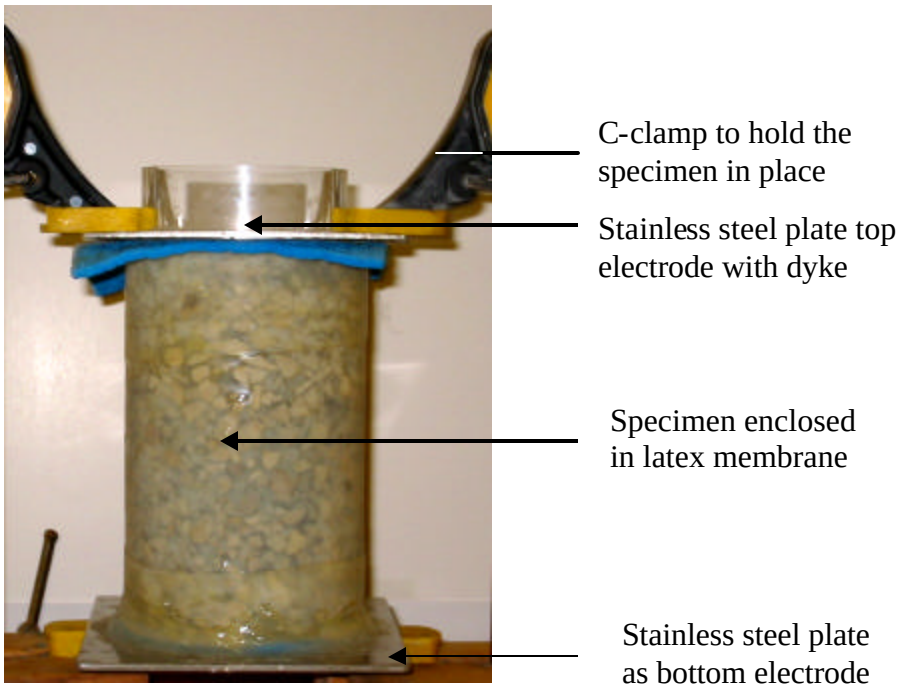

Figure 10.3 Specimen set up for EIS experiments

CHAPTER 11: POROSITY AND MECHANICAL PROPERTIES OF FIBER REINFORCED EPC

11.1General

This chapter deals with the fundamental mechanical properties (flexural strength), and porosity of fiber reinforced EPC. The influence of aggregate size and gradation on the porosity and the mechanical properties are presented, and compared with those of plain EPC. The central idea of this chapter therefore is to bring out the significant features of the pore structure of fiber reinforced EPC and develop an understanding of how it affects the other properties.

11.2 Influence of Fibers on Porosity of Fiber Reinforced EPC

The influence of addition of 0.5% and 1.5% polypropylene fibers by volume on the porosity of EPC is shown in Figure 11.1. It could be observed from this figure that there is no significant variation in porosity with the addition of fibers. The fibers might exert a pore-filling effect thereby reducing the porosity, but at the same time could aid in separating the aggregates further, thus negating the effect of pore filling. A combination of these mechanisms explains the reason for lack of change in porosity.

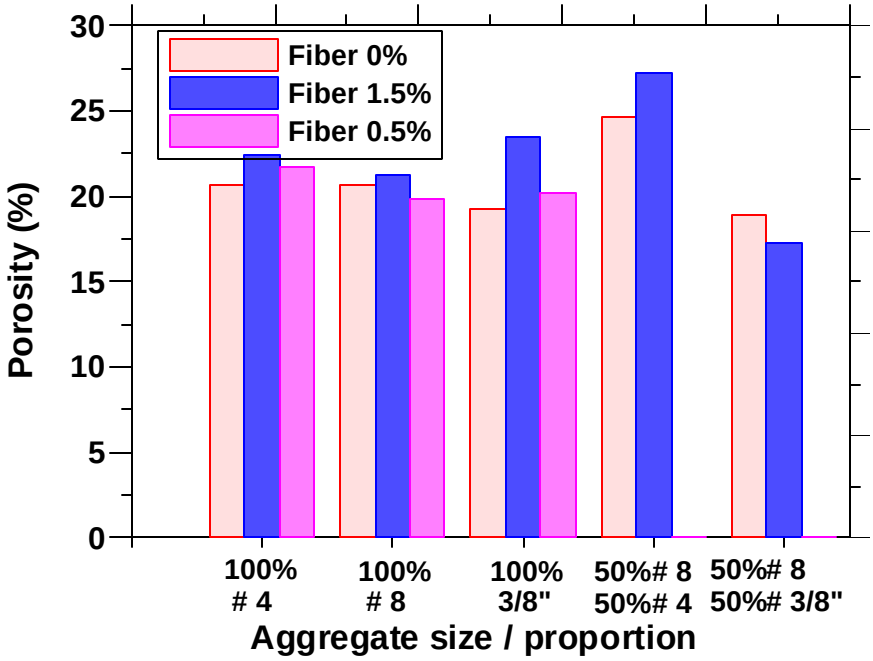

Figure 11.1 Influence of fibers on porosity

11.3 Influence of Fibers on Flexural Strength of Fiber Reinforced EPC

The influence of 0.5% and 1.5% by volume of polypropylene fibers on the flexural strength of EPC is shown in Figure 4.12. The purpose of incorporating fiber reinforcement was not to increase the flexural strength of the material, but to ascertain its influence in acoustic absorption behavior, as well as in fracture. It has been proven that flexible fibers at low volumes as used in this study does not aid in increasing the flexural strength, and this observation is validated in Figure 11.2. In highly porous systems as EPC, fibers may prove beneficial in enhancing the post-peak behavior by bridging the pores.

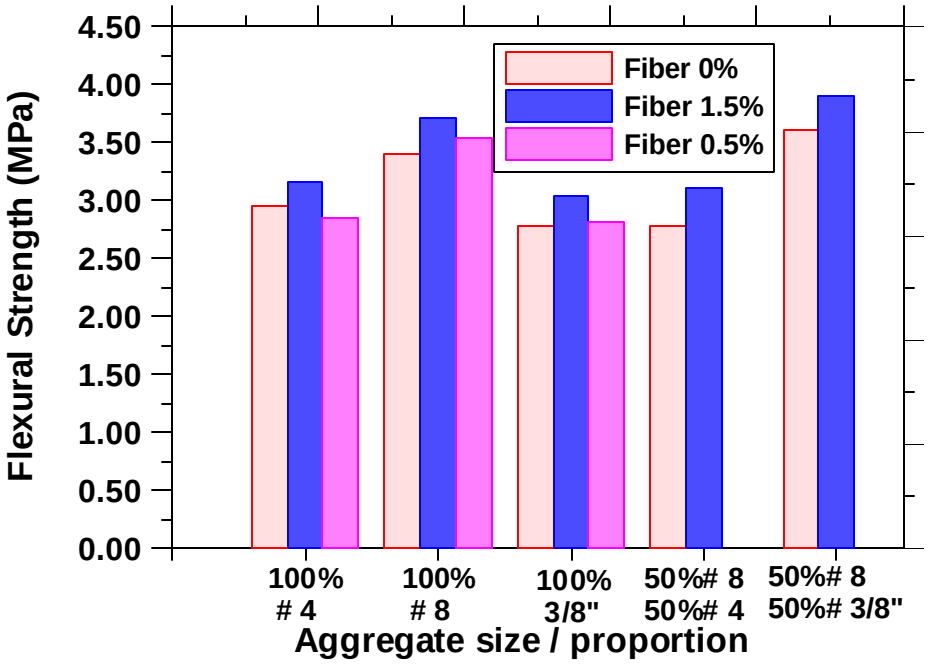

Figure 11.2 Influence of fibers on flexural strength

CHAPTER 12: ACOUSTIC ABSORPRITON OF FIBER REINFORCED EPC

12.1 General

This chapter reports the results of acoustic absorption studies on fiber reinforced EPC carried out using the impedance tube. The acoustic absorption spectra (plot of acoustic absorption coefficient against frequency) for F-EPC made using both single sized aggregates as well as aggregate blends are provided. Polypropylene fibers (50 mm long, and around 1-2 mm wide) used in conjunction with EPC mixtures were believed to affect the acoustic absorption properties because of their extremely low stiffness and the manner in which they may bridge the large pores in EPC. This chapter deals with the effect of fibers on the absorption properties of EPC.

12.2 Acoustic Absorption of Single Sized Aggregate Mixtures Incorporating Fibers

The influence of varying volume fractions of polypropylene fibers on the acoustic absorption characteristics of EPC mixtures made using single sized aggregates (# 8, # 4, and 3/8") is discussed here. Figure 12.1 shows the acoustic absorption spectra of EPC mixtures made using # 4 aggregates alone, incorporating 0%, 0.5% and 1.5% polypropylene fibers.

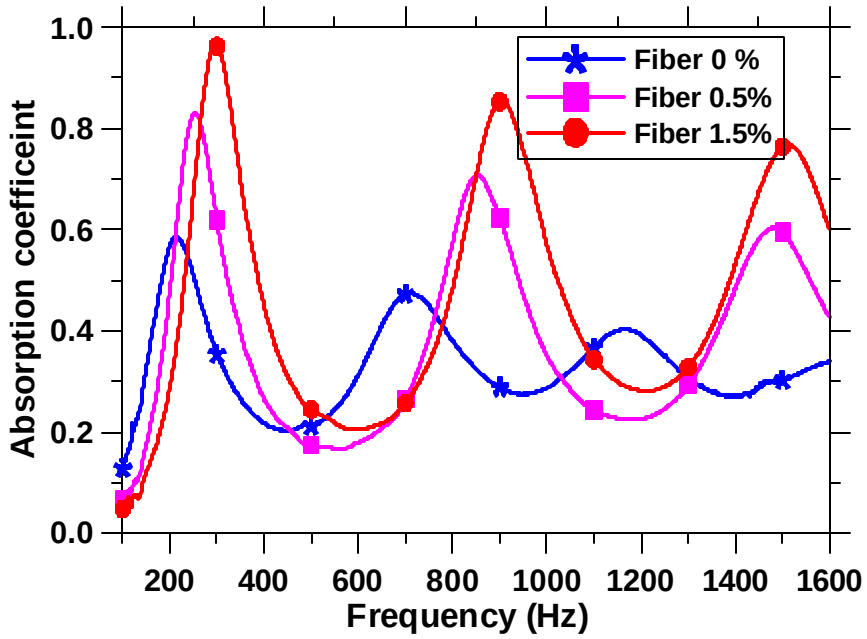

Figure 12.1 Influence of fibers on the acoustic absorption of EPC made with # 4 aggregates

It can be observed from this plot that the maximum acoustic absorption coefficient (α) increases with fiber volume. α increases from around 0.60 for a mixture with no fibers to around 0.95 for a mixture with fiber volume of 1.5%. The plausible explanation for this behavior is as follows: The long polypropylene fibers in the mixture bridge some of the large pores. When sound waves passing through the open pore structure of EPC impinges on the fibers, a part of the energy is lost in viscous interaction with the fibers, whereas another part is lost in setting up the fibers into vibration. With an increased fiber volume, the losses due to both of these mechanisms increase, resulting in an increased acoustic absorption.

Figure 12.2 depicts the acoustic absorption spectra of EPC mixtures made using 3/8" aggregates alone.

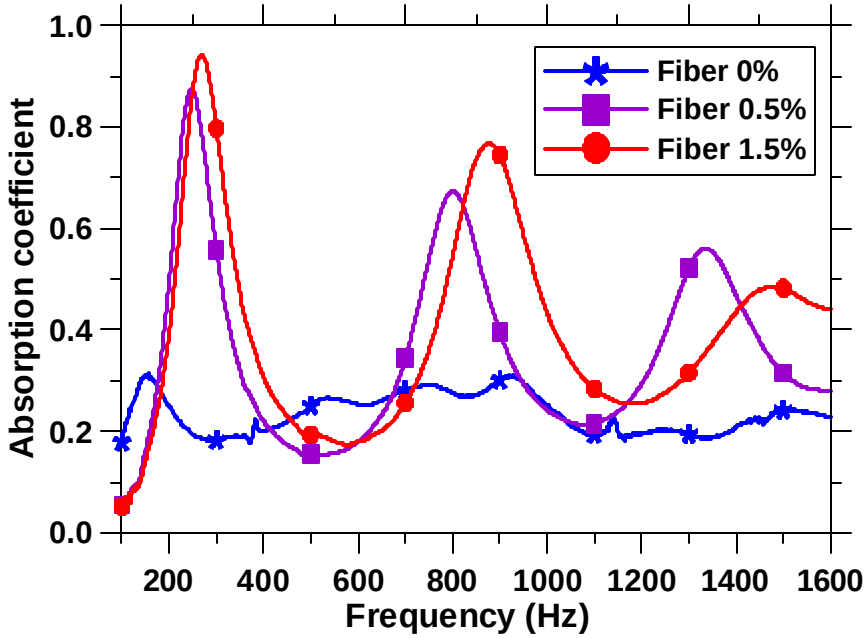

Figure 12.2 Influence of fibers on the acoustic absorption of EPC made with 3/8" aggregates

The behavior is similar to the mixtures with # 4 aggregates alone, even though a drastic increase in acoustic absorption with fiber addition is observed in this case. The maximum acoustic absorption coefficient increases from around 0.30 for mixtures without fibers to around 0.95 for those with a fiber volume of 1.5%. It is believed that larger pore sizes in EPC mixtures with 3/8" aggregates contribute to this phenomenon. While larger pore sizes result in higher acoustic reflection, and consequently lower absorption for mixtures without fibers [Marolf et al. 2003], the addition of fibers effectively reduces the pore sizes, resulting in reduced acoustic reflection. Moreover, the viscous losses of the pore network is also increased, contributing to increased absorption. Due to the larger pore sizes, the effective length of the fibers spanning the pores also could be larger, thereby dissipating more energy through the vibration mechanism. A synergy of all these effects could be responsible for the extremely efficient acoustic absorption characteristics of EPC mixtures with 3/8" aggregates, incorporating fibers.

The absorption spectra of EPC mixtures made using # 8 aggregates alone are shown in Figure 12.3.

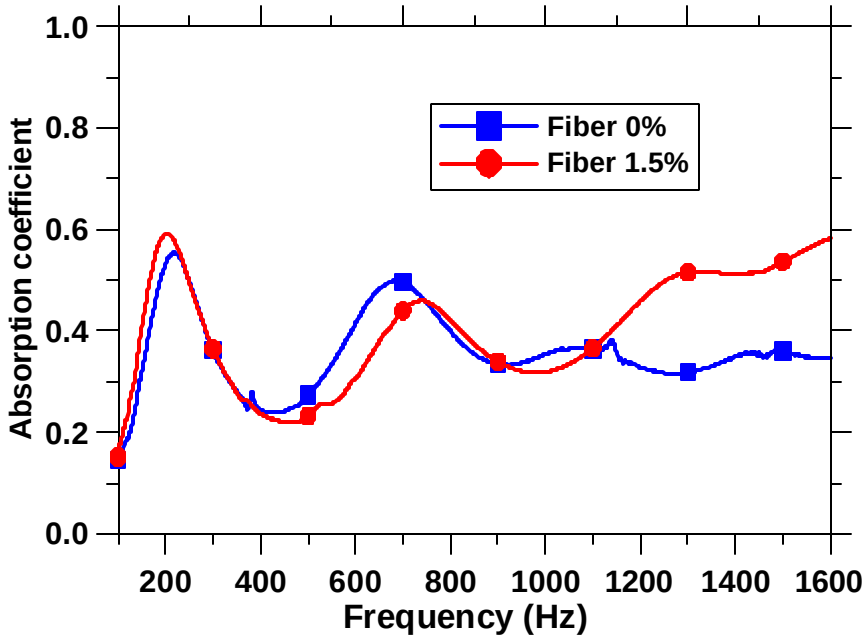

Figure 12.3 Influence of fibers on the acoustic absorption of EPC made with # 8 aggregates

This plot shows that EPC mixtures incorporating fibers, with only # 8 aggregates show a completely different behavior as compared to the ones with either # 4 aggregates or 3/8" aggregates shown in Figure 12.1 and 12.2 respectively. There is no significant increase in acoustic absorption with increase in fiber volume in this case. This behavior can also be explained taking into account the pore sizes in these mixtures. The mixtures with # 8 aggregates have a lower pore size than those with # 4 aggregates. The pore sizes in mixtures with # 8 aggregates are not much larger than the width of the fibers. Therefore, even though some energy may be expended in setting up the fibers into vibration, due to the partial closure of the pore network by the fibers, there is more acoustic reflection, effectively rendering the maximum absorption coefficient same.

The above results indicate that it is possible to tailor the pore structure of EPC by using fibers to enhance acoustic absorption characteristics. Mixtures with pore sizes larger than the fiber width show markedly increased acoustic absorption. The detrimental effects of a larger pore size could thus be overcome by the use of flexible fibers. When the pore size is in the range of the fiber width, use of fibers does not provide substantial advantages.

12.3 Acoustic Absorption of Blended Aggregate Mixtures Incorporating Fibers

Two EPC mixtures with different aggregate blends incorporating fibers were studied to understand the influence of fibers on the acoustic absorption of blended systems. Figure 12.4 shows the acoustic absorption spectra for a mixture with 50% # 4 and 50% # 8 aggregates, whereas Figure 12.5 is the spectra for 50% # 8 and 50% 3/8" aggregate blend.

A mixture with a blend of 50% # 8 and 50% # 4 is one of the most promising plain EPC mixtures with respect to acoustic absorption [Marolf et al. 2003]. Figure 12.4 also shows that this mixture is the most promising when fibers are incorporated. The reason for the effectiveness of this mixture could be the fact that it has the optimal pore size and tortuosity to provide maximum acoustic absorption, in addition to the reasons given in the previous section.

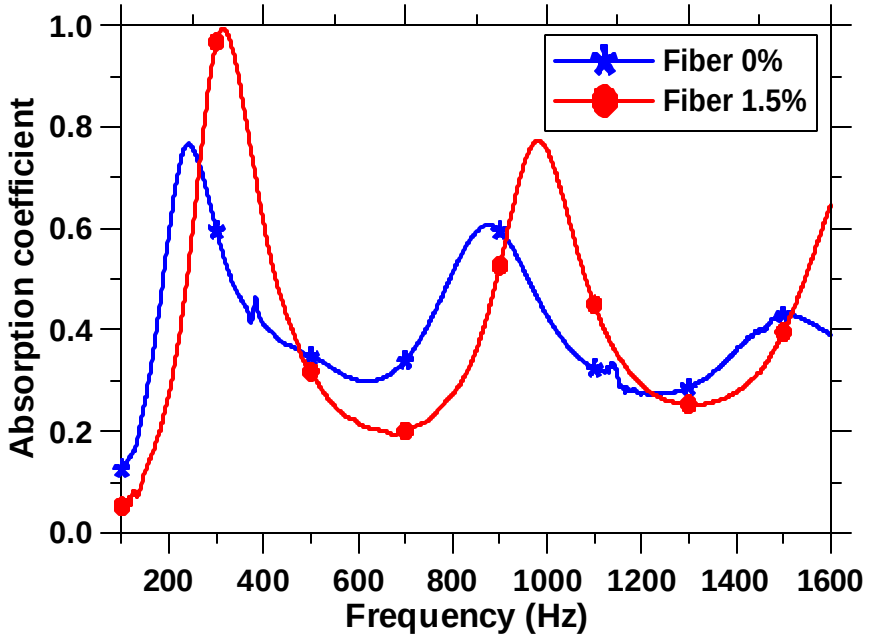

Figure 12.4 Influence of fibers on the acoustic absorption of EPC made with 50% # 8 and 50% # 4 aggregates

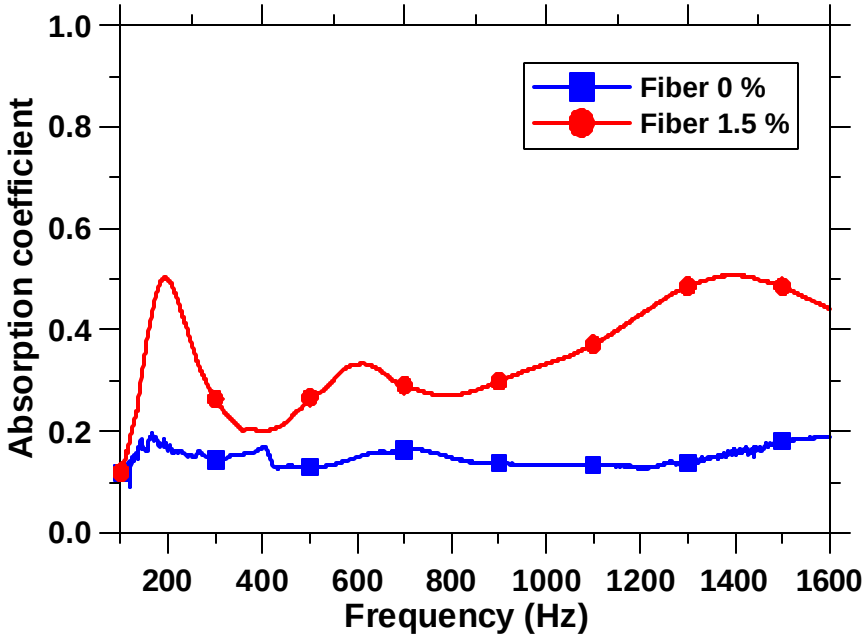

Figure 12.5 Influence of fibers on the acoustic absorption of EPC made with 50% # 8 and 50% 3/8” aggregates

From Figure 12.5, it could be noticed that the fibers improve the acoustic performance of the EPC mixture with a blend of 50% # 8 and 50% 3/8" aggregates, though the maximum acoustic absorption coefficient is not very high as compared to a blend of # 4 and # 8 aggregates. This mixture without fibers performs poorly because of the fact that the # 8 aggregates fill in the pores of the system with 3/8" aggregates, reducing the effective porosity. Adding fibers therefore does not significantly affect the pore structure, however the improvement is due to the fact that the fibers vibrate to dissipate some energy.

The above results indicate that it is possible to tailor the pore structure of EPC by using fibers to enhance acoustic absorption characteristics. Mixtures with pore sizes larger than the fiber width show markedly increased acoustic absorption, as shown in Fig.12.6.

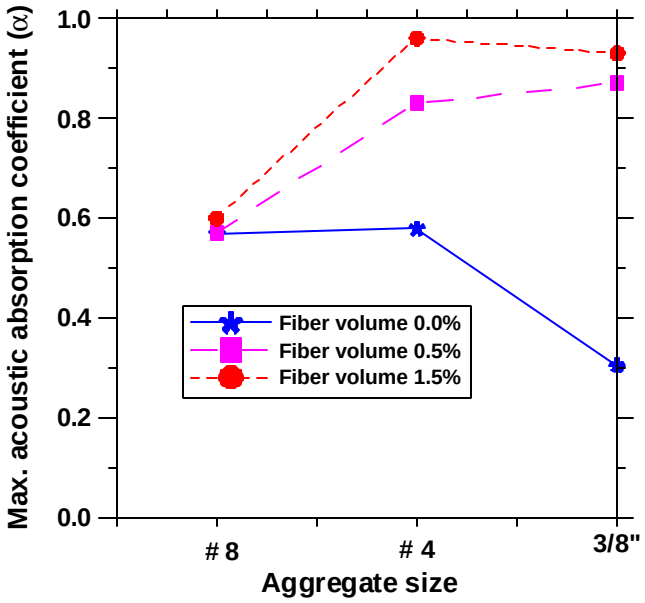

Figure 12.6 Variation in maximum acoustic absorption coefficient as a function of aggregate sizes

While the maximum acoustic absorption coefficient decreases with increasing aggregate sizes (correspondingly, increasing pore sizes) for plain EPC mixtures, the trend is reversed for fiber reinforced mixtures. The detrimental effects of a larger pore size could thus be overcome by the use of flexible fibers. Preliminary research also indicated that fiber reinforcement may have additional benefits by way of improving the toughness and fracture resistance of EPC.

12.4 Characterizing the Pore Structure of Fiber Reinforced EPC

It has previously been shown that porosity alone is an inadequate predictor of the performance of EPC systems (Neithalath et al., 2003); rather pore connectivity also must be considered in prediction of acoustic and hydraulic properties of EPC. To determine the pore connectivity factors for EPC mixtures reinforced with polypropylene fibers, a modified parallel model, as shown in Equation 12.1 is used.

$$s_{eff} = s_p f_p b_p + s_s \qquad 12.1$$

where σ_{eff} is the effective conductivity of the sample, σ_p, and σ_s are the conductivities of the electrolyte and the solid phase respectively, ϕ_p is the pore volume fraction (determined by weighing the specimen in dry and saturated conditions), and β_p is the pore connectivity factor.

Using two different electrolyte conductivities ($\sigma_{p\text{-}3}$ = 4.40 S/m and $\sigma_{p\text{-}10}$ = 12.40 S/m) obtained by saturation using two different concentrations of NaCl (3% and 10%), the effective conductivities ($\sigma_{eff\text{-}3}$ and $\sigma_{eff\text{-}10}$) are calculated using the bulk resistances from

Eq. (3). The pore connectivity factor (β_p) can then be calculated as shown in Equation 12.2

$$b_p = \frac{(s_{eff-10} - s_{eff-3})}{f_p (s_{p-10} - s_{p-3})} \qquad 12.2$$

The pore connectivity factors for plain as well as fiber reinforced EPC mixtures are shown in Fig. 12.7

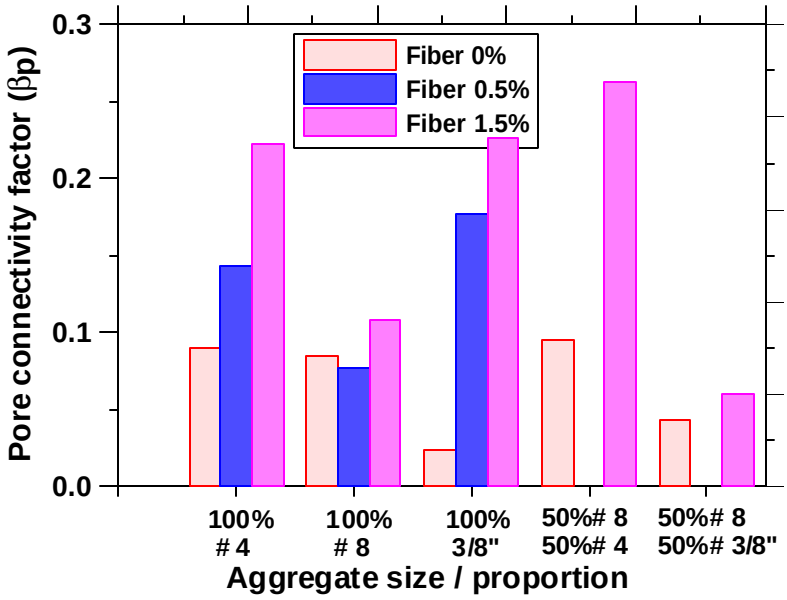

Figure 12.7 Influence of fiber volume and aggregate proportions on pore connectivity factor

It can be seen from this figure that the pore connectivity factors are typically higher for mixtures with fibers, and they increase with increase in fiber volume. The mixture with 100% # 8 aggregates does not show a considerable increase in β_p with increase in fiber volume where as the mixture with 100% 3/8" aggregates shows the largest increase. This leads to the premise that the addition of fibers bridges the pores,

and significantly influence the pore connectivity factors. Similar observations were made with respect to acoustic absorption coefficient also where it was seen that mixtures with 100% # 8 aggregates (smaller pore sizes) did not benefit from the addition of fibers, whereas mixtures with 100% 3/8" aggregates (larger pore sizes) showed a drastic increase in absorption coefficient. The maximum acoustic absorption coefficients of mixtures with and without fibers are compared in Fig. 12.8.

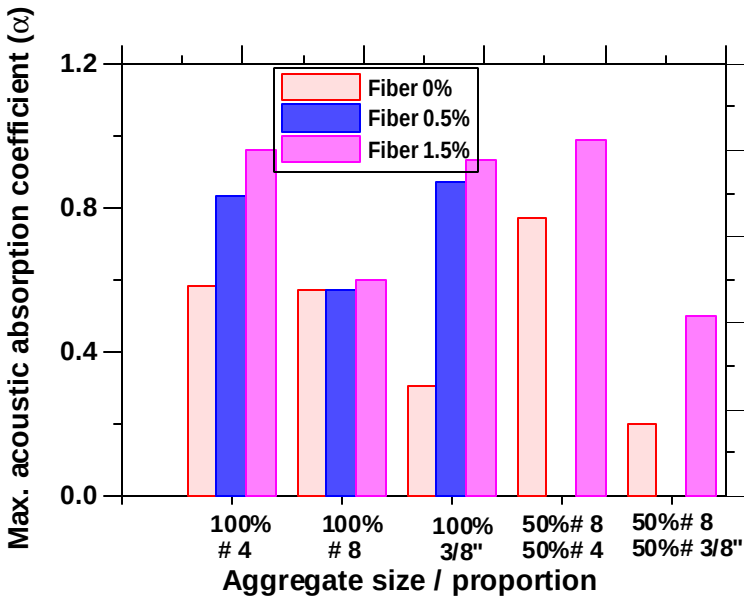

Figure 12.8 Influence of fiber volume and aggregate proportions on maximum acoustic absorption coefficient

The similarities between Figs. 12.7 and 12.8 are immediately evident. The variation in acoustic absorption coefficient with fiber volume for different aggregate sizes and proportions follow a similar trend as the pore connectivity factor, reiterating the fact that pore connectivity factor for EPC mixtures is a very good indicator of the acoustic absorption characteristics of the material.

12.5 Summary

This chapter has dealt with the influence of flexible polypropylene fiber inclusions on the acoustic absorption of EPC. It was observed that the fibers significantly enhance the acoustic absorption of EPC depending on the pore sizes of the material. EPC mixtures that did not show an increase in absorption with fiber addition were found to have smaller pore sizes. The mechanisms by which the fibers enhance the acoustic efficiency of EPC are (i) reducing the effective pore size, (ii) increasing the tortuosity of the sound channels, thereby forcing the waves to travel longer, and (ii) vibration of the fibers.

CHAPTER 13: SUMMARY AND CONCLUSIONS

13.1 General

This chapter summarizes the research findings pertaining to the influence of polypropylene fibers on the acoustic absorption of Enhanced Porosity Concrete.

13.2 Conclusions

1. The addition of polypropylene fibers at fairly low volumes does not significantly affect the porosity of the EPC system
2. The flexural strength of EPC systems reinforced with polypropylene fibers are not significantly higher than those without fibers
3. Addition of polypropylene fibers increases the maximum acoustic absorption coefficient of EPC. The increase is significant for mixtures having larger pore sizes as opposed to those with smaller pore sizes. The mechanisms responsible for this behavior are believed to be: (i) pore size reduction by fibers, and increase in path length of sound waves since they have to travel around the fibers, and (ii) energy expended in setting the fibers into vibration.

LIST OF REFERENCES

Akers, S.A.S., and Studinka, J.B., “Ageing behavior of cellulose fiber cement composites in natural weathering and accelerated tests”, International Journal of Cement Composites and Lightweight Concrete, Vol.11, No.2, 1989, pp 93-97.

Allard, J. F., “Propagation of sound in porous media – modeling sound absorbing materials”, Elsevier Applied Science, 1993.

ASTM C 1259-01., “Standard test method for dynamic Young’s modulus, shear modulus and Poisson’s ratio for advanced ceramics by impulse excitation of vibration”, ASTM International, Pennsylvania.

ASTM C 1437-01., “Standard test method for flow of hydraulic cement mortar”, ASTM International, Pennsylvania.

ASTM C 192-00, “Standard method of making and curing concrete test specimens in the laboratory”, American Society of Testing and Materials, Pennsylvania.

ASTM C 666-03, “Standard test method for resistance of concrete to rapid freezing and thawing”, American Society of Testing and Materials, Pennsylvania, 2000.

ASTM C 78-02, “Standard method for flexural strength of concrete (using simple beam with third point loading)”, American Society of Testing and Materials, Pennsylvania, 2002.

ASTM E 1050-98, “Standard test method for impedance and absorption of acoustic materials using a tube, two microphones and a digital frequency analysis system”, American Society of Testing and Materials, Pennsylvania, 1998.

Balaguru, P. N., and Shah, S. P., “Fiber reinforced cement composites”. McGraw-Hill Inc., 1992.

Balaguru, P., "Contribution of fibers to crack reduction of cement composites during the initial and final setting period", ACI Materials Journal, Vol. 91, No.3, 1994, pp. 280-88.

Bentur, A., "Long term performance of fiber reinforced cements and concretes", Proceedings of Advances in cement and concrete, ASCE, 1994, pp. 223-234.

Bernhard, R. J., "The state of the art of quiet highways", Presentation at the 88th Purdue Road School, March 2002.

Biot, M.A., "Generalized theory of acoustic propagation in porous dissipative media", Journal of the Acoustic Society of America, Vol. 34, 1962, pp. 1254-1264.

Blankenhorn, P. R., Blankenhorn, B. D., Silsbee, M. R., and DiCola, M., "Effects of fiber surface treatments on mechanical properties of wood fiber-cement composites", Cement and Concrete Research, Vol.31, 2001, pp. 1049-55.

Blankenhorn, P. R., Silsbee, M. R., Blankenhorn, B. D., DiCola, M., and Kessler K., "Temperature and moisture effects on selected properties of wood fiber-cement composites", Cement and Concrete Research, Vol.29, 1999, pp. 737-41.

Bledzki, A.K., and Gassan, J., "Composites reinforced with cellulose based fibers", Progress in Polymer Science, Vol.24, 1999, pp. 221-274.

Bouguerra, A., Sallee, H., de Barquin, F., Dheilly, R.M., and Queneudec, M., "Isothermal moisture properties of wood-cementitious composites", Cement and Concrete Research, Vol. 29, 1999, pp. 339-347.

Brennan, M.J., and To, W.M., "Acoustic properties of rigid frame porous materials – an engineering perspective", Applied Acoustics, Vol. 62, 2001, pp. 793-811.

BRITE/EURAM project BE 3415 “Surface properties of concrete roads in accordance with traffic safety and reduction of noise”, November 1994.

Bussian, A.E., “Electrical conductance in a porous medium”, Geophysics, Vol. 48, No.9, 1983, pp. 1258-1268.

Chen, C. P, &and Lakes, R. S., “Analysis of high loss viscoelastic composites”, Journal of Materials Science, Vol.28, 1993, pp. 4299-4304.

Chowdhury, S. H., “Damping characteristics of reinforced and partially prestressed concrete beams”. Ph.D Thesis, Griffith University, Australia, 1999.

Christensen, B.J., Coverdale, R.T., Olson, R.A., Ford, S.J., Garboczi, E.J., Jennings, H.M., and Mason, T.O., “Impedance spectroscopy of hydrating cement based materials: Measurement, interpretation and application”, Journal of American Ceramic Society, Vol. 77, 1994, pp. 2789-2804.

Corr, D.J., Monteiro, P.J.M., and Bastacky, J., “Microscopic characterization of ice morphology in entrained air voids”, ACI Materials Journal, Vol.99, No.2, 2002, pp. 190-195.

Descornet, G., “Low-noise road surface techniques and materials”, Proceedings of Inter Noise 2000, Nice, France, August 2000.

Descornet, G., Faure, B., Hamet, J.F., Kestemont, X., Luminari, M., Quaresma, L., and Sandulli, D., “Traffic noises and road surfaces: State of the art”, SIRRUS project, Belgian Road Research Center, Brussels, March 2000.

Descornet, G., Fuchs, F., and Buys, R., “Noise reducing concrete pavements”, Proceedings of the Fifth International Conference on Concrete Pavement and Rehabilitation, Purdue University, Indiana, 1993, Vol.2, pp. 93-98

Francois, H.J., and Michel, B., 'Acoustical characteristics of porous pavements: A new phenomenological model', Proceedings of Inter Noise 93, (Leuven, Belgium, 1993), 641-646.

Fu, X., and Chung, D. D. L., "Vibration damping admixtures for cement". Cement and Concrete Research, Vol. 26, No.1, 1996, pp. 69-75.

Gerharz, B., "Pavements on the base of polymer-modified drainage concrete", Colloids and Surfaces A: Physicochemical and Engineering Aspects, Vol. 152, 1999, pp 205-209.

Glover, P.W.J., Hole, M.J., and Pous, J., "A modified Archie's law for two conducting phases", Earth and Planetary Science Letters, Vol. 180, 2000, pp. 369-383.

Iwase, T., "Acoustic properties of porous pavement with double layers and its reduction effects for road traffic noise", Proceedings of Inter Noise 2000, Nice, France, August 2000.

Katz, A.J., and Thompson, A.H., "Quantitative prediction of permeability in porous rock", Physical Review B, Vol. 34, 11, 1986, pp. 8179-8181.

Kim, P.J., Wu, H.C., Lin, Z., Li, V.C., deLhoneux, B., and Akers, S.A.S., "Micromechanics-based durability study of cellulose cement in flexure", Cement and Concrete Research, Vol.29, 1999, pp. 201-208.

Kompella, M. K., and Lambros, J., "Micro mechanical characterization of cellulose fibers". Polymer Testing, Vol. 21, No.5, 2002, pp. 523-530.

Lakes, R. S., "Extreme damping in composite materials with negative stiffness phase", Physical Review Letters, Vol.86, No.13, 2001, pp. 2897-2900.

Lakes, R. S., Kose, S., and Bahia, H., "Analysis of high volume fraction irregular particulate damping composites". Transactions of the ASME, Vol.124, 2002, pp. 174-78.

Lange, D. A., Ouyang, C., and Shah, S. P., "Behavior of cement based matrices reinforced by randomly dispersed microfibers", Advanced Cement Based Materials, Vol.3, 1996, pp. 20-30.

Mac Vicar, R., Matuana, L.M., and Balatinecz, J.J., "Aging mechanisms in cellulose fiber reinforced cement composites", Cement and Concrete Composites, Vol.21, 1999, pp. 189-196.

Majumdar, A.J., and Walton, P.L., "Durability of fiber cement composites", Proceedings of Durability of concrete – Volume II, SP 126-40, ACI, 1991, pp. 745-771.

Marikunte, S., and Soroushian, P., "Statistical evaluation of long term durability characteristics of cellulose fiber reinforced cement composites", ACI Materials Journal, Vol.91, No.6, 1994, pp. 607-616.

Naaman, A. E., "SIFCON: Tailored properties for structural performance", Proceedings of International RILEM/ACI workshop: High performance fiber reinforced cement composites, Mainz, 1991, pp. 18-38.

Natesaiyer, K.C., and Hover, K.C., "The protected paste volume of air entrained cement paste – Part I", Journal of Materials in Civil Engineering, Vol.4, No.2, pp. 166-184.

Nelson, P. M., "Designing porous road surfaces to reduce traffic noise", TRL Annual Review, Transportation Research Laboratories, UK, 1994.

Nelson, P. M., and Phillips, S. M., "Quieter road surfaces", TRL Annual Review, Transportation Research Laboratories, UK, 1994.

Neville, A.M., "Properties of Concrete", 4th Edition, Addison Wesley Longman, 1996.

Nissoux, J-L., Gnagne, C., Marzin, J., Lefebvre, J-P., and Pipien, G., "A pervious cement concrete wearing course below 73 dB(A)", Proceedings of the Fifth International

Conference on Concrete Pavement and Rehabilitation, Purdue University, Indiana, 1993, Vol.2, pp. 269-284.

Permanent International Association Road Congresses (PIARC), "Report of the Technical Committee on Concrete Roads, Marrakesh, 1991.

Powers, T.C., "Basic considerations pertaining to freezing and thawing tests", Proceedings of the American Society for Testing and Materials, 1955, Vol. 55, pp. 1132-1155.

RILEM CPC 11.3., "Absorption of water by immersion under vacuum", Materials and Structures, Vol. 17, 1984, pp. 391-94.

Sandberg, U., and Ejsmont, J. A., "Tyre / Road noise reference book", Informex, Kisa, Sweden, 2002.

Sarigaphuti, M., Shah, S. P., and Vinson, K. D., "Shrinkage cracking and durability characteristics of cellulose fiber reinforced concrete", ACI Materials Journal, Vol.90, No.4, 1993, pp. 309-18.

Soroushian, P., and Marikunte, S., "Moisture sensitivity of cellulose fiber reinforced cement", Proceedings of Durability of Concrete – Volume II, Second international conference, SP 126-44, ACI, 1991, pp. 821-835.

Soroushian, P., and Marikunte, S., "Reinforcement of cement based materials with cellulose fibers", Proceedings of Thin section fiber reinforced concrete and ferrocement, SP-124, ACI, Detroit, 1990, pp. 99-124.

Soroushian, P., and Ravanbakhsh., “High early strength concrete: Mixture proportioning with processed cellulose fibers for durability”, ACI Materials Journal, Vol.96, No.5, 1999, pp. 593-599.

Soroushian, P., Marikunte, S., and Won, J. P., “Statistical evaluation of mechanical and physical properties of cellulose fiber reinforced cement composites”, ACI Materials Journal, Vol. 92, No. 2, 1995, pp. 172-80.

Soroushian, P., Shah, Z., and Won, J. P., “Optimization of wastepaper fiber-cement composites”, ACI Materials Journal, Vol.92, No.1, 1995, pp. 82-92.

Synder, K.A., Ferraris, C., Martys, N.S., and Garboczi, E.J., “Using impedance spectroscopy to assess the viability of rapid chloride test for determining chloride conductivity”, Journal of Research of the National Institute of Standards and Technology, Vol. 105, No. 4, 2000, pp. 497-509.

Vinson, K. D., and Daniel, J. I., “Specialty cellulose fibers for cement reinforcement”, Proceedings of Thin section fiber reinforced concrete and ferrocement, SP-124, ACI, Detroit, 1990, pp. 1-18.

Voronina, N., “An empirical model for rigid frame porous materials with low porosity”, Applied Acoustics, Vol. 58, 1999, pp. 295-304.

Wang, C. N., and Torng, J. H., “Experimental study of the absorption characteristics of some porous fibrous materials”, Applied Acoustics, Vol.62, 2001, pp. 447-59.

Wang, X., and Lu, T. J., “Optimized acoustic properties of cellular solids”, Journal of the Acoustic Society of America, Vol. 106, No.2, 1999, pp. 756-765.

Wassilieff, C., “Sound absorption of wood based materials”, Applied Acoustics, Vol. 48, No.4, 1996, pp. 339-56.

Wayson, R.L., “NCHRP Synthesis 268 - Relationship between pavement surface texture and highway traffic noise”, Transportation Research Board, National Academy Press, Washington D.C, 1998.

Weiss, W.J., and Olek, J, “Development of quiet and durable porous cement concrete paving materials”, Proposal No. 571-1284-0007, Institute of Safe, Quiet, and durable highways, Purdue University, 2001.

Whittington, H.W., McCarter, J., Forde, M.C., “The conduction of electricity through concrete”, Magazine of Concrete Research, Vol. 33, No.114, 1981, pp. 48-60.

Wolfe, R. W., and Gjinolli, A., “Cement bonded wood composites as an engineering material”, Proceedings of The use of recycled wood and paper in building applications, Forest products society, Madison, Wisconsin, 1996, pp. 84-91.

Wolfe, R. W., and Gjinolli, A., “Durability and strength of cement-bonded wood particle composites made from construction waste”, Forest Products Journal, Vol.49, No.2, 1999, pp. 24-31.

Yang, J., and Jiang, G., “Experimental study on properties of pervious concrete pavement materials”, Cement and Concrete Research, Vol. 33, 2003, pp. 381-386.

Zwikker, C., and Kosten, C. W., “Sound absorbing materials”. Elsevier Publishing Company Inc., 1949.